

Dissertation

submitted to the
Combined Faculties for the Natural Sciences and Mathematics
of the Ruperto-Carola University of Heidelberg, Germany
for the degree of
Doctor of Natural Sciences

presented by
Martina Klünemann, MSc
Born in: Haselünne, Germany
Oral examination: March 30th, 2017

Human gut bacteria interactions with host-targeted drugs

Referees:

Dr. Anne-Claude Gavin

Prof. Dr. Rob Russell

“I don't know, and I would rather not guess.”

(Frodo in “The Lord of the Rings” by J.R.R. Tolkien)

Acknowledgements

First of all I would like to thank Kiran for taking me on as a PhD student, advising me and having just another idea for an interesting experiment. Your light-hearted spirit, inquisitiveness and last minute polishing of manuscripts did shape my idea of science for the better.

Furthermore I like to thank my thesis advisory committee members Anne-Claude Gavin, Rob Russell, Christoph Steinbeck and Carsten Schultz for advise, feedback and thorough questioning during our regular meetings. In particular, I would like to thank Anne-Claude and Rob for accepting my thesis for examination.

I love to thank the Patil group as a whole and Melanie Tramontano, Sergej Andrejev and Filipa Pereira in particular. Thank you for getting me started in the lab and keeping me motivated. Thanks for discussions and sword fights and chocolate and the one or other kick in the butt. I am happy to have shared the last four years with you guys!

I would also like to thank the Typas group, especially Manuel Banzhaf and Lisa Maier, for mentoring, sharing their knowledge on bacteria and screening, hosting experiments in their sometimes crowded lab without ever complaining, and being in general a positive influence on the EMBL community.

Of course I want to mention the rest of the EMBL community as well. Thanks guys for discussions, friendship, coffee breaks, pizza session, hugs, and last but definitely not least parties! I made friends with many of you and my life is richer and better for it. Thank you especially Deepikaa Menon for kicking my butt, and thank you Simone Li for being amazing in general. Thank you for the last four years of friendship and support and slightly odd ideas and trips. Simone, without you I would have gone crazy but I will nevertheless remember forever that you are the reason I didn't get enough cookies during my predoc course!

I am eternally thankful for Daniela Begolo, without you I would have died. Thanks for saving me from starvation, dehydration, and boredom. You are one of the best and have been there for good and bad times. Thank you!

I also want to thank my other friends without whom I wouldn't be who I am, especially Katha Wilmes, Kadda Pallmer and the Münsteraner Crew. You guys are amazing. Particularly, I am deeply grateful to Phillip Ihmor and Neda Kazemie for getting me started with and keeping motivated during thesis writing. Johannes Sonnenholzner is acknowledged for providing me with an almost perfect playlist. Thank you!

Last but not least I would like to thank my family. Danke, dass ihr immer da seid egal was passiert. Vielen Dank für Umarmungen, Zuspruch, Ablenkung, Interesse an dem was ich tue, und Vertrauen darauf, dass schon was bei rum kommt. Vielen Dank für alles!

This thesis was written in memory of the Cookie and Wine Connection.
We did it!

Abstract

Studies as early as in the 70s showed that the gut and its intrinsic gut microbiota is a possible site of drug modification and later studies confirmed that human microbiota metabolism with its diverse set of genes can be a cause for drug side effects. Yet, our knowledge of the biochemical capabilities of gut bacteria to interact with or metabolize therapeutic drugs remains largely incomplete. To our knowledge, there has not been any systematic screen of xenobiotic-microbial interactions elucidating how wide-spread bacterial drug modification is across therapeutic drugs or the gut microbiota. In my PhD work, I tested, under anaerobic conditions, 450 bacteria-drug interactions covering 25 metabolically diverse gut bacteria and 18 structurally diverse FDA-approved drugs. This revealed almost 50 novel bioaccumulation or biotransformation links between 19 bacterial species and 10 drugs. The implicated bacteria are phylogenetically diverse, including commensals, probiotics and bacteria associated with diseases. The affected drugs span diverse indication areas, from asthma (montelukast) to depression (duloxetine and aripiprazole). As a case in point, the results from this bacteria-drug interaction study are followed upon in more details through investigation of interactions involving duloxetine – a widely used antidepressant. I found that duloxetine induces higher diversity in synthetic bacterial communities, and its bioaccumulation by community members affects the community dynamics. Following, I found that duloxetine affects the native metabolism of *B. uniformis* and *C. saccharolyticum*, in particular the purine metabolism. These interactions might in turn influence bacterial behavior in a community. To find the direct protein targets of duloxetine in *C. saccharolyticum*, I used click chemistry-based methods and proteomics. Two of the five strongly enriched binding proteins are part of a NADH:quinone dehydrogenase complex. Two potential underlying mechanisms for duloxetine interactions are suggested: i) Duloxetine inhibits NADH:quinone dehydrogenase by binding to its quinone binding site. The resulting NADH excess leads to a change in downstream pathways like purine metabolism. ii) Duloxetine binds competitively on the NADH binding site of NADH:quinone dehydrogenase and other proteins.

In addition to discovering new xenobiotic interactions, the study highlights a new dimension to gut microbiota-drug interactions, namely bioaccumulation, which so far has been largely overlooked. My results suggest that bioaccumulation of drug compounds might be a common feature to many gut bacteria and thus have broad and far-reaching implications for drug dosage decisions and personalized medicine.

Zusammenfassung

Bereits in den 70er Jahren zeigten Studien, dass der Darm und sein intrinsisches Darmmikrobiom ein möglicher Ort für die Modifikation von Medikamenten ist. Spätere Studien bestätigten, dass der Stoffwechsel des menschlichen Mikrobiom mit seinen im Vergleich zum menschlichen Genom unterschiedlichen Satz an Genen eine Ursache für Medikamentennebenwirkungen sein kann. Unser Wissen über die biochemischen Fähigkeiten von Darmbakterien mit therapeutischen Wirkstoffen in Wechselwirkung zu treten oder diese zu metabolisieren, bleibt jedoch weitgehend unvollständig. Unseres Wissens nach gibt es bis jetzt keine systematische Studie von xenobiotisch-mikrobiellen Wechselwirkungen, die darlegen könnte, wie weit verbreitet bakterielle Modifikation von therapeutische Arzneimitteln durch das Darmmikrobiom ist. In meiner Doktorarbeit habe ich unter anaeroben Bedingungen 450 Bakterien-Wirkstoff-Wechselwirkungen getestet, die 25 metabolisch verschiedene Darmbakterien und 18 strukturell verschiedene, FDA-zugelassene Medikamente abdecken. Dies zeigte fast 50 neue Zusammenhänge, Bioakkumulationen oder Biotransformationen, zwischen 19 Bakterienarten und 10 Wirkstoffen auf. Die betroffenen Bakterien sind phylogenetisch unterschiedlich, einschließlich Kommensalen, probiotischen Bakterien und Bakterien, die mit Krankheiten assoziiert sind. Die betroffenen Medikamente erstrecken sich über diverse Indikationsbereiche, von Asthma (Montelukast) bis hin zu Depression (Duloxetin und Aripiprazol). Als typisches Beispiel werden die Ergebnisse dieser Bakterien-Wirkstoff-Wechselwirkungsstudie anhand von Wechselwirkungen mit Duloxetin, einem weit verbreiteten Antidepressivum, genauer untersucht. Duloxetin induziert eine höhere Diversität in synthetischen Bakteriengemeinschaften, und seine Bioakkumulation durch Gemeinschaftsmitglieder beeinflusst die Gemeinschaftsdynamik. Weiterhin beeinflusst Duloxetin den nativen Metabolismus von *B. uniformis* und *C. saccharolyticum*, insbesondere den Purinstoffwechsel. Diese Wechselwirkungen könnten wiederum das bakterielle Verhalten in einer Gemeinschaft beeinflussen. Um die direkten Proteintargets von Duloxetin in *C. saccharolyticum* zu finden, verwendete ich Klick-Chemie-basierte Methoden und Proteomics. Zwei der fünf stark angereicherten Proteine sind Teil eines NADH:Quinone-Dehydrogenase-Komplexes. Zwei mögliche zugrundeliegende Mechanismen für Duloxetin-Wechselwirkungen werden vorgeschlagen: i) Duloxetin hemmt NADH:Quinone-Dehydrogenase durch Bindung an seine Quinone-Bindungsstelle. Der resultierende NADH-Überschuss führt zu einer Veränderung in Downstream-

Stoffwechselwegen wie dem Purinstoffwechsel. ii) Duloxetin bindet kompetitiv an der NADH-Bindungsstelle von NADH:Quinone-Dehydrogenase.

Neben der Entdeckung neuer xenobiotischer Wechselwirkungen unterstreicht die Studie eine neue Dimension der Mikrobiota-Wirkstoff-Wechselwirkungen, nämlich die der Bioakkumulation, die bisher weitgehend übersehen wurde. Meine Ergebnisse legen nahe, dass die Bioakkumulation von Wirkstoffen ein gemeinsames Merkmal vieler Darmbakterien sein kann und somit breite und weitreichende Implikationen für Arzneimitteldosierungsentscheidungen und personalisierte Medizin aufweist.

Table of contents

ACKNOWLEDGEMENTS	I
ABSTRACT	III
ZUSAMMENFASSUNG	V
TABLE OF CONTENTS	VII
LIST OF FIGURES.....	XIII
LIST OF TABLES.....	XV
1 INTRODUCTION.....	17
1.1 The human gut microbiota and its xenometabolism	17
1.1.1 The human gut microbiota.....	17
1.1.2 Hierarchy of xenometabolic interactions in the gut	18
1.2 Promiscuous enzymes drive and enlarge xenometabolic interactions	20
1.3 Enzyme availability and interaction between xeno- and native metabolism.....	22
1.3.1 Bacterial metabolism can change xenobiotics.....	22
1.3.2 Xenobiotics can change bacterial metabolism	22
1.4 Community structure influences xenometabolic interactions.....	23
1.4.1 Community structure determines possible interactions	23
1.4.2 Xenobiotics influence gut microbiota composition and structure 25	
1.5 Host-microbiota co-metabolism of xenobiotics	25
1.6 The gut-brain axis and depression	27
1.6.1 Duloxetine and its pharmacokinetics and -dynamics.....	29
1.7 Aims and Outline of the Thesis	30
1.7.1 Aims	30
1.7.2 Outline.....	31
2 HUMAN GUT BACTERIA INTERACTIONS WITH HOST-TARGETED DRUGS.....	32
2.1 Introduction	32
2.1.1 Why investigate bacteria-drug interactions?.....	32

2.1.2	Human gut bacteria investigated in this study.....	33
2.1.3	Experimental setup of bacteria-drug interaction screen and depletion-mode assay	34
2.2	Results.....	38
2.2.1	Drug Selection.....	38
2.2.2	Bacteria-Drug Interaction Screen	41
2.2.3	Depletion-mode assay.....	48
2.2.4	Summary: Bacteria-Drug interactions are specific	51
2.3	Discussion and Outlook.....	53
2.4	Clarification of contribution	58
3	DULOXETINE AFFECTS BACTERIAL GROWTH AND INDUCES CHANGES IN BACTERIAL COMMUNITIES	59
3.1	Introduction.....	59
3.1.1	Why investigate bacterial interactions with duloxetine?	59
3.1.2	Why investigate interactions in a synthetic community?	60
3.1.3	Aims and Experimental outline.....	61
3.2	Results.....	63
3.2.1	Growth effects of duloxetine.....	63
3.2.2	Bacterial community shifts induced by duloxetine	65
3.3	Summary and Discussion	67
3.4	Clarification of contribution	71
4	HUMAN GUT BACTERIA CHANGE THEIR NATIVE METABOLISM UPON DULOXETINE EXPOSURE	73
4.1	Introduction.....	73
4.1.1	Why investigate bacterial duloxetine metabolism?	73
4.1.2	How to investigate bacterial metabolism: Untargeted metabolomics	74
4.1.3	Experimental Outline and Aims	75
4.2	Untargeted metabolomics of duloxetine interactions using ¹ H NMR spectroscopy.....	77
4.2.1	Experimental setup.....	77
4.2.2	Results	77
4.2.3	Summary.....	79
4.3	Untargeted metabolomics of bacterial duloxetine depletion using LC- MS/MS	80

4.3.1	Experimental setup	80
4.3.2	Duloxetine is depleted in all conditions.....	81
4.3.3	Systemic investigation of changes in mass features	84
4.3.4	Feature annotation and pathway analysis.....	85
4.4	Summary and Discussion.....	90
4.5	Clarification of contribution.....	94
5	DULOXETINE BINDS TO A NADH:QUINONE DEHYDROGENASE AND PURINE PATHWAY MEMBERS	95
5.1	Introduction	95
5.1.1	Why investigate protein interactions of duloxetine?	95
5.1.2	Aims and Experimental Outline	96
5.1.3	Pull-down and proteomics of duloxetine binding proteins.....	97
5.1.4	Overexpression of candidate proteins.....	98
5.2	Results	99
5.2.1	Duloxetine binding protein enrichment.....	99
5.2.2	Homologous overexpression of protein candidates.....	105
5.2.3	Heterologous overexpression of protein candidates.....	106
5.3	Summary and Discussion.....	108
5.3.1	Summary	108
5.3.2	Duloxetine as NADH:quinone dehydrogenase inhibitor at quinone binding site.....	110
5.3.3	Duloxetine as nucleotide mimicking electron acceptor	111
5.3.4	Alternative explanations	113
5.3.5	Conclusion	113
5.4	Clarification of Contribution.....	114
6	DISCUSSION AND OUTLOOK	115
6.1	Summary of Results.....	115
6.1.1	Bioaccumulation of xenobiotics is a wide-spread characteristic of the human gut bacteria and affects community dynamics.....	115
6.1.2	Bacterial NADH:quinone dehydrogenase and purine metabolism are likely affected by duloxetine	116
6.2	Discussion.....	119
6.2.1	Side effects of host-targeted drugs are mediated through the gut microbiota.....	119

6.2.2	Duloxetine influences depression symptoms through impact on gut microbiota.....	122
6.2.3	Deprotonated, negatively charged drugs are less likely to be sequestered	123
6.2.4	Potential of host-targeted drugs as antibiotic adjuvants.....	124
6.2.5	Duloxetine inhibits bacterial NADH:quinone dehydrogenase and affects purine metabolism	126
6.3	Conclusion	127
7	MATERIALS AND METHODS	129
7.1	Growth conditions and media	129
7.2	UPLC methods	130
7.2.1	UPLC-UV methods.....	130
7.2.2	Data analysis.....	132
7.3	Bacteria-Drug Interaction Screen	133
7.3.1	Drug Selection.....	133
7.3.2	Experimental setup.....	134
7.3.3	Data analysis.....	135
7.4	Community Assembly Assay	136
7.4.1	Experimental Setup	136
7.4.2	DNA extraction and 16S barcode sequencing library preparation	137
7.4.3	16S barcode sequencing analysis.....	138
7.5	Other <i>in vitro</i> assays	138
7.5.1	Depletion-mode assay.....	138
7.5.2	Growth curves for IC50 determination.....	139
7.5.3	Resting Cell and Lysate assay.....	139
7.5.4	Duloxetine pull down assay	140
7.5.5	Homologous overexpression of protein candidates	141
7.5.6	Heterologous overexpression of protein candidates	142
7.6	Untargeted Metabolomics with NMR.....	143
7.7	Untargeted Metabolomics with LC-MS/MS	144
7.7.1	Experimental setup.....	144
7.7.2	Mass spectrometry method.....	144
7.7.3	Data analysis.....	145
7.8	Proteomics	146

7.8.1	Sample preparation.....	146
7.8.2	Mass spectrometry method and protein identification	147
7.8.3	Data analysis	148
REFERENCES		149
APPENDIX		162
A.	Side effect keywords	162
B.	Bacteria-Drug Interactions	163
C.	<i>C. saccharolyticum</i> growth curves and IC50	167

List of Figures

Figure 1: Hierarchal organization of xenobiotic interactions with the human gut microbiota.	19
Figure 2: Examples of promiscuous enzyme-drug interactions in bacteria.....	21
Figure 3: Chemical structure of duloxetine.	29
Figure 4: Experimental outline bacteria-drug interaction screen and depletion-mode assay.....	36
Figure 5: Drug Selection workflow and result.....	39
Figure 6: Technical replicates of UPLC injections from bacteria-drug interaction screen.	43
Figure 7: Density distribution of drug depletion in bacteria-drug interaction screen.	44
Figure 8: Reproducibility of significant growth fold changes in bacteria-drug interaction screen.	46
Figure 9: Heatmap of growth effects in bacteria-drug interaction screen.....	47
Figure 10: Examples of bacterial drug degradation from the depletion-mode assay.	50
Figure 11: Bacteria-drug interactions.	52
Figure 12: Community assembly assay outline.	62
Figure 13: IC50s for duloxetine.....	64
Figure 14: Growth curves with duloxetine.	65
Figure 15: Community composition of duloxetine assembly assay.	66
Figure 16: Duloxetine depletion in community assembly assay.....	67
Figure 17: Outline of untargeted metabolomics experiments.	76
Figure 18: NMR spectra comparing <i>B. uniformis</i> treated with duloxetine to controls.	79
Figure 19: Technical and biological replicates of untargeted metabolomics.....	82
Figure 20: Depletion of duloxetine in untargeted metabolomics.....	83
Figure 21: PCA of mass features from untargeted metabolomics.....	83
Figure 22: Comparing fold changes of duloxetine treated bacteria to controls.	85
Figure 23: Alkynated duloxetine.	97
Figure 24: Volcano plot of proteins detected in pull down.....	100
Figure 25: Heatmap of protein blast alignment.	101

Figure 26: Duloxetine depletion in <i>E. coli</i> homologous overexpression.	106
Figure 27: Duloxetine depletion in <i>E. coli</i> heterologous overexpression.....	107
Figure 28: NADH:quinone dehydrogenase.	109
Figure 29: Enriched metabolites and enzymes in purine pathway of <i>C.</i> <i>saccharolyticum</i>	118
Figure 30: Outline of bacteria-drug interaction screening plates.	134
Figure 31: Growth curves of <i>C. saccharolyticum</i> exposed to a dilution series of duloxetine.	167
Figure 32: Duloxetine IC50 determination for <i>C. saccharolyticum</i>	167

List of Tables

Table 1: Selection of species in bacteria-drug interaction screen.....	34
Table 2: Drugs selected for the Bacteria-Drug Interaction Screen.....	40
Table 3: Duloxetine depletion in NMR spectroscopy samples. Interference indicates duloxetine peaks, which partially interfered with peaks in bacteria only treated sample.	78
Table 4: KEGG Pathways enriched in significantly changed mass features.	88
Table 5: Species-specific annotations of top 10 changed mass features.	89
Table 6: GO term enrichment (most specific) for 55 enriched proteins.	102
Table 7: KEGG Pathway enrichment analysis for 55 enriched proteins represented by 33 EC numbers.	104
Table 8: Gut Microbiota Medium (GMM).....	129
Table 9: Recipe for LB medium.....	130
Table 10: UPLC methods.	131
Table 11: UPLC method description by drug	131
Table 12: Indirect gut related side effects from SIDER database.....	162
Table 13: Direct gut related side effects from SIDER database.....	163
Table 14: Drug depletion in bacteria-drug interaction screen.....	163
Table 15: Growth effects from bacteria-drug interaction screen.....	164
Table 16: Drug depletion in depletion-mode assay.....	165

1 Introduction

The text of the following chapter sections 1.1-1.5 has mainly been taken from the review Klünemann et al. (2014) and has been originally written by myself. I modified and updated it according to the needs of this thesis introduction.

1.1 The human gut microbiota and its xenometabolism

1.1.1 The human gut microbiota

With the help of metagenomics tools, it is now possible to determine the identity of a large fraction of the microbial species colonizing the human gut (Qin et al. 2010; Human Microbiome Project Consortium. 2012). These tools are also revealing the genetic repertoire of the gut microbiome in an unprecedented detail. The resulting rich datasets are enabling the characterization of the gut microbial communities and their association with health (Blaser et al. 2013).

The gut microbiota has been shown to modify or metabolize several kinds of xenobiotics, from novel cancer drugs through millennia old analgesics to dietary components (Goldman et al. 1974; Azad Khan et al. 1983; Sousa et al. 2008; Wallace et al. 2010; Zheng et al. 2013; Clayton et al. 2009). Recent studies have also highlighted the feasibility of exploiting and manipulating this microbial-mediated xenometabolism to improve the host health or to prohibit medicinal side effects. For example, Wallace et al. showed that a deleterious biotransformation of the cancer drug Irinotecan can be averted by inhibiting bacterial β -glucuronidase (Wallace et al. 2010). On a more general level, probiotic bacteria like *Lactobacillus* sp. have been shown to ease *C. difficile*-associated diseases, diarrhea and other side effects of antibiotics (Cimperman et al. 2011; Hickson 2011).

Thanks to the advances in various omics technologies, molecular pathways of xenometabolism and other xenobiotic interactions in the gut microbiota have now

started to unfold through the identification of responsible microorganisms and enzymes (Ravcheev & Thiele 2016; Wang et al. 2011; Haiser et al. 2013). In parallel to these advances stemming from metagenomics, more and more evidence is piling up supporting the key role of gut microbiota in xenometabolism (Sousa et al. 2008; Clayton et al. 2009; Zheng et al. 2013). In particular, metabolomics has made it possible to trace the metabolic fate of xenobiotic compounds (Segata et al. 2013; Wikoff & Anfora 2009; van Duynhoven et al. 2011), which, together with metagenomics, is leading to the recent resurgence in the research on xenometabolism (Sowada et al. 2014; Johnson et al. 2012; Wilson & Nicholson 2016).

Understanding xenobiotic interactions in the gut is a highly challenging task due to three main reasons: the widespread promiscuity of metabolic enzymes, the compositional complexity of the gut microbiota, and the interactions between the host and the microbial-mediated xenometabolism. Due to the widespread promiscuity of metabolic enzymes (Khersonsky & Tawfik 2010; Ekins 2004; Oguri 1994), the number of possible routes through which a xenobiotic compound can interact with or get metabolized or modified by increases combinatorially with the enzymatic repertoire of the microbiota. The compositional diversity and spatial heterogeneity of the microbiota and the host-microbiota interaction through the enterohepatic cycle adds another layer to this complexity.

1.1.2 Hierarchy of xenometabolic interactions in the gut

Xenometabolism is the enzyme-mediated biochemical transformation of a xenobiotic, meaning non-native, compound. Other xenometabolic interactions can involve the disturbance of native metabolism by the xenobiotic compound. The general metabolic interactions that a xenobiotic compound can undergo in the gut microbiota can be conceptually organized into three levels: community, species and enzymes (Figure 1). Complex xenometabolic pathways often emerge through the functional interplay within and across these hierarchical levels. At the outermost level, the spatial and compositional structure of the microbial community influences the survival, activity and procreation of species in the gut environment, and hence the overall xenometabolism (Figure 1c). At the

intermediate level, individual species determine and control the enzyme availability for the xenometabolism (Figure 1b). At the innermost level, the enzymes perform the actual biotransformations owing to their promiscuity (Figure 1a).

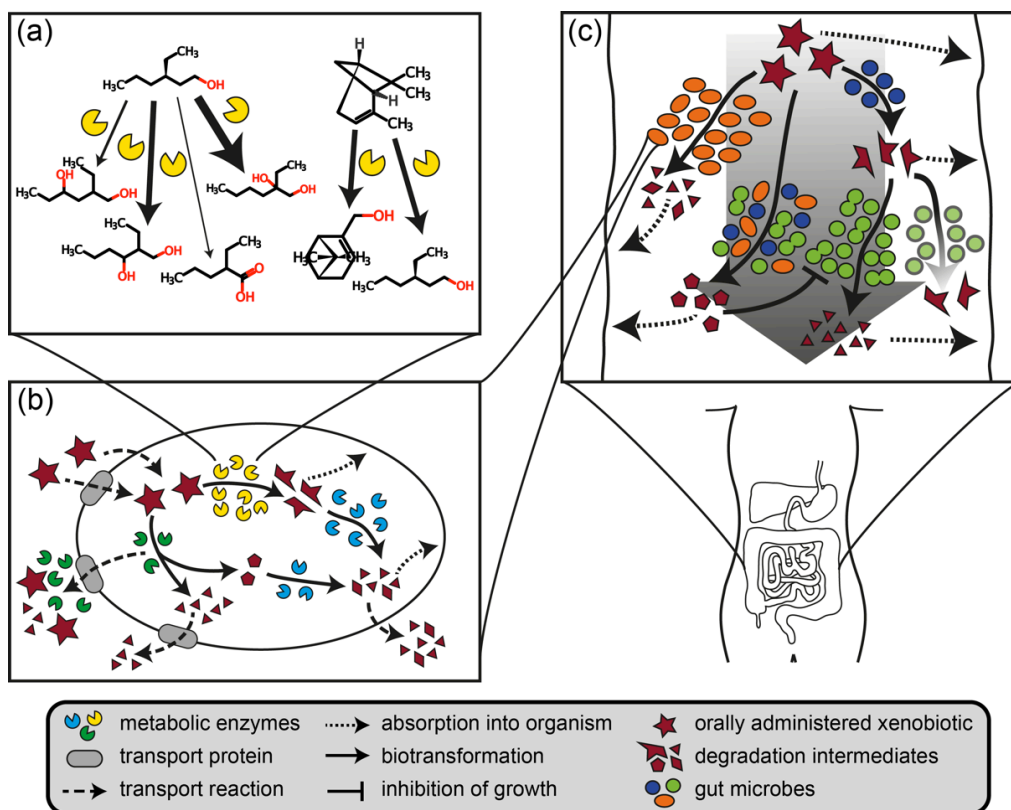


Figure 1: Hierarchical organization of xenobiotic interactions with the human gut microbiota.

(a) Enzyme-level xenometabolism. Promiscuous enzymes like cytochrome P450 have broad substrate specificities and can biotransform different xenobiotics. Enzyme moonlighting can also lead to different modifications of a given xenobiotic compound. (b) Species-level xenometabolism. Xenometabolic enzymes are usually found in the cytosol of microbial cells, but some can be secreted as well. A xenobiotic compound can undergo different biotransformations within a microbe before its metabolites are exported into the gut lumen, or used by the microorganism as a nutrient. (c) Community-level xenometabolism. A xenobiotic or its derivatives can be absorbed and/or modified by the host, excreted from the gut, or modified by the gut microbiota in many alternative ways. Different species in the microbiota can transform a given xenobiotic into different compounds, which can be further metabolized by the same or different microbes. Depending on the metabolic status of certain bacteria, a xenobiotic might be degraded or not. The xenobiotics and the degradation intermediates are also affected by the structure of the microbiota and *vice versa*. Figure adapted from (Klünemann et al. 2014)

As a consequence, the gut microbiome can alter the disposition, toxicity, and efficacy of therapeutic drugs in different ways (Swanson 2015): 1) Activation or Inactivation of a xenobiotic by metabolic modification. 2) Sequestration or bioaccumulation by binding the xenobiotic. 3) Reactivate a xenobiotic already detoxified by liver metabolism. 4) Generating metabolic intermediates, which are

metabolized to toxic compounds by the host. 5) Microbial metabolites and xenobiotics compete directly for host enzymes. The following chapter will focus on potential mechanism behind gut microbial xenobiotic metabolism and its consequences on the host while also highlighting how xenobiotics influence the gut microbiota in return. The different levels of regulation conceptualized in Figure 1 structure the following parts of introduction.

1.2 Promiscuous enzymes drive and enlarge xenometabolic interactions

Enzymes can often bind to more compounds (substrate promiscuity) and catalyze more reactions (functional moonlighting) than those listed in traditional databases like KEGG (Kanehisa et al. 2014), and thus may exhibit functions and biochemical features beyond the current description (Khersonsky & Tawfik 2010; Ekins 2004). This promiscuity is the key driver of xenobiotic metabolism (Figure 1a). Indeed, xenobiotic metabolism in the liver is also driven by highly promiscuous enzymes like cytochrome P450 oxidases and glutathione S-transferases (Jakoby & Ziegler 1990). In microbial systems, enzyme promiscuity has been as yet mainly investigated in the context of bioremediation of toxic compounds from the environment (Wu et al. 2012), or, in the context of biotechnological production of valuable chemical compounds (Soni C Banerjee 2005; Gao et al. 2011). For a comprehensive review on the biotransformation of xenobiotics mediated by the gut microbial enzymes and its similarity to bioremediation, see Haiser & Turnbaugh (2013).

Specific links between xenometabolism and the responsible enzyme are scarcely known for gut microbes. However, numerous enzyme-xenobiotic compound relationships have been described in other biological systems, particularly in the context of liver metabolism (Jakoby & Ziegler 1990; Holzhütter et al. 2012; Valerio & Long 2010). To obtain an overview of the bacterial enzymes relevant for xenobiotic metabolism, I compiled a xenobiotic-enzyme network for exemplary xenobiotics (Figure 2) based on interactions obtained from the

1.3 Enzyme availability and interaction between xeno- and native metabolism

1.3.1 Bacterial metabolism can change xenobiotics

One of the well-known examples of xenometabolism that is specific to a particular gut bacterium is the metabolism of Digoxin by *Eggerthella lenta* (Haiser et al. 2013). Although such specificity of xenometabolism is scarcely known for other compounds, links between bacterial species and metabolites have been observed in several studies (Zheng et al. 2013; Wang et al. 2011; Mahmood et al. 2015; Shu et al. 1991). Not only metabolic interactions can be species specific but also sequestration. For example, the binding of L-DOPA to surface proteins of *Helicobacter pylori* interferes with the treatment of Parkinson's disease and it improves again after eradication of the pathogen (Pierantozzi et al. 2006; Niehues & Hensel 2009). Such correlations can be used to narrow down the list of potential biotransforming species for a given xenobiotic compound.

While the nature and the abundance of different enzymes harbored by a species will determine the possibilities and limits of the xenobiotic interactions and xenometabolism, the interactions between xeno- and native metabolism will impact the dynamics and efficiency of the actual xenometabolic pathways. One step towards understanding species level xenometabolic interactions is to assess its enzymatic repertoire and map the corresponding metabolic network.

1.3.2 Xenobiotics can change bacterial metabolism

The metabolic activity status of a bacterium can also have a strong influence on the probability of biotransformations, which can subsequently impact the entire community (Allison et al. 2011; Tamura et al. 2013; Cai et al. 2015). Some xenobiotics can also directly influence the microbial metabolism, e.g. by invoking changes in gene expression (Maurice et al. 2013; de Freitas et al. 2016). Such feed-forward phenomena increase the challenges for investigating xenometabolic interactions. Metatranscriptomic and metaproteomic studies can help to identify

the metabolic state of a given species and to understand the response of microbial native metabolism to the perturbations introduced by xenobiotics (Booijink et al. 2010; Kolmeder et al. 2012; Pérez-Cobas et al. 2013; Cai et al. 2015). Another method to investigate if and how bacterial native metabolism is affected makes use of recent advances in (meta)metabolomics (Jacobs et al. 2008; Davey et al. 2013; Johnson et al. 2012; Vernocchi et al. 2016). Thus, xenobiotics can alter the composition of the intestinal microbiota as well as the microbial gene expression and metabolism.

1.4 Community structure influences xenometabolic interactions

1.4.1 Community structure determines possible interactions

A typical gut microbiota consists of hundreds of diverse microbial species (Human Microbiome Project Consortium. 2012; Qin et al. 2010). This compositional complexity, combined with the spatial heterogeneity of the microbiota (Rey et al. 2013; Dunne 2001; Yang et al. 2005; Hao & Lee 2004) poses arguably the biggest challenge for investigating the xenometabolism in the gut. A microbial consortium can interact with and transform a certain xenobiotic compound in qualitatively different ways than any single species (Figure 1c). A community is especially more likely to perform multiple consecutive transformation steps due to the larger enzymatic repertoire and thus the likelihood is higher that at least some of the many species would express a given enzyme under a given condition.

The spatial structure of the gut microbiota is a critical factor for xenometabolism (Donaldson et al. 2015; Rey et al. 2013; Yang et al. 2005; Dunne 2001). For example, a biotransformation of a xenobiotic might require an acidic environment and thus would be performed by microbes residing closer to or in the small intestine, whereas microbes in the distal colon would perform subsequent steps of the xenometabolism.

The composition of the gut microbiota is strongly influenced by several environmental and host-dependent factors including nutrient supply, peristaltic movements and the host's immune system (Hao & Lee 2004; Hooper et al. 2012). In turn, the gut microbiota can act as an ecosystem engineer influencing some of these factors (Costello & Stagaman 2012). Regarding species composition, individual gut microbiota are often considerably different from each other (Human Microbiome Project Consortium. 2012). Interestingly, these diverse microbiotas can converge regarding their functional repertoire, for example, when seen from the viewpoint of the represented metabolic capabilities (Human Microbiome Project Consortium. 2012; Abubucker et al. 2012). Accordingly, in a recent metaproteomic analysis, Kolmeder et al. (2012) observed temporally stable expression for a core protein pool of the human intestinal microbiota. From a xenometabolism perspective, these observations suggest that different microbiota may exhibit common functionalities despite compositional dissimilarities. However, the dependency of xenometabolism on the microbial community composition can be highly complex (Figure 1c). It has been shown that differences in microbial composition is associated with differences in xenometabolic gene capacity (Das et al. 2016). Hence the functional implications of the convergent metabolic potential remain to be evaluated.

A source of diversity in xenometabolism that can arise even between species with similar metabolic capabilities is the disparity in their ability to secrete enzymes, and to uptake/excrete xenobiotics and derivative xenometabolites (Nikaido 1996; Lee et al. 2010; Sorg et al. 2014). A given xenometabolic process may involve a complex combination of intra- and extra-cellular biotransformation processes (Figure 1b). In the gut lumen, secreted enzymes can transform the original xenobiotic compound or its metabolic derivatives secreted by other microbes. Inside the cells, biotransformation is limited to the enzyme repertoire of the respective bacterium, but likelihood of biotransformation may be higher due to higher proximity between the xenobiotic and the transforming enzyme(s).

1.4.2 Xenobiotics influence gut microbiota composition and structure

Secreted enzymes, native metabolites and xenometabolites can positively or negatively impact the whole community (Lee et al. 2010; Riley & Wertz 2002; Sorg et al. 2014). Thus, the xenometabolic processes and the gut microbiota can reciprocally impact each other. Many examples of xenobiotic influence on gut microbiota composition have been described in recent years (Catry et al. 2015; Jackson et al. 2016; Cai et al. 2015; Davey et al. 2013). Particular noteworthy is a study which disentangled the effect of metformin, an antidiabetic drug, on the gut microbiome composition from the effect of diabetes or metabolic syndrome (Forslund et al. 2015). Effects of proton pump inhibitors or antidepressants have also been shown in large cohort studies (Jackson et al. 2016; Zhernakova et al. 2016). In a few studies, which investigated a cause for a shift in microbiome composition, an effect of the xenobiotic on bacterial gene expression or metabolism was observed (Cai et al. 2015; Catry et al. 2015; Kaufman & Griffiths 2009). However, most of these changes have been observed in host-mediated systems, thus the shift in microbiota composition could also be caused by the host and not by the xenobiotic directly interacting with the bacteria.

1.5 Host-microbiota co-metabolism of xenobiotics

After ingestion and passage of xenobiotics through the stomach, the alkalization of the intestinal content is critical for the enzyme activity and subsequently for xenometabolism within the small intestine. Absorption to the bloodstream can occur by many different ways such as active transport, facilitated diffusion, pinocytosis or passive diffusion. Absorbed substances are transported via the portal vein to the liver, where metabolism of most xenobiotics takes place (Chhabra 1979; Gad 2007). Following the absorption of drugs from the stomach and gut, biotransformation in the gastrointestinal epithelial tissue and liver can drastically alter their bioavailability and pharmacokinetics (Chhabra 1979). This so-called first pass metabolism consists of two phases and it alters the activity of

xenobiotics and/or converts them into more water-soluble compounds, often leading to detoxification and eventual excretion (Chhabra 1979; Gad 2007). In phase I it is usually mediated by cytochrome P450 enzymes and it introduces reactive or polar chemical groups enabling further detoxification reactions. In phase II the enzymes catalyze conjugation reactions to transform compounds to less toxic forms and increase the water-solubility for easier excretion. In many cases, this so-called 'first-pass metabolism' not only includes metabolism by the liver but also that by the gut microbiota (Björkholm et al. 2009).

The co-metabolism by the liver and the gut microbiota can also lead to the circulation of xenobiotics between these two metabolic compartments, constituting the enterohepatic cycle. During the enterohepatic circulation, an unchanged xenobiotic or its biotransformed metabolite can be excreted back into the small intestines via the bile (Gad 2007; Kaminsky & Zhang 2003). Xenobiotics can be biotransformed first either by the liver or the microbiota and then further modifications can occur in the other system (Clayton et al. 2009; Wallace et al. 2010). Together, the intestinal absorption barrier, phase I and II metabolism and excretion constitute the defense mechanism of the human body against foreign (toxic) substances.

The intestinal microbiota adds to the possibilities and complexity of human metabolism in general and xenometabolism particularly. In general, the microbiota has a strong impact on human metabolism, immune system and potentially behavior (Wikoff & Anfora 2009; Hooper et al. 2012; Heijtz et al. 2011; Cai et al. 2015). In particular, the interconnectivity between the intestinal tract and other metabolic compartments makes it essential to view xenometabolic processes as a co-metabolism by the host and the microbiota (Swanson 2015). The examples of such co-metabolism include pro-drugs like mesalazine, which are activated by the gut microbiota and then detoxified by the liver (Azad Khan et al. 1983). Another prominent example is irinotecan, a cancer drug, which is first glucuronidated by the liver and then, through enterohepatic circulation, transferred back to the gut, where it is further metabolized by the gut microbiota (Wallace et al. 2010). Intriguingly, the xenobiotic co-metabolism can be further

interconnected by the mutual regulation of host and microbiota gene expression in response to a xenobiotic. For example, the intestinal microbiota can mediate changes in the hepatic gene expression and the xenometabolism thereof in response to a xenobiotic (Björkholm et al. 2009). For an extensive review of gut microbiota-host xenobiotic co-metabolism see Carmody & Turnbaugh (2014).

1.6 The gut-brain axis and depression

An intriguing example where all different factors of host system, microbiota and drug interactions act in concert is the gut-brain axis, which is particularly relevant for the development and treatment of depression. The human gut microbiota, the gut and the central nervous system are closely connected through an exchange of numerous metabolites and hormones (Collins & Bercik 2009; O'Mahony et al. 2015). In particular at the functional level, the gut microbiota plays an important role in maturation of the immune and nervous system (Sharon et al. 2016). Microglia, the immune cells of the brain, and the blood-brain-barrier are potentially trained and influenced by the microbiota. Newly emerging data suggest the importance of communication between the gut and the brain in disorders as diverse as anxiety, depression, cognition, and autism spectrum disorder (Sharon et al. 2016). Other data from animal studies indicate that changes in behavior can change the microbiome composition, and that these changes have effects on inflammation signals in the GI tract (Collins & Bercik 2009). In turn, prebiotics and probiotics have a mood lightening effect or effects on brain activity in human subjects (Schmidt et al. 2014; Tillisch et al. 2013). Especially serotonin synthesis is closely connected to the gut and 90% of serotonin is located in the enterochromaffin cells in the GI tract, where it regulates intestinal movements (Berger et al. 2009). Additionally, the gut microbiome is able to modulate host tryptophan metabolism, which in turn affects serotonin synthesis and production of neuroactive metabolites (O'Mahony et al. 2015). Thus, there is substantial overlap between behaviors influenced by the gut microbiota and those, which rely on intact serotonergic neurotransmission like mood or appetite.

The development of depression seems to be closely linked with a change in microbiota (Foster & McVey Neufeld 2013). Patients with major depressive disorder have a different gut microbiome than healthy subjects (Zheng et al. 2016), and also in comparison to patients in remission (Jiang et al. 2015). Mice treated with feces from patients showed depressive-like symptoms (Jiang et al. 2015; Zheng et al. 2016). However, in both cases the studies did not control for the use of antidepressants, thus a change in microbiome might be induced by medication. Two studies that investigated population cohorts found an association between certain antidepressant treatments and changes in the diversity of gut bacteria (Falcony et al. 2016; Zhernakova et al. 2016). In turn these studies did not control for depression among subjects.

Another factor to be considered is that many antipsychotics induce weight gain (Dent et al. 2012). Weight gain can be caused by a change in microbiota (Musso et al. 2011) or because of differences in life style and nutrition change the microbiota (Turnbaugh et al. 2009; Zhernakova et al. 2016). Thus, on the one hand the observed changes in microbiome composition in patients with depression could be caused by the weight gain induced by antidepressive treatment. On the other hand, the weight gain might be caused through medication changing the microbiome (Davey et al. 2013; Morgan et al. 2014). Differences in weight gain can be observed between medications from the same class. For example duloxetine induces weight gain, while the structurally similar antidepressant fluoxetine does not (Dent et al. 2012).

Interestingly, many antipsychotic drugs have antimicrobial properties and can *in vitro* augment the efficacy of antibiotics (Jeyaseeli et al. 2012; Jeyaseeli et al. 2006; Ayaz et al. 2015; Munoz-Bellido et al. 2000). For antidepressants, which act as serotonin reuptake inhibitors blocking a molecular pump, these effects have been associated with blocking drug efflux pumps in bacteria (Bohnert et al. 2011). Different antidepressants affect bacteria with different efficiencies (Munoz-Bellido et al. 2000; Kalaycı et al. 2015). Additionally, as some antidepressants have antimicrobial effects on their own they have to directly affect bacterial physiology as well (Munoz-Bellido et al. 2000).

Taking these studies together, an interaction between depression, medication and gut microbiota is likely, but cause and consequence are yet difficult to assess. In the next part I will shortly introduce the specific antidepressant duloxetine, as much of the following study is based on it.

1.6.1 Duloxetine and its pharmacokinetics and -dynamics

Antidepressants are widely prescribed medications treating various forms of depression and anxiety, and the number of patients receiving antidepressive treatment is on the rise worldwide. In the US, duloxetine (Trade name: Cymbalta) is one of the most commonly prescribed antidepressant, and is in the top 20 pharmaceutical products by sales volume in 2013 (PMLive 2015). It is a norepinephrine and serotonin reuptake inhibitor (SNRI), which leads to a longer exposition of synapses to these neurotransmitters, which in turn has a mood-lightening effect. Duloxetine binds selectively with high affinity to both norepinephrine (NE) and serotonin (5-HT) transporters and lacks affinity for monoamine receptors within the central nervous system (Wernicke et al. 2005). It is also in use or investigated for treating stress-induced urinary incontinence. Common side effects are nausea, insomnia, and dizziness, which are consistent with the pharmacology of the molecule as it interacts with the hormonal and nervous system (Wernicke et al. 2005). Another side effect of duloxetine that is common to many antidepressants is weight gain (Dent et al. 2012) but also constipation. Chemically, it is a naphthalene with a sulfur hetero cycle and an secondary amine group attached (Figure 3).

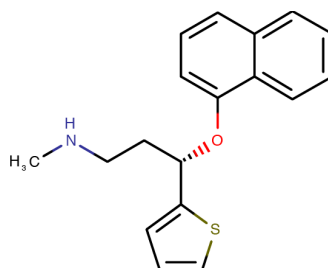


Figure 3: Chemical structure of duloxetine.

Duloxetine is a thiophene derivative. It acts as a selective neurotransmitter reuptake inhibitor for serotonin and noradrenalin (SNRI).

Duloxetine has a long half-life after oral administration of around 11h, and its metabolites are systemically cleared only after up to 120 hours (Lantz et al. 2003). It is mainly metabolized in the liver, and is hepatotoxic in higher doses. Duloxetine interacts with many cytochrome P450 enzymes, but is mainly metabolized by CYP1A2 and CYP2D6. Duloxetine's main metabolites are excreted to 70% in urine and to 20% in feces after extensive first and second phase detoxifying metabolism. The major biotransformation pathways for duloxetine involve oxidation of the naphthyl ring at either the 4-, 5-, or 6-positions followed by further oxidation, methylation, and/or conjugation. Conjugated metabolites are mainly found in the urine. In feces, 4-hydroxy duloxetine and an unidentified polar metabolite are the main metabolites (Lantz et al. 2003). Duloxetine's metabolites 5-hydroxyduloxetine, 6-hydroxyduloxetine and 6-hydroxy-5-methoxyduloxetine have been shown to inhibit 5HT and/or NE transporters and hence are possibly contributing to duloxetine's therapeutic impact (Kuo et al. 2004). Chan et al. (2011) reported that the hepatotoxicity of duloxetine is possibly not related to the bioactivation of its thiophene moiety, or its transient binding of CYP1A2, but might be due to the epoxidation of its naphthyl ring. As all experiments are performed with the pure compound, it should be noted that duloxetine is sensitive to neutral, acidic and alkaline hydrolysis, but stable to oxidative stress (Sinha et al. 2009)

1.7 Aims and Outline of the Thesis

1.7.1 Aims

Studies as early as in the 70s showed that the gut and its intrinsic gut microbiota is a possible site of drug modification (Goldman et al. 1974) and later studies confirmed that human microbiota metabolism with its diverse set of genes can be a cause for drug side effects (Wallace et al. 2010; Haiser et al. 2014; Sousa et al. 2008). The general metabolic processes a xenobiotic compound can potentially undergo in the gut are known in principle (Wilson & Nicholson 2016; Koppel & Balskus 2016). However, the specifics of when, where, and how are often unclear.

The biomodification of a xenobiotic compound is hard to predict from the compound structure alone, since it is also dependent on the chemical environment and enzyme availability (Nicholson 2002). Thus, our knowledge of the biochemical capabilities of gut bacteria to interact with or metabolize therapeutic drugs remains largely incomplete.

The goal of this study was to conduct a systematic screen of xenobiotic-microbial interactions elucidating the potential of gut bacteria to modify or sequester host-targeted drugs. Insights into gut bacterial-drug interactions can facilitate prediction of xenobiotic biotransformation, which is highly valuable since it can reduce the cost of developing drugs and prevent unnecessary testing for toxicity (Klünemann et al. 2014). Furthermore, together with other data from metagenomic sequencing this knowledge can foster personalized dosage (for better pharmacokinetics) and personalized medicine, thus reducing side effects (Clayton et al. 2006). In conclusion, the aim of my PhD work is to find gut bacteria-drug interactions *in vitro* and then investigate potential underlying mechanisms.

1.7.2 Outline

In chapter 2, I present results from a bacteria-drug interaction screen and investigations into the mode of bacterial drug depletion. Results from this interaction study are followed upon in more details through investigation of gut bacterial interactions with the antidepressant duloxetine. As gut bacteria live as part of a community, interactions of duloxetine with different bacterial targets within a defined community context are assessed and presented in chapter 3. In chapter 4, I present results from investigating the effect of duloxetine on bacterial native metabolism, which may in turn influence bacterial behavior in a community. In chapter 5, to find a mechanistic explanation for bacteria-duloxetine interactions, I explored the direct protein targets of duloxetine using click-chemistry based methods and proteomics. In the last chapter I give a summary of all findings, discuss how they connect to current research and propose further research directions.

2 Human gut bacteria interactions with host-targeted drugs

In this chapter I will describe the experimental basis for the rest of my PhD work presented in this thesis. I will explain why and how a gut bacteria-drug interaction screen and follow-up on the depletion-mode of bacterial drug depletion is conducted. I will describe the results from both experiments separately and give summary of findings from both screens in the end. Then I will discuss the limitations and implications of the results for specific bacteria-drug interactions. In the end I will give a short outlook on further experiments.

2.1 Introduction

2.1.1 Why investigate bacteria-drug interactions?

Studies in the 70s showed that the gut and its intrinsic gut microbiota is a possible site of drug degradation (Goldman et al. 1974) and later studies confirmed that human microbiota metabolism with its diverse set of genes can be a cause for side effects (Wallace et al. 2010; Haiser et al. 2014). It has been shown recently that xenobiotics-gut microbiota-host interactions have major impacts on health in a microbiota dependent manner (Zheng et al. 2013). Additionally, the drugs can influence the human microbiota itself, which might cause side effects (Forslund et al. 2015). Prediction of xenobiotic biotransformation is highly valuable since it can reduce the cost of developing drugs and prevent unnecessary testing for toxicity. Furthermore, in context with other data from metagenomic sequencing and detailed knowledge of the pharmacodynamics/kinetics of the drug it can foster personalized dosage boosting treatment efficiency. Knowing the effects of a drug on the microbiota and its effect on the drug can lead to development of new treatment strategies having the microbiota as its primary target (Swanson 2015). To predict efficacy or potential toxic side effects one has

thus to investigate how the xenobiotic metabolism of gut bacteria influences the degradation and absorption of the drugs.

The general metabolic processes a xenobiotic compound can potentially undergo in the gut are known in principle. However, the specifics of when, where, and how are often unclear. The biodegradation of a xenobiotic compound is hard to predict from the compound structure alone, since it is also dependent on the chemical environment and enzyme availability. Thus, for most current drugs it is not known if and how they are affected by the human gut microbiota and in turn how the microbiota is affected by drugs (Patterson & Turnbaugh 2014).

To our knowledge, there has not been any systematic study of xenobiotic-microbial interactions elucidating how wide-spread bacterial drug interaction is across therapeutic drugs or the gut microbiota. We therefore planned a medium-scale systematic study researching the interactions between therapeutic drugs and human gut bacteria *in vitro* in monocultures. We aimed to investigate around 500 pairwise interactions, one drug-bacteria interaction at a time.

2.1.2 Human gut bacteria investigated in this study

In this study, I used a subset of a panel of cultivatable human gut bacteria (96 strains representing 74 species) being used in a variety of projects at EMBL-Heidelberg. These were rationally selected to cover a broad range of phylogenetic and metabolic characteristics of the human gut microbiota. Parameters for selection included: i) relative abundance higher than 10^{-5} , ii) prevalence higher than 90% in metagenomic datasets of healthy persons, iii) cultivability in monocultures, and iv) availability of an annotated genome. Additional species were included to cover probiotics, opportunistic pathogens and species representing particular metabolic features like mucin degradation or xenobiotic biotransformation. A subset of this selection was used in the bacteria-drug interaction screen presented in this study. Besides covering the main phyla present in the human gut, the focus here was to cover potentially metabolic diverse but phylogenetically similar species. This focus allows narrowing down quickly on relevant genes potentially involved in a bacteria-drug interaction. Additionally,

bacteria known to be involved in xenobiotic interactions like *E. lenta* were included (Haiser et al. 2014). The final selection used in the screen can be found in Table 1. Bacteria strains were purchased from ATCC or DMSZ strain collections.

Table 1: Selection of species in bacteria-drug interaction screen.

Gram stain	Phylum	Species	Strain	NCBI tax ID
negative	Bacteroidetes	<i>Bacteroides fragilis</i>	EN-2; VPI 2553	272559
negative	Bacteroidetes	<i>Bacteroides thetaiotaomicron</i>	E50(VPI 5482)	226186
negative	Bacteroidetes	<i>Bacteroides uniformis</i>	VPI 0061	411479
negative	Bacteroidetes	<i>Bacteroides uniformis</i> HM-715	CL03T00C23	997889
negative	Bacteroidetes	<i>Bacteroides uniformis</i> HM-716	CL03T12C37	997890
negative	Bacteroidetes	<i>Bacteroides vulgatus</i>	DSM-1447	435590
positive	Actinobacteria	<i>Bifidobacterium animalis</i> subsp. <i>lactis</i>	BI-07	742729
positive	Actinobacteria	<i>Bifidobacterium longum</i> subsp. <i>infantis</i>	S12	391904
positive	Actinobacteria	<i>Bifidobacterium longum</i> subsp. <i>longum</i>	E194b (Variant a)	
positive	Firmicutes	<i>Clostridium bolteae</i>	WAL 16351	411902
positive	Firmicutes	<i>Clostridium ramosum</i>	113-I; VPI 0427	445974
positive	Firmicutes	<i>Clostridium saccharolyticum</i>	WM1	610130
positive	Firmicutes	<i>Coprococcus comes</i>	VPI CI-38	470146
positive	Actinobacteria	<i>Eggerthella lenta</i>	1899 B; VPI 0255	479437
negative	Proteobacteria	<i>Escherichia coli</i> ED1a	ED1a	585397
negative	Proteobacteria	<i>Escherichia coli</i> IA11	IA11	585034
positive	Firmicutes	<i>Eubacterium rectale</i>	A1-86	657318
negative	Fusobacteria	<i>Fusobacterium nucleatum</i>	1612A; VPI 4355	190304
positive	Firmicutes	<i>Lactobacillus gasseri</i>	AM 63	324831
positive	Firmicutes	<i>Lactobacillus paracasei</i>	LPC-37	
positive	Firmicutes	<i>Lactobacillus plantarum</i>	WCFS1	220668
positive	Firmicutes	<i>Lactococcus lactis</i>	IL1403	272623
positive	Firmicutes	<i>Ruminococcus gnavus</i>	VPI C7-9	411470
positive	Firmicutes	<i>Ruminococcus torques</i>	VPI B2-51	411460
positive	Firmicutes	<i>Streptococcus salivarius</i>	275	

2.1.3 Experimental setup of bacteria-drug interaction screen and depletion-mode assay

The number of interactions investigated was mainly limited by the detection method for the drugs. For detection the drug is separated from media compounds by liquid chromatography, thus each drug has a different chromatographic method. As all drugs need to be detected in the same screen, establishing the different methods using the same buffer system was challenging and time-

consuming. Within the constraints of analytics, I selected drugs to investigate a broad diversity of them spanning a wide therapeutic area and a spectrum of chemical structures. For a detailed description of drug selection and experimental conditions refer to method section 7.3 on page 133.

The experimental investigation was set up in two parts: first a screening part investigating a broad range of potential bacteria-drug interactions and then assaying the depletion hits from the screen to determine the mode of depletion (Figure 4). The bacteria-drug interaction screen was conducted in 96 well plates with 150µl of medium, growth was monitored during 48h anaerobic incubation, and bacteria were removed by centrifugation before extracting the spent medium in organic phases to measure the drug concentration. Extraction protocol was implemented with a pipetting robot. As shown in the plate outline in Figure 4, I used one bacteria-free control per plate and drug, but triplicates for each bacteria-drug interaction. All bacteria-drug interactions were screened in biological duplicates.

Bacteria-drug interaction screen

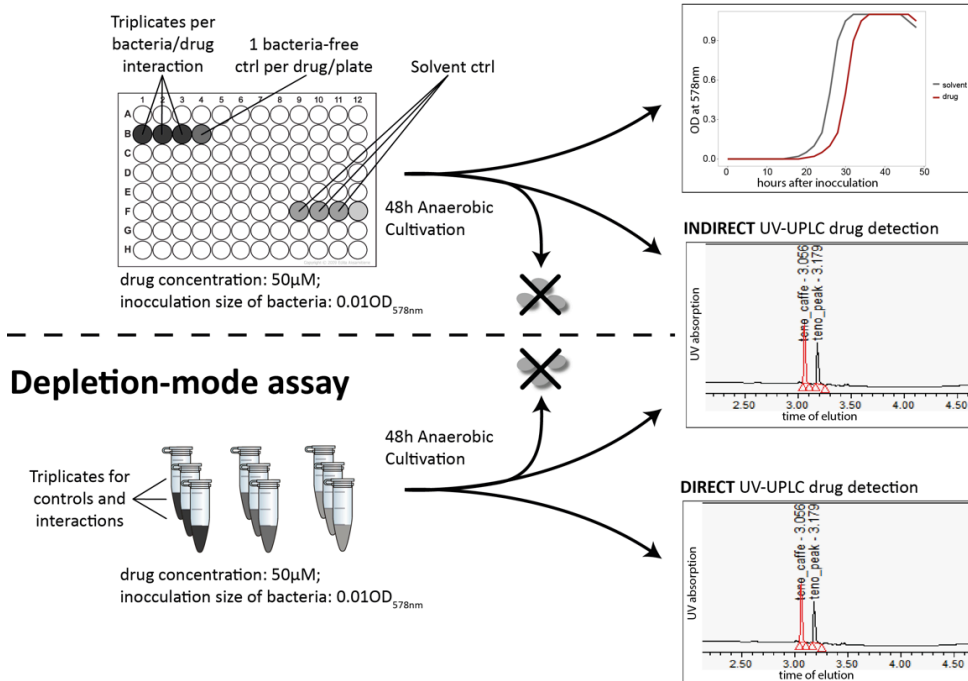


Figure 4: Experimental outline bacteria-drug interaction screen and depletion-mode assay.

Interactions were studied in two ways: first a screen in 96-well plates to find potential bacteria-drug interactions and then a depletion-mode assay of the hits to distinguish between bioaccumulation and metabolism of drug compounds. For indirect drug detection, bacterial cultures were removed by centrifugation and the supernatant was extracted and analyzed.

As bacteria are removed before extraction of the spent medium, drug compounds can be depleted in the screen for multiple reasons: compounds can be bound to bacteria or to secreted extracellular proteins, compounds can be taken up by bacteria and stored inside, or compounds can be metabolized, either completely or biotransformed to a different, maybe less bacteriotoxic form. Whereas the first two effects are bioaccumulations and have implications mainly on drug dosage and maybe bacterial physiology and community dynamics, the latter can create compounds toxic to humans and lead to serious side effects (Zheng et al. 2013). Hence I designed a depletion-mode assay to distinguish between bioaccumulation of drug compounds by bacteria and a biotransformation of drug compounds by bacteria.

In the depletion-mode assay I extract the same culture in two different ways: indirectly by removing first the bacteria using centrifugation and then extracting the drug from the spent media and directly by adding the extraction solvent

directly to the whole culture consisting of bacteria, extracellular components and spent media (Figure 4). Indirect extraction hits would confirm the interaction found in the bigger bacteria-drug interaction screen whereas hits from direct extractions point to a metabolic interaction as the original drug compound is removed from the whole culture. The assay was conducted in 2ml eppendorf tubes with 1ml of medium, and after 48h incubation under agitation samples were split for direct and indirect extraction. This way the same samples could be used to investigate if the drug-bacteria interaction was bioaccumulation or biotransformation of the drug. Each interaction and their controls were assayed at least in triplicates.

Bacteria-drug interaction screen and depletion-mode assay both used a drug concentration of 50 μ M, which in most cases approximates the concentration of one pill (0.02-3mmol) diluted in the volume of the gut (approx. 2.5L). The inoculation OD₅₇₈ of 0.01 and incubation of the bacteria anaerobically for 48h at 37°C was also the same.

The concentrations of all drug compounds in the bacteria-drug interaction screen and depletion-mode assay are determined by UV-UPLC methods. The methods applied here use UV absorption and elution time for identification by comparison to a standard. To be able to measure all selected drugs within one screen with the available instrument, chromatographic conditions needed to be optimized using a maximum of 4 different mobile phases, while one of them needed to be pure water and one an organic phase respectively. Another parameter for optimization was time. For optimal separation of compounds a longer chromatography with a less steep gradient is usually preferable, but would increase the measurement time for the whole screen strongly since approximately 6000 injections were to be expected.

2.2 Results

2.2.1 Drug Selection

The aim of this drug selection was to get a diverse set of drugs for screening, representing different medical indications and structural drug classes, while also selecting the drugs that are causing microbiota-associated side effects. I focused on host-targeted drugs, excluding antibiotics on purpose as those are studied in bacterial context heavily already and in these cases drug-to-bacteria interactions were deemed more likely than bacteria-to-drug interactions. An overview of the drug selection procedure is shown in Figure 5a. In general, information about drug side effects are taken from SIDER database (Kuhn et al. 2016), information about drug pharmacology from DrugBank (Law et al. 2014).

Using the side effect database SIDER (Kuhn et al. 2010), I selected around 90 drugs with a directly gut microbiota related side effect (e.g. bloating, diarrhea) and 120 drugs with a more indirectly gut microbiota related side effect (e.g. arteriosclerosis, weight gain). Furthermore, drugs without any gut related side effects and drugs known to be metabolized by bacteria were added to the selection as controls. From these compounds with a molecular weight higher than 500 Dalton were generally excluded to focus on small molecule drugs. I only selected orally administered drugs as they have a higher chance of passing into the gut in high concentrations compared to intravenously applied drugs. Furthermore, drugs which are taken regularly to treat chronic diseases or in high dosage or have a long half-life and poor bioavailability are also more likely to reach the gut. Finally, an emphasis was put on drugs with high market revenue, thus increasing the relevance of potential findings to a broader population.

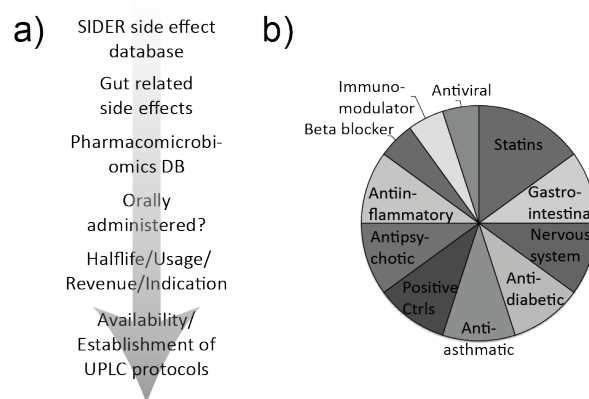


Figure 5: Drug Selection workflow and result.

a) Drug selection started with approximately 1000 annotated drugs from the SIDER side effect database (Kuhn et al. 2016), which were filtered for their gut related side effects. Drug selection was enriched from another database (Saad et al. 2012) for known or suspected interactions with the gut microbiome, before filtered for oral administration and manually curated for overall interest. Final selection was filtered for availability from vendors and establishment of UPLC methods. b) Pie chart classifying selected compounds by disease indication.

After this selection procedure 30 drugs were left, and for 18 of them a chromatographic method with the same buffer system and internal standard could be established. 3 of the final 18 drugs are drugs with known specific bacterial interactions, which serve as positive and negative controls to recapitulate known biological interactions. The selected drugs, the therapeutic indication and the primary reason for selection (e.g. control) are shown in Table 2 and different therapeutic indications covered are shown in Figure 5b.

Table 2: Drugs selected for the Bacteria-Drug Interaction Screen.

ChEMBL ID	Drug	Indication	Acute/chronic	Selection	pKa*	Stock conc.	Solvent
CHEMBL112	Acetaminophen	Minor pain; Fever	acute	Usage widely spread; high dosage	9.38	50 mM	water
CHEMBL1112	Aripiprazole	Psychosis; Depression	chronic	Weight fluctuations; top selling product	7.46	50 mM	DMSO
CHEMBL1751	Digoxin	Arrhythmia	acute	Negative control; only depleted by <i>E. lenta</i>	4.43	50 mM	DMSO
CHEMBL502	Donepezil HCl	Alzheimer's disease	chronic	Long half-life; gastrointestinal side effects	8.62	23 mM	water
CHEMBL1175	Duloxetine HCl	Depression; Anxiety disorders	chronic	Weight gain; top selling product	9.7	100 mM	DMSO
CHEMBL1138	Ezetimibe	Cholesterol reduction	chronic	High % fecal excretion; top selling product	9.7	10 mM	DMSO
CHEMBL1454	Levamisole HCl	Parasitic worm infections; tested for cancer treatment	acute	Withdrawn due to coagulation side effects; in trial as colon cancer drug; bacterial metabolism	6.98	50 mM	water
CHEMBL841	Loperamide HCl	Diarrhea; IBD	both	Usage very common	9.41	50 mM	DMSO
CHEMBL137	Metronidazole HCl	Antibiotic for anaerobic bacteria	acute	Positive control; degradation and growth	3.09	50 mM	water
CHEMBL787	Montelukast Na	Acute asthma; Seasonal allergies	chronic	Gastrointestinal disturbances; chronic use	4.3	50 mM	DMSO
CHEMBL1790041	Ranitidine HCl	Peptic ulcer	acute	Vitamin B12 deficiency; bacterial metabolism	8.08	100 mM	DMSO
CHEMBL193240	Roflumilast	Asthma; COPD	chronic	Gastrointestinal side effects are dose limiting	8.74	10 mM	DMSO
CHEMBL121	Rosiglitazone	Diabetes	chronic	Withdrawn due to increase in heart attacks	6.23	100 mM	DMSO
CHEMBL1496	Rosuvastatin Ca	Cholesterol reduction	chronic	Mechanism of action unclear; top selling	3.8	10 mM	DMSO
CHEMBL1064	Simvastatin	Cholesterol reduction;	chronic	Mechanism of action of statins unclear; top selling product	13.5	100 mM	DMSO
CHEMBL421	Sulfasalazine	Rheumatoid Arthritis; IBD	chronic	Positive control; metabolized by many bacteria	2.4	100 mM	DMSO
CHEMBL483	Tenofovir	HIV	chronic	Flantulence; top selling product	2.07	10 mM	DMSO
CHEMBL1020	Disoproxil Fumarate	Rheumatoid Arthritis,	both	Mild coronary and gastrointestinal side effects	3.5	100 mM	water

*Sources of most basic pKa values are Drugbank (Law et al. 2014), ChEMBL (Bento et al. 2014), and Toxnet (Wexler 2001) databases.

Special emphasis has been put to select proper controls for the bacteria-drug interaction screen to be able to estimate the biological relevance of screening results and compare them to known biology. Metronidazole, sulfasalazine and digoxin are drugs with known and well-described bacterial interaction mechanisms. Metronidazole is an antibiotic against anaerobic bacteria, which upon reduction of its nitro group by bacteria inhibits their growth by introducing DNA double strand breaks. It serves as a control both for growth inhibition and drug depletion. Sulfasalazine is an inflammation inhibitor used in the treatment of ulcerative colitis. It is a prodrug, which becomes active upon cleavage of its azobond by bacterial azoreductases, and thus serves as a control for bacterial drug depletion without strong effects on their growth. As most bacteria possess azoreductases a broad interaction with many bacteria in the screen is expected (Mahmood et al. 2015). Digoxin has been shown to be metabolically modified only by a specific strain of *Eggerthella lenta* (Haiser et al. 2013; Haiser et al. 2014). Thus, it serves as a negative control with no expected interaction with other bacteria than *E. lenta* and provides clues about the specificity of the screen. For levamisole and ranitidine metabolic bacteria-drug interactions have been reported previously as well (Shu et al. 1991; Basit & Lacey 2001), although mechanism and specificity is less clear as for the dedicated controls metronidazole, sulfasalazine and digoxin. This bacteria-drug interaction screen can aid in elucidating specificity in their bacterial interactions and also show the impact of levamisole and ranitidine on bacterial growth.

2.2.2 Bacteria-Drug Interaction Screen

The aim of the bacteria-drug interaction screen was to test if gut bacteria deplete drugs in their growth medium and if this depletion is impacting the growth of the respective bacteria. Drugs and respective controls had been selected as described before (see results 2.2.1), and an UPLC readout after extraction had been established for them (see methods 7.2.). Growth was monitored by OD₅₇₈ readout, every 2 hours for the first 12h and then approximately every 8h until the end of the 48h growth curves. The following describes in short the analysis and

results of the interaction screen. First I will describe results from investigating bacterial drug depletion, and then I will describe the impact of the screened drugs on the growth of bacteria.

Drug depletion in the bacteria-drug interaction screen

UPLC methods had been established to separate drugs from medium compounds and estimate their concentration based on area under the curve. As shown in Figure 6, double injections of the same sample have a high correlation for each respective drug detection method. However, throughout the screen it became apparent that between-sample variability can be high and is mostly dependent on different LC columns. LC columns are susceptible to clogging up and breakdown of their matrix, and need to be exchanged regularly otherwise the LC method loses sensitivity. Peak shape and thus area under the curve of the respective drug peak are highly dependent on the performance state of LC column. Thus, comparing samples measured on different LC columns or even at different measurement times on the same column is difficult.

A way to analyze data from the screen and compare results between different LC columns or between samples measured on the same column but at different usage stages is to focus on one biological replicate at a time, and then compare results from different biological replicates. Samples from one biological replicate of bacteria-drug interaction are on the same 96-well plate, which is measured in one LC run, and thus samples from one biological replicate are measured on the same LC column. Variability within one biological replicate is therefore minimal, but comparatively high between different biological replicates. Thus, I decided to calculate the depletion of bacteria-drug interaction in comparison to its respective control from the same LC run.

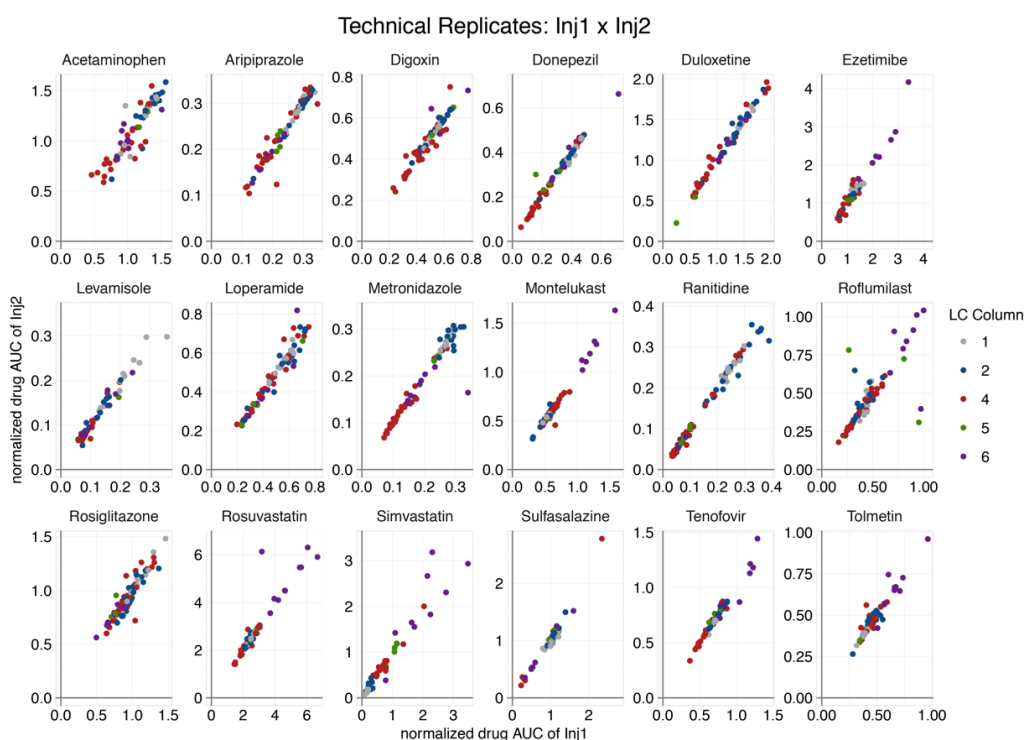


Figure 6: Technical replicates of UPLC injections from bacteria-drug interaction screen. Dots represent double injections of drug control, containing no bacteria. Axes show area under curve of drug peak normalized by peak of internal standard caffeine from UPLC measurements. Throughout the screen different LC columns have been used, indicated by the different colors.

The density distribution of drug depletion in comparison to the replicate-specific control (Figure 7) shows that the positive controls for degradation metronidazole and sulfasalazine are depleted in most interactions. Furthermore, the negative control digoxin is only depleted in its specific interaction with *Eggerthella lenta*. Thus, the bacteria-drug interaction screen is recapitulating expected results and might allow exploration of additional biologically relevant interactions.

Similar to digoxin five other drugs like tolmetin or rosuvastatin have a very small distribution centered on zero. Drugs with this kind of density distribution show no bacterial depletion and might be considered inert in respect to gut bacterial degradation. Acetaminophen and ezetimibe have a narrow distribution around zero as well but show specific and relatively strong interactions with *Escherichia coli* *iAi1* or *Clostridium* as they form a separate distribution. Acetaminophen is completely depleted, ezetimibe to 60%.

Interestingly, 8 of the 15 tested drugs show a shift of their density towards depletion, indicating interactions with many bacteria. These interactions might be relatively minor like in the case of ranitidine or montelukast or strong as in the case of simvastatin. Duloxetine, aripiprazole and roflumilast show a depletion of up to 50% in many cases but almost no example of an interaction that is stronger than that. Levamisole on the other hand seems to have not only weak interactions but also strong interactions with some bacteria, indicated by an additional density around 80% depletion.

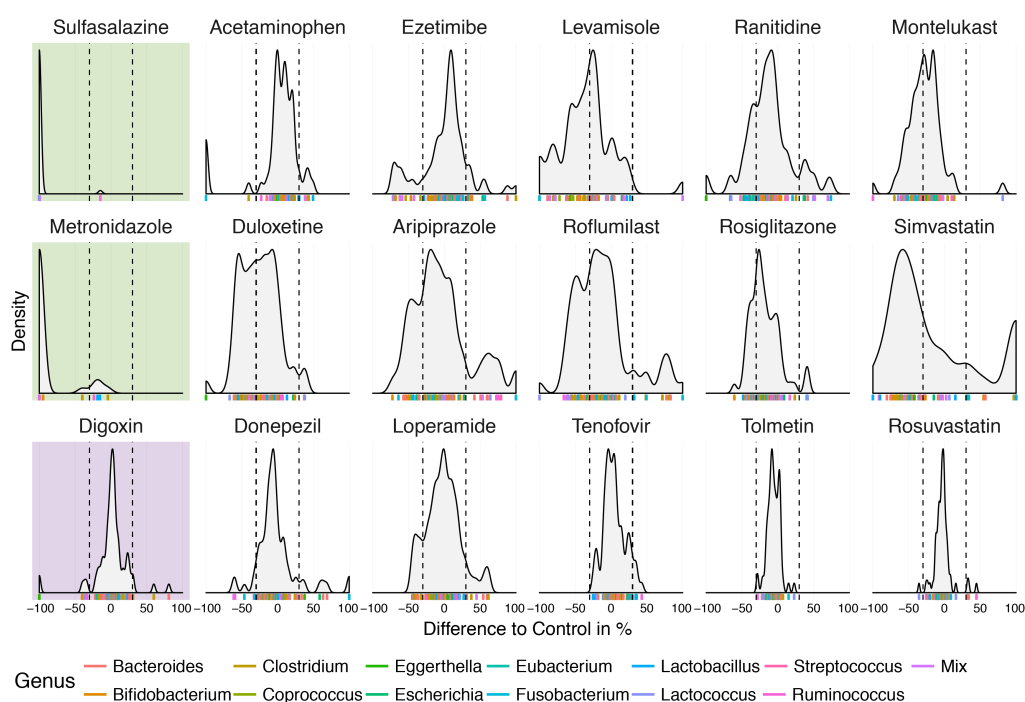


Figure 7: Density distribution of drug depletion in bacteria-drug interaction screen.

Density distribution of drug depletion in comparison to bacteria-free control for each drug respectively. Ticks in the rug below indicate different replicates, colored by genus of the respective tested species. Background colors indicate positive (green) and negative (blue) drug controls for depletion. Dashed lines in each plot mark a 30% threshold for bacteria-drug interaction.

Some drugs show a high variability in their density distribution of depletion, with a shift to the right indicating an increase of drug concentration in comparison to the replicate-specific control. In most cases these seem to be non-repetitive outliers, which might be caused by a failing column. But in some cases like simvastatin, aripiprazole or roflumilast these can be indicative of a problematic LC method and results from these interactions should be considered with caution.

The density distribution of the negative control digoxin shows a biological or screening variability of around $\pm 30\%$. Within this cutoff no bacteria show an interaction with digoxin except the expected interaction with *E. lenta*. Also other drugs like tenofovir or ezetimibe vary this much, having their density distributed mainly between 30% depletion and 30% increase. Thus, I decided to apply a threshold of at least 30% depletion when comparing the different bacteria-drug interactions between biological replicates. A study by Haiser et al. on digoxin showed that a depletion of this degree could lead to implications in mammalian drug efficacy, which gives additional support for this decision (Haiser et al. 2013).

If a bacteria-drug interaction showed at least 30% depletion in both biological replicates, it was considered biologically interesting and is considered a drug depletion hit in this gut bacteria-drug interaction screen. Two tables listing all the specific interactions can be found in the appendix B. In summary, 55 novel interactions were found encompassing 20 different bacterial strains and 11 different drugs. If interactions from simvastatin are excluded because of its poor robustness in LC quality, these numbers change to 49 interactions encompassing 19 bacterial strains.

Growth effects in the bacteria-drug interaction screen

Growth curves were recorded using optical density of the bacterial cultures in each well at a wavelength of 578nm as readout. To correct for noisy growth the maximum OD reached within each growth curve was annotated and manually curated. Noisy growth was often associated with an aggregation of bacteria and can vary across different drug conditions for the same bacterium, but this was not further quantified. After annotation, fold changes in comparison to the respective solvent control were calculated for each bacteria-drug interaction (Student's t test, $\alpha < 0.05$). The reproducibility of significant changes in bacterial growth is high (Figure 8). Many changes are lethal or lead to a strong decrease in maximum OD. However, a few drugs seem to induce better growth than in control conditions.

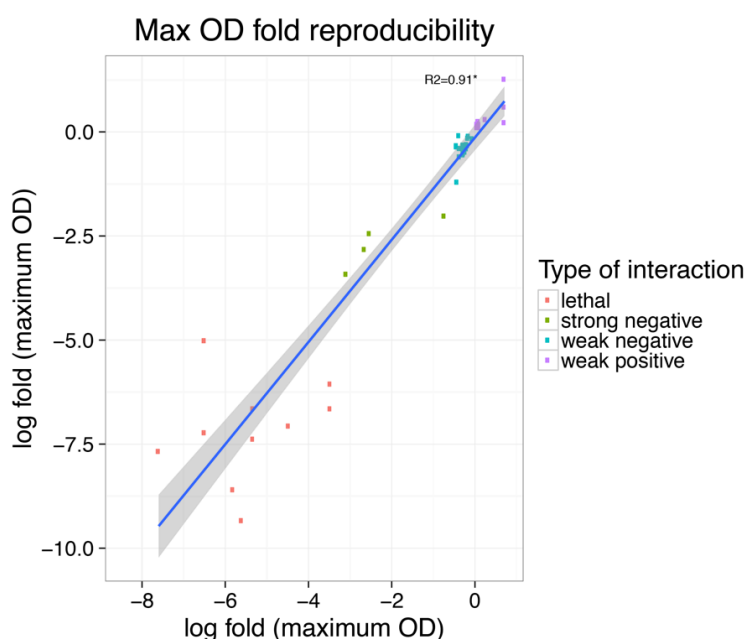


Figure 8: Reproducibility of significant growth fold changes in bacteria-drug interaction screen.

Log₂ fold changes of maximum OD at 578nm adsorption wavelength of two biological replicates for significantly changed interactions (Student's t test, $\alpha < 0.05$; Spearman correlation). Interactions with a log₂ fold change above 0.5 are considered strong. Data analyzed by Sergej Andrejev.

As expected the antibiotic metronidazole shows strong growth inhibition of many bacteria (Figure 9). Still, some bacteria like *E. coli ED1a* or *L. gasseri* are not influenced in their maximum OD by 50 μ M metronidazole. Also as expected when screening non-antibiotics, most drugs show very little effect on the growth of most bacteria. Unexpectedly, quite a lot of interactions tend to induce a weak growth advantage in comparison to the control. A possible explanation is differences in the cytotoxic solvent DMSO, which is 0.5% in the control but depending on the drug compound varies between 0.05% to 0.5% (Table 2). However, this effect is certainly also bacteria-specific as mostly *E. rectale* and *E. lenta* seem to benefit.

Interestingly, loperamide and duloxetine affect the growth of a number of bacteria (Figure 9). Both kill *E. rectale*, negatively affect *E. coli IAI1* and support the growth of *L. lactis* and possibly *B. longum subsp. longum*. Loperamide additionally strongly impacts the growth of *B. longum subsp. infantis*. This is especially interesting as those two bacteria are closely related but show opposite drug responses. Digoxin increase the growth of its degrader *E. lenta*, while weakly inhibiting the growth of *E. coli IAI1* and *R. torques* (Figure 9).

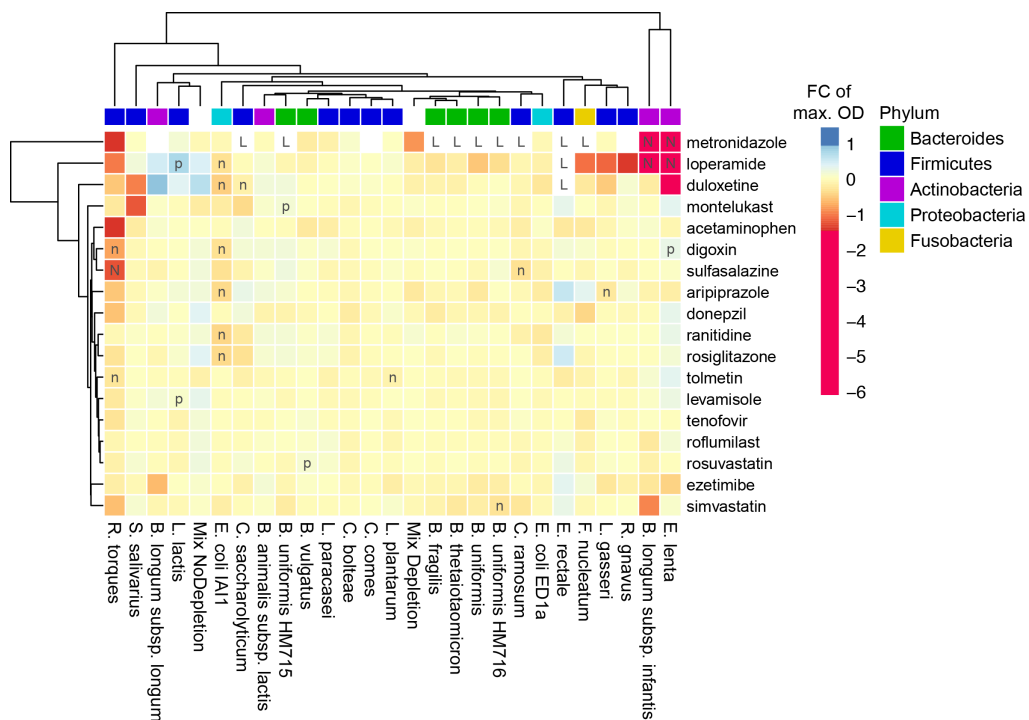


Figure 9: Heatmap of growth effects in bacteria-drug interaction screen.

Letters indicated significant changes (student's t test, $\alpha < 0.05$): L-lethal; N-strong negative; n-weak negative; p-weak positive. Interactions with a \log_2 fold change above 0.5 are considered strong. Clustering based on average linking. Data analyzed by Sergej Andrejev.

Some bacteria like *R. torques* and *E. coli IAI1* are influenced by several drugs (Figure 9). In the case of *E. coli IAI1* the effects are not strong but because its growth curves are very smooth, they are highly reproducible. Interestingly though *E. coli ED1a*, a close relative with comparably smooth growth curves, is not significantly influenced in its growth by any drug. *R. torques* grows slowly and has a comparatively long lag phase. This might increase its sensitivity to drug interactions. *L. lactis* shows significant growth promotion in response to two different drugs, loperamide and levamisole, and is not negatively influenced by other drugs.

In general, clustering of the growth profile reveals Bacteroides tend to have more similar, common drug responses, while phyla like Firmicutes and Actinobacteria are more diverse in their drug response (Figure 9). However, phylogenetic clusters are not strong and even closely related species like *E. coli IAI1* and *E. coli ED1a* or *B. uniformis HM715* and *B. uniformis HM716* do differ in their drug response. Interestingly, the two Actinobacteria *E. lenta* and *B. longum*

infantis cluster closely and have growth profile distinct from all other bacteria in the screen.

Summary

In summary, the gut bacteria-drug interaction screen revealed many potential bacteria-drug interactions, showing that many bacteria potentially deplete drugs from their growth medium as well as that some drugs can impact growth of several bacteria. However, during the screening process it became apparent that those interactions are highly sensitive to environmental conditions like differences in medium composition and anaerobicity. Also technical difficulties around the stability of UPLC measurements throughout screening increased the variability of the screen and cast doubt on some results. Additionally, these results brought about the question if the drug depletion is a metabolic degradation or modification as in the case of sulfasalazine or digoxin, or rather a bioaccumulation of the drug from the medium without any structural modification by the bacteria. Thus, we decided to implement an assay to address this question and to confirm and estimate the robustness of interactions found in the screen.

2.2.3 Depletion-mode assay

The depletion-mode assay was aimed to characterize the hits of the previous bacteria-drug interaction screen to distinguish between bioaccumulation of the drug and bacterial metabolic biotransformation. To reach this aim bacterial cultures were extracted in two different ways: indirectly after removing bacteria by centrifugation, and directly with all bacterial cells and extracellular proteins still present. After extraction, drug concentration was measured by UPLC. For drug depletion, 49 novel interactions were found in the screen encompassing 19 different bacteria and 10 different drug compounds. Of those I tested 28 interactions in the assay, encompassing all 10 drugs and 13 different bacteria strains. As control also known metabolic interactions between bacteria and sulfasalazine and the specific interaction between *E. lenta* and digoxin were tested.

All interactions were tested at least in triplicates, confirmed interactions often repeated additionally.

For the controls all interactions could be confirmed in the depletion-mode assay conditions. Controls showed depletion in indirect and direct extractions (appendix B). 19 of the tested 28 novel interactions showed depletion in at least the indirect extraction, meaning roughly 70% of the interactions from the bacteria-drug interaction screen could be confirmed. For 11 interactions a significant depletion (FDR controlled Student's t-test, $\alpha < 0.05$) was also found in direct extractions. However, applying an additional threshold of at least 20% depletion leaves only 7 interactions with potentially metabolic modifications of the drug compound. Four of these direct interactions are with levamisole, and two with montelukast (Figure 10). While all interactions of levamisole are potentially metabolic modifications, most other interactions of montelukast are bioaccumulations. Only in its interaction with *R. gnavus* and *B. longum subsp. infantis* montelukast was consistently confirmed to be depleted when directly extracted. Levamisole is likely to be metabolically modified by all bacteria depleting it, while montelukast is sequestered or modified depending on the bacterium it interacts with.

The other mentioned direct interaction is donepezil and *F. nucleatum*. Two additional interactions show a significant depletion only in the direct extraction, but not in the indirect extraction. This is usually caused by an unusual high variation in the indirect extraction, and the respective mean is still indicating depletion (appendix B).

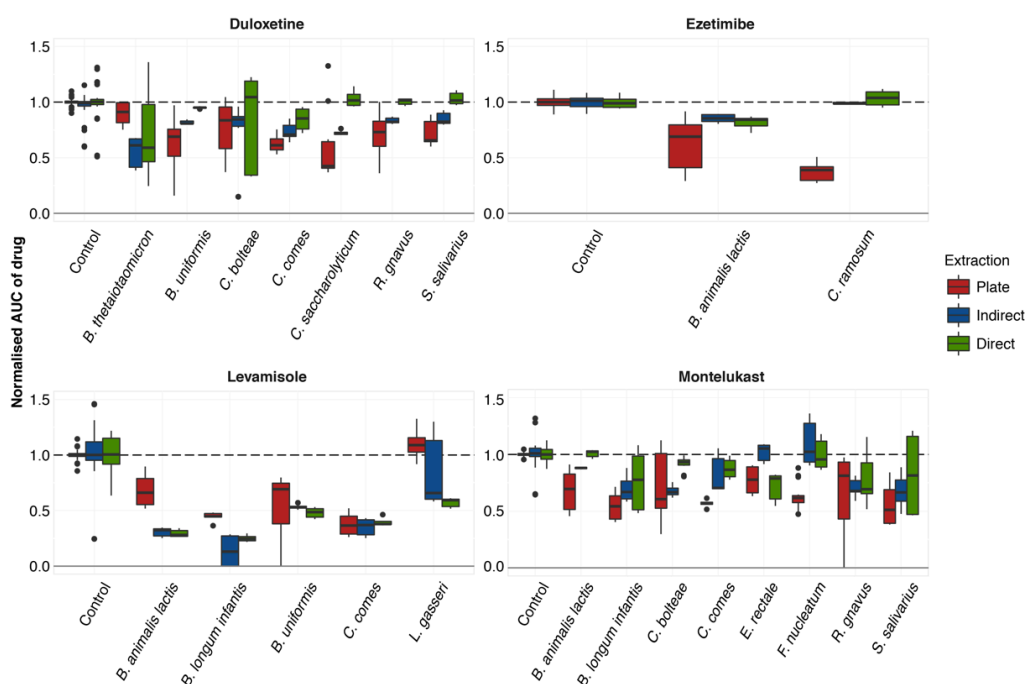


Figure 10: Examples of bacterial drug degradation from the depletion-mode assay.

Boxplots show normalized values for each bacteria-drug interaction and different metabolite extraction methods. Plate: Extractions from bacteria-drug interaction screen; Indirect: Extractions of supernatant in depletion-mode assay; Direct: Extraction of whole bacterial culture in depletion-mode assay. AUC normalized by mean of respective controls from each batch or plate. Dashed line indicates mean of bacteria-free controls.

Ezetimibe showed very specific interactions in the bacteria-drug interaction screen being only depleted by two bacteria: *B. animalis subsp. lactis* and *C. ramosum*. Interestingly, the strong interaction with *C. ramosum* could not be confirmed by the depletion-mode assay, the weaker interaction with *B. animalis subsp. lactis* however shows a weak depletion in both assay extractions as well.

Duloxetine is another interesting case, as it shows eight interactions in the interaction screen, of which five were tested in the depletion-mode assay: *B. uniformis*, *C. bolteae*, *C. comes*, *C. saccharolyticum* and *R. gnavus*. Additionally, I tested *S. salivarius* as it showed a strong tendency for depletion in one biological replicate, and *B. thetaiotaomicron* as a negative control as it showed no depletion in the screen (Figure 10). The depletion-mode assay confirmed all interactions but made clear that most interactions of bacteria with duloxetine are bioaccumulations, as most of the drug can be recovered after extracting the whole bacteria culture. Curiously however, the in the bacteria-drug interaction screen inert interaction between duloxetine and *B. thetaiotaomicron* is now positive, in

indirect and direct extractions. This happens similarly for the interaction of *L. gasseri* and levamisole, which is also inert in the screen but shows depletion in a direct extraction in the depletion-mode assay.

Thus, while roughly 70% of the interactions from the bacteria-interaction screen could be confirmed with the depletion-mode assay and 35% of those are likely biotransformations, it also became clear that the screen is not finding all possible potential bacteria-drug interactions.

2.2.4 Summary: Bacteria-Drug interactions are specific

The bacteria-drug interaction screen and the following depletion-mode assay showed that many bacteria could interact with human-targeted therapeutic drugs. The results from both experiments are summarized in Figure 11. The screen showed that 20 out of 25 tested bacteria deplete at least one drug compound in their growth medium, and 11 out of 15 drug compounds are depleted by at least one bacterium. From 375 tested bacteria-drug interactions 49 revealed a depletion of a drug in the medium, and 22 an effect on the maximum growth capacity of bacteria. The single tested Fusobacterium *F. nucleatum* accounts for 15% of the found drug depletion interactions. Bacteroidetes phyla on the other hand accounts for 24% of the interactions tested, but only for 16% of the depletion interactions found. With the exception of *E. coli IA11*, therapeutic drugs mainly affect the growth of gram-positive bacteria.

Interestingly, only in six interactions the same drug, which is depleted from the medium, affects also the growth of the respective bacterium. Digoxin is promoting the growth of *E. lenta*, montelukast is promoting *B. uniformis* HM715 growth and duloxetine is inhibiting growth of *C. saccharolyticum*. All three drugs, which are depleted by *E. coli IA11*, are also inhibiting its growth. *E. coli IA11* is relatively sensitive to both kinds of drug interaction, especially in comparison to *E. coli ED1a*, which only depletes acetaminophen (Figure 11).

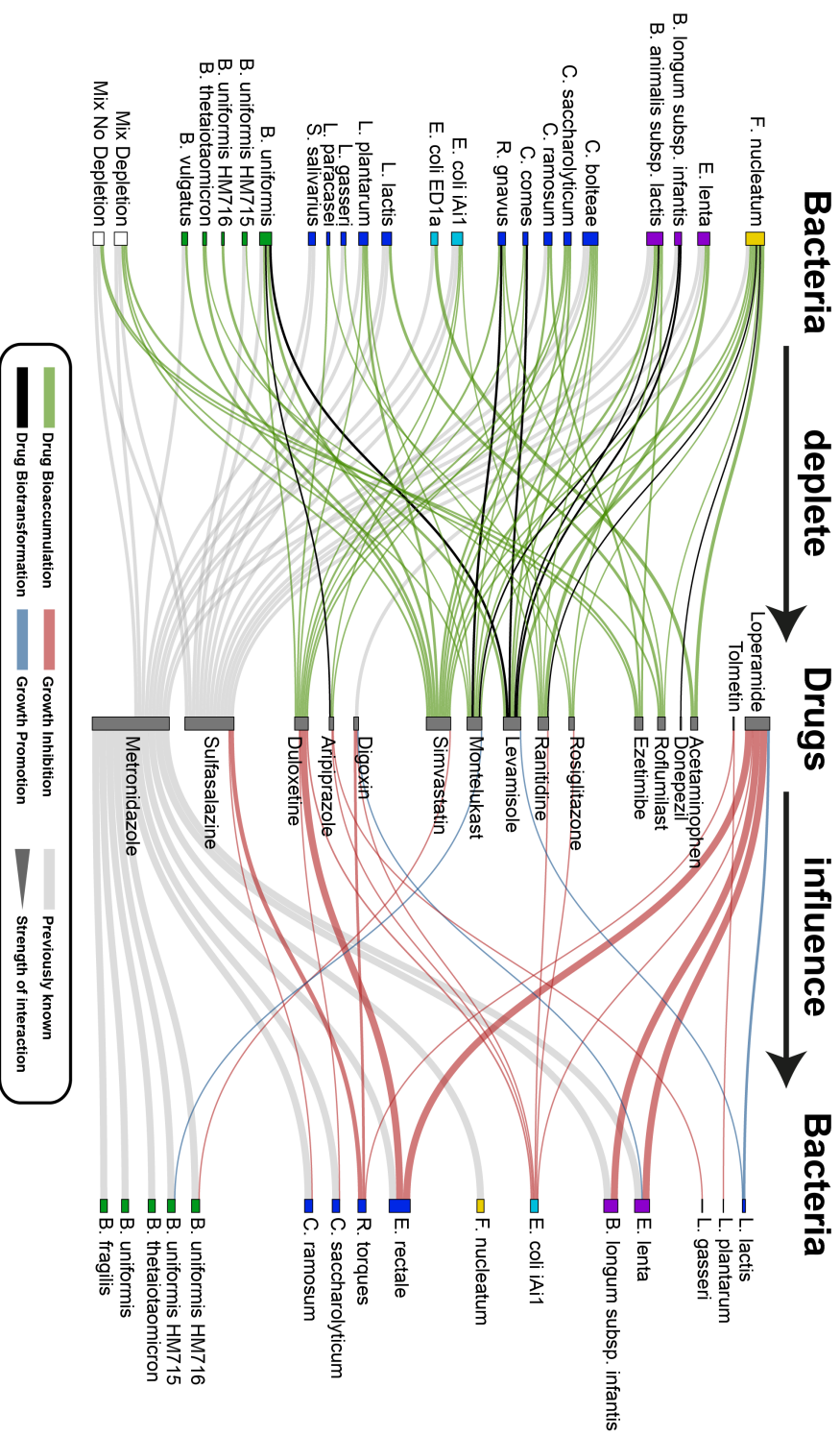


Figure 11: Bacteria-drug interactions.

Bacteria-drug interactions found in the screen. Drug bioaccumulation: at least 30% depletion in both biological replicates. Growth effect: student's t test, $\alpha < 0.05$, hit in both biological replicates. Drug biotransformations found in depletion-mode assay indicated in black. Interactions from bacteria-drug interaction screen only and are not corrected for non-hits from depletion-mode assay as not all hits were tested. Growth data analyzed by Sergej Andreev.

An unexpectedly divergent response when comparing drugs is the bacterial response to simvastatin and rosuvastatin. Both drugs act similarly in humans, but rosuvastatin interacts with no bacterium in any tested way, whereas simvastatin is depleted by ten different bacteria and inhibits the growth of one. Contrasting this finding both duloxetine and aripiprazole, which are both antidepressant drugs, interact with a diverse set of bacteria having an impact both on depletion and growth (Figure 11). Bacteria not interacting with any drug besides controls are *B. fragilis*, *B. longum subsp. longum* and *S. salivarius*. The only drug not interacting with any bacterium is tenofovir.

Besides single bacteria, I also tested two bacterial communities consisting of five members each in the bacteria-drug interaction screen. One community consisted of bacteria showing strong depletion of drugs in the first tested biological replicate of the bacteria-drug interaction screen (Mix Depletion in Figure 11), the other of bacteria showing little to no depletion (Mix NoDepletion in Figure 11). Strikingly, a mix of bacteria not depleting drugs on their own depletes ezetimibe in a community. Bacteria depleting duloxetine or ranitidine on their own lose this ability in community. However, as community composition cannot be interfered from growth alone this might also be caused by a loss of specific depleting bacteria from the community.

2.3 Discussion and Outlook

The aim of the bacteria-drug interaction screen was to test if gut bacteria deplete drugs in their growth medium and if this depletion is impacting the growth of respective bacteria. Additionally, assaying the mode of depletion found in the screen we wanted to address the question if the drug depletion is a metabolic degradation or modification as in the case of sulfasalazine or digoxin, or rather a sequestration or bioaccumulation of the drug from the medium without any structural modification by the bacteria.

In summary, the results from the bacteria-drug interaction screen and the depletion-mode assay show a broad potential of human gut bacteria to interact with human-targeted drugs in a specific manner. Bacterial growth is affected in a drug-species specific manner. Some drugs like loperamide and duloxetine affect a broader bacteria spectrum, and act both as inhibitor and promoter of bacterial growth depending on the bacterial species and strain. Bioaccumulation of drug compounds from the medium might be a common feature of many bacteria-drug interactions, and some drugs like duloxetine or montelukast show a strong tendency to interact with bacteria in this manner. Interestingly, bacteria, which deplete drug compounds from the medium, are usually not affected in their growth by those compounds. Thus, this bacteria-drug interaction screen shows a new dimension to microbiota interactions, which so far has often been overlooked.

However, unfortunately the bacteria-drug interaction screen and also the depletion-mode assay suffered from methodological difficulties comprised of LC hypersensitivity and medium-batch dependent variation. To improve on this kind of screen a growth medium less sensitive to batch-to-batch variations is recommended as well as a LC detection method, which relies less on retention time but more on the inherent features of each compound, like mass spectrometry. Additionally, OD measurements should be performed at least every hour if possible to improve sensitivity in growth curves comparison for the already highly variably growth of natural isolates. This would also allow correcting the strength of drug depletion for the amount of biomass in the culture. I will now discuss specific interactions, which proved to be stable across most conditions, in more detail and then give an outlook for further experiments.

For levamisole and ranitidine metabolic interactions with bacteria have been shown before albeit the specific bacterial players remained unclear (Shu et al. 1991; Basit & Lacey 2001). Bacterial metabolism opens the thiazole-ring of levamisole, and cleaves the N-oxide bond of ranitidine. Shu et al. suggest that mainly Clostridiales and Bacteroides species are responsible for the levamisole ring opening. Besides those species, the bacteria-drug interaction screen suggests

also Bifidobacteria and other Firmicutes like *C. comes* and *L. gasseri* can modify levamisole. Basit and Lacey do not suggest specific bacteria for ranitidine metabolism, but my screen suggests a diverse set of bacteria interact with it except Bacteroides species. However, when replicated in the depletion-mode assay only *F. nucleatum* truly degraded ranitidine, whereas for all other interactions it could be recovered after extracting the whole culture. Thus, different to what the authors suggest in their study, ranitidine metabolism might not be widely common but relatively specific to some microbiota containing the low prevalent species *F. nucleatum* (Li et al. 2014).

Montelukast is a leukotriene receptor antagonist used in the treatment of asthma, with common side effects like diarrhea and inflammation of the gastrointestinal tract. Glucuronidated metabolites of montelukast have been found and it gets mainly eliminated via bile and thereafter feces. However, in rats enterohepatic cycling has not been shown for montelukast (FDA 1997), although colonic metabolites of drug detoxification are expected (Balani et al. 1997). In the bacteria-drug interaction screen and following depletion-mode assay montelukast is sequestered by many bacteria, biotransformed by *R. gnavus* and *B. longum* subsp. *infantis*, and shows a weak growth promoting effect on *B. uniformis* HM715. In a different screen testing for growth effects only, similar species were affected (Lisa Maier (Typas group EMBL), personal communication). This suggests that montelukast is selectively interacting with bacteria. If montelukast is exposed to gut bacteria, its side effects might be caused by bacterial interactions. Bacterial metabolites of montelukast might be toxic to enterocytes causing an inflammation, or it has an effect on the bacterial community structure as a whole leading to diarrhea. The only reported interaction of montelukast with bacteria so far is an increase of bacterial growth in nasal cavity of mice treated with montelukast (Khoury et al. 2006).

Three lipid-lowering agents were tested in the bacteria-drug interaction screen: simvastatin and ezetimibe are commonly given together as standard therapy against high cholesterol, rosuvastatin usually alone. As cardiovascular diseases are highly prevalent in westernized cultures, with almost every fourth

person over the age of 40 in the USA using a statin drug (Gu et al. 2014). All statins act as inhibitors of HMG-CoA reductase in the liver preventing production of cholesterol, whereas ezetimibe likely binds NPC1L1 in gut and liver preventing absorption of cholesterol into systemic cycling. Side effects of simvastatin and ezetimibe are diarrhea and gastritis, whereas the only gut related side effect of rosuvastatin is constipation. Interestingly, ezetimibe and simvastatin are strongly depleted by gut bacteria, whereas rosuvastatin shows no interaction with any. For simvastatin no information about drug modification was obtained. However, it is a prodrug and roughly 60% of its original dose is excreted in feces, making activation in the gut a likely explanation for its gastrointestinal side effects. Colonic metabolism of simvastatin has been shown already (Aura et al. 2011). Additionally, simvastatin and ezetimibe treatment does change relative abundance of *Lactobacillus* species in the gut microbiota of mice (Catry et al. 2015). Thus, especially simvastatin but also ezetimibe might have unfavorable impacts on the microbiota whereas the synthetic statin rosuvastatin might be free of these effects and thus a preferred treatment option for long-term treatment in cardiovascular diseases.

Loperamide is a non-selective calcium blocker used as antidiarrheal treatment. It is not strongly absorbed from the gut, and is thus mainly excreted unmetabolized with the feces. A recent study showed that loperamide could weaken the membrane of gram-negative pathogenic bacteria, but is not as effective as an antibiotic adjuvant against gram-positive bacteria (Ejim et al. 2011). However, in my bacteria-drug interaction screen besides *E. coli IAI1* it mainly affects the growth of gram-positive bacteria. Interestingly, duloxetine has a similar growth effect profile as loperamide but in contrast is depleted by many bacteria. It is classified as an inhibitor of sodium-dependent transporters. Thus, it is possible that duloxetine has a similar destabilizing effect on the bacterial cell membrane but caused by a different underlying mechanism than in loperamide.

To be specific, duloxetine is an antidepressant of the class selective serotonin-norepinephrine reuptake inhibitor (Lantz et al. 2003). Another antipsychotic drug in the screen is aripiprazole, a serotonin reuptake inhibitor with dopaminergic

effects acting on different enzymes than duloxetine (Burriss et al. 2002). Both drugs have side effects like weight fluctuations, constipation and diarrhea. Duloxetine is heavily metabolized and mainly detoxified through the liver, but 20% of its metabolites are excreted in feces. Aripiprazole is also detoxified hepatically, but around 18% of the original dose is excreted unchanged in feces. Both drugs show a range of interactions in the bacteria-drug interaction screen and depletion-mode assay, both affect bacterial growth, are depleted and possibly modified. Other researchers found that aripiprazole and fluoxetine, a drug structurally very similar to duloxetine, and also a number of other antidepressants could act as inhibitors of intracellular bacterial pathogens (Czyż et al. 2014). Additionally, many antidepressants have antimicrobial activity or enhance the action of antibiotics (Munoz-Bellido et al. 2000; Kalaycı et al. 2015). These findings together suggest that interactions between antidepressants and bacteria might be a robust phenomenon. Interestingly, recent metagenomic deep sequencing studies showed that use of antidepressants is associated with a change in microbiota composition (Zhernakova et al. 2016; Falcony et al. 2016). Thus, the observed gastrointestinal side effects of duloxetine and aripiprazole might be caused by bacterial interactions in the gut. Recently, more evidence is accumulating that gut microbiota and depression are linked with each other (Jiang et al. 2015; Foster & McVey Neufeld 2013; Heijtz et al. 2011). Antidepressive medication might play a role in this link, and so far few studies have investigated interactions between medication, disease and the gut microbiota as a whole.

The findings from bacteria-drug interaction screen and depletion-mode assay suggest that sequestration of drug compounds from the medium might be a common feature of many bacteria-drug interactions, and for specific drugs this bioaccumulation might lead to gastrointestinal side effects potentially caused by a change in gut microbiota composition. Thus, further investigations into bacterial drug and native metabolism and drug effects on bacterial communities could help elucidate potential causes of drug side effects. In general, these findings show a new dimension to microbiota interactions, which so far has often been overlooked.

2.4 Clarification of contribution

I designed the bacteria-drug interaction screen in collaboration with Manuel Banzhaf (Typas group, EMBL). Extractions of screening plates were conducted together with Manuel, otherwise I conducted all experiments from the screen and depletion-mode assay in this chapter. I setup the UPLC methods, and analyzed and interpreted the resulting depletion data. Sergej Andrejev (Patil group, EMBL) analyzed the growth curves. Melanie Tramontano (Patil group, EMB) and Lisa Maier (Typas group, EMBL) provided a lot of feedback and discussions for data interpretation and screen/assay optimization.

3 Duloxetine affects bacterial growth and induces changes in bacterial communities

In this chapter I investigate the effects of one drug compound, the widely used antidepressant duloxetine, on a synthetic bacterial community. I first explain why I selected duloxetine and why I test in a synthetic community. After explaining the experimental set up, I describe the growth effects of duloxetine on bacteria grown in monoculture and then its effect on bacterial community composition. In the end, I discuss potential explanations derived from ecological principles for a change in bacterial community composition upon duloxetine exposure and suggest further possibilities for research.

3.1 Introduction

3.1.1 Why investigate bacterial interactions with duloxetine?

Results from the bacteria-drug interaction screen and depletion-mode assay suggest that sequestration of drug compounds from the medium might be a common and specific feature of many bacteria-drug interactions. Additionally, the mixed bacteria communities tested in the screen suggest that bacteria might behave different in community than in monocultures. To gain insights into how drug bioaccumulation would impact at the level of a community, I decided to focus on the specific example of duloxetine. Findings from my bacteria-drug interaction screen and from literature suggest that interactions between antidepressants and bacteria might be a robust phenomenon (Zhernakova et al. 2016; Czyż et al. 2014; Munoz-Bellido et al. 2000). Furthermore, the gut microbiota plays an important role in the development of depression and other mental diseases (Jiang et al. 2015; Foster & McVey Neufeld 2013). Antidepressive medication might play a role in this link. Side effects of antidepressive medication often include changes in the weight of patients (Dent et al. 2012), a morbidity

often associated with the microbiome as well (Musso et al. 2011). So far only few studies have investigated interactions between medication, disease and the gut microbiota as a whole for any disease, diabetes and metformin treatment being a well researched exception (Forsslund et al. 2015).

In the bacteria-drug interaction screen described in the previous chapter two antidepressants, duloxetine and aripiprazole, were investigated, both showing several interactions with gut bacteria. In the screen, the SSRI duloxetine is sequestered by nine different bacterial strains, one of them likely transforming it, and inhibits the growth of three strains, one of them also sequestering it (Figure 11). The partial dopamine agonist aripiprazole is sequestered by three different strains, all of which also sequester duloxetine, and inhibits the growth of two other strains (Figure 11). Preliminary experiments showed that duloxetine is also sequestered when exposed to bacteria resting in PBS, but not by the spent medium of bacteria usually sequestering duloxetine. Preliminary experiments with aripiprazole showed that its interaction in many cases is sensitive to changing environmental conditions like differences in oxygen or medium composition, and additionally its LC method was instable. Thus, I decided to subsequently focus on gut bacterial interactions with duloxetine. A detailed introduction to duloxetine is given in the introduction chapter 1.6.1 on page 29.

3.1.2 Why investigate interactions in a synthetic community?

A natural bacterial community is usually complex and often not completely defined. In case of the human gut microbiota the community can consist of up to a thousand bacterial strains (Human Microbiome Project Consortium. 2012). This complexity is hard to disentangle as specific members are hard to manipulate and other community members can counterbalance specific bacterial interactions. In an experiment the final read-out from a community is thus an integral of all interactions taking place within the community. To address this challenge a simplified synthetic community can guide the discovery of underlying principles and inter-species dependencies. If communities are constructed with isolates from

a natural system, the evolved co-dependencies can often be preserved (Stadie et al. 2013; Ponomarova & Patil 2015).

One way to investigate bacterial community dynamics is in the context of adaptive laboratory evolution (ALE). ALE can be as easily implemented with communities as with single strains, and usually involves repeated transfers of inoculum from a growing culture into fresh medium with the same or sequentially stronger selective pressure. ALE is typically used to explore evolutionary dynamics of single strains towards a specific or unspecific selective pressure (Lenski et al. 1991). It is a common tool especially in microbial synthetic bioengineering to adapt a genetically modified organism like yeast or *E. coli* to a production environment and to investigate the cause of those adaptations (Dragosits & Mattanovich 2013). However, it is also increasingly used in basic science to investigate co-dependencies in evolving communities. Especially structured environments like biofilms with distinct evolutionary pressures can be well investigated with this approach (Martin et al. 2016). A selective and distinct evolutionary pressure like drug exposure should allow a fast adaptation of the community towards the pressure by selecting for less affected members or members beneficial for the whole community. In a long-term experiment genetic adaptations might additionally occur.

3.1.3 Aims and Experimental outline

To investigate whether duloxetine has an effect on bacterial communities, I decided to assemble a synthetic community consisting of bacteria sequestering duloxetine and bacteria being affected in their growth by duloxetine. These communities were exposed to duloxetine and as control to its solvent DMSO respectively (Figure 12). Every 48h, an inoculum of the evolved community was transferred into fresh medium containing either duloxetine or DMSO. The remaining bacterial community from each transfer was pelleted and subjected to 16s barcode sequencing to estimate the relative abundance of community members. Additionally, the duloxetine concentration in the bacteria-free spent medium was determined. Thus, the experiment allowed following the

establishment of a potentially stable community. From similar experiments within our research group we expected a relatively stable community within five transfers, whereas stochastic population bottleneck and founder effects seem to dominate the first two transfers.

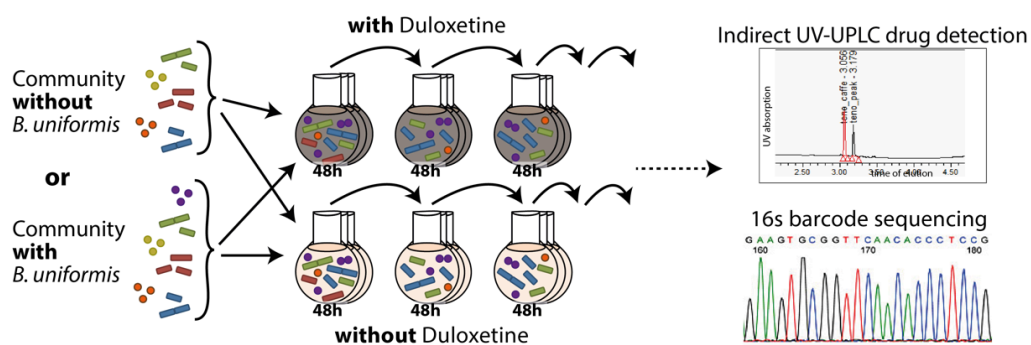


Figure 12: Community assembly assay outline.

Two different communities were tested in a community assembly assay: a five-member bacterial community without *B. uniformis* and a six-member community with *B. uniformis*. Communities were inoculated with a total OD₅₇₈ of 0.01 in GMM with or without duloxetine but respective solvent. An inoculum from the evolved culture was transferred every 48h to fresh media conditions. Each culture was 16s barcode sequenced and the duloxetine remaining in the medium was assessed.

I designed two different bacterial communities to not only assess the effect of duloxetine on a community, but also to investigate if duloxetine bioaccumulation can affect the community structure. Duloxetine bioaccumulation by community members could potentially aid in the survival of bacterial species, which are growth sensitive to duloxetine. One of the bacteria depleting duloxetine the strongest was *B. uniformis*. It is highly prevalent and abundant in the gut microbiome (Qin et al. 2010; Li et al. 2014) and has been associated with improved metabolic functions of the microbiome (Gauffin Cano et al. 2012). Thus, I designed a community with and without *B. uniformis* (Figure 12). Other community members sequestering duloxetine consisted of *S. salivarius* and *B. thetaiotaomicron*, the latter is potentially additionally modifying duloxetine. As a species inhibited in growth by duloxetine *E. rectale* was included in the community. *L. gasseri* and *R. torques*, which so far had not shown any interactions with duloxetine, were added to increase the likelihood that a community consisting of more than one member species was formed. The species selection represents the main phyla in the gut, Bacteroidetes and Firmicutes, and are distinguishable by 16s barcode sequencing.

Duloxetine bioaccumulation and biotransformation by single species had been assessed with the bacteria-drug interaction screen and depletion-mode assay as described in the previous chapter. However, as techniques for growth readout had improved in the lab and in the screen only one concentration of duloxetine was assessed, I decided to also assess the growth sensitivity of synthetic community members to duloxetine. A better characterization of bacterial response to duloxetine can reveal more details about differences between bacterial species and might allow an easier interpretation of results from the community assembly assay.

3.2 Results

3.2.1 Growth effects of duloxetine

The aim of the duloxetine dilution growth curves was to estimate the sensitivity of bacteria towards duloxetine, which were later used in the community assembly assay. Sensitivity is recorded as concentration inhibiting 50% of the effective growth (IC₅₀). The strongest effect on growth by duloxetine was usually seen around the inflection point of the exponential growth phase. To approximate this point in each bacterial species, I first estimated the time point at which the bacteria not exposed to duloxetine reached half the maximum OD. For this time point I recorded the respective OD of all duloxetine exposed growth curves and fitted a local regression from which I estimated the IC₅₀ (Figure 13). *B. thetaiotaomicron*, *B. uniformis*, *L. gasseri* and *R. torques* all have an IC₅₀ around 100 μ M for duloxetine. *S. salivarius* is more sensitive with an IC₅₀ of 40 μ M, and *E. rectale* is the most duloxetine sensitive species with an IC₅₀ around 30 μ M.

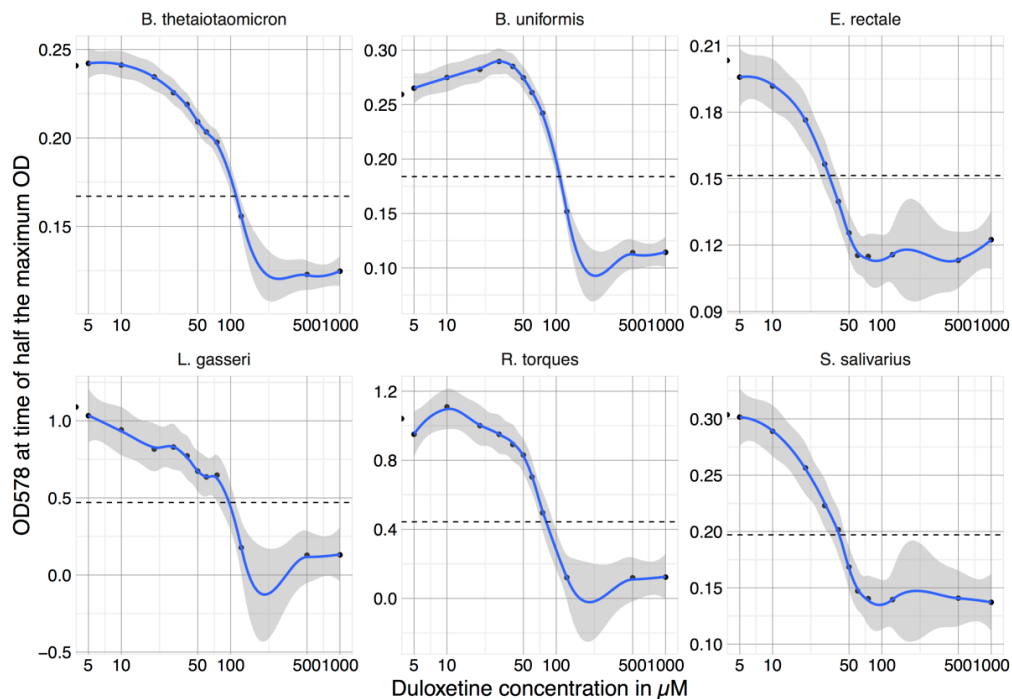


Figure 13: IC50s for duloxetine.

Dilution series of duloxetine in 1% DMSO. Underlying growth curves taken for 24h in GMM in triplicates. OD at half maximum OD time point of control used as effect response. Dashed line indicates 50% of half-maximum OD, to estimate corresponding inhibitory concentration (IC50). Curves are fitted with R function “loess”, span parameter equals 0.5.

Sensitivity to a drug is not always reflected only in a shift in exponential growth but also in a prolonged lag phase or a reduced maximum OD (Figure 14). The community assembly assay concentration is 50 μM duloxetine. At this concentration only *B. uniformis* is not affected in its growth, all other bacteria have growth deficiencies. As expected from the IC50, *E. rectale* is strongly delayed in growth. Interestingly, it recovers half of the growth when reducing the duloxetine concentration by just 20% to 40 μM . Even though *B. thetaiotaomicron* has a much higher IC50, its growth rate is affected already at the lower duloxetine concentration of 50 μM . Some bacteria besides being affected in lag or exponential phase have a noisier growth with duloxetine than without, e.g. *L. gasseri* or *R. torques*. This seemed to correspond to a stronger aggregation of bacteria in the culture as observed by eye. However, this effect could not be quantified so far.

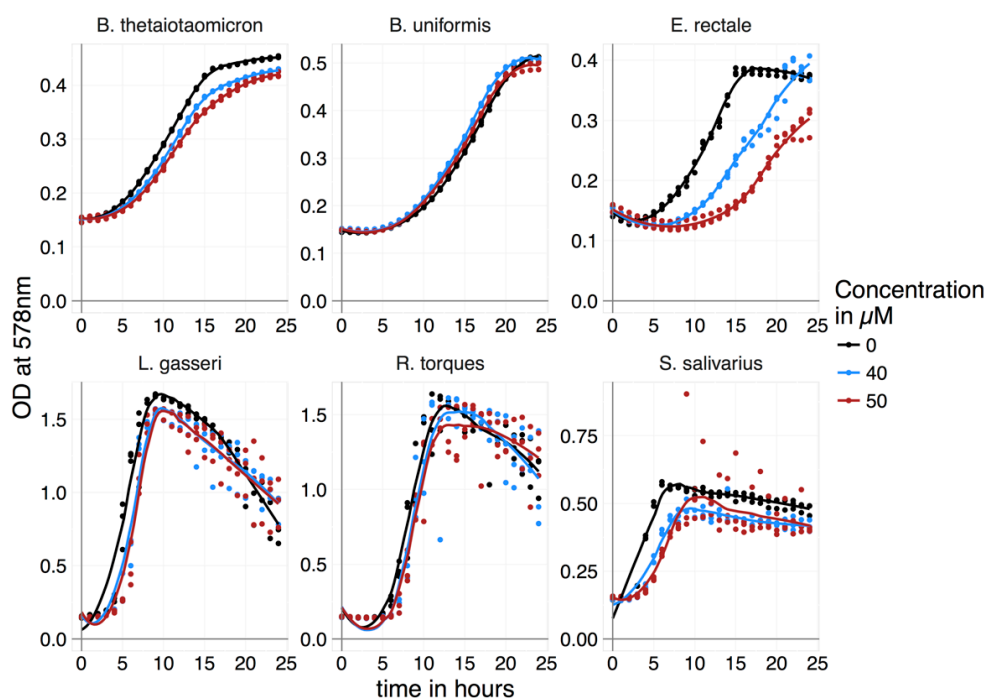


Figure 14: Growth curves with duloxetine.
 24h growth curves in GMM with respective concentration of duloxetine with 1% DMSO as solvent. Curves fitted for triplicates with local regression using R's loess function.

3.2.2 Bacterial community shifts induced by duloxetine

The aim of the community assembly assay was to investigate first whether duloxetine has an effect on bacterial community composition, and second whether bacteria sequestering duloxetine modify this effect. The presence of duloxetine in the medium increases the community diversity in both bacterial communities (Figure 15). Without duloxetine, two or three bacteria respectively dominate the community from the second transfer on, whereas with duloxetine four or five bacteria respectively coexist in the community. Interestingly, in both communities *E. rectale*, the bacterium most sensitive to duloxetine, is relatively abundant in the presence of duloxetine, whereas without duloxetine it is superseded in most transfers. Also *L. gasseri* profits from the presence of duloxetine, whereas *R. torques* is below detection limit in any bacterial community.

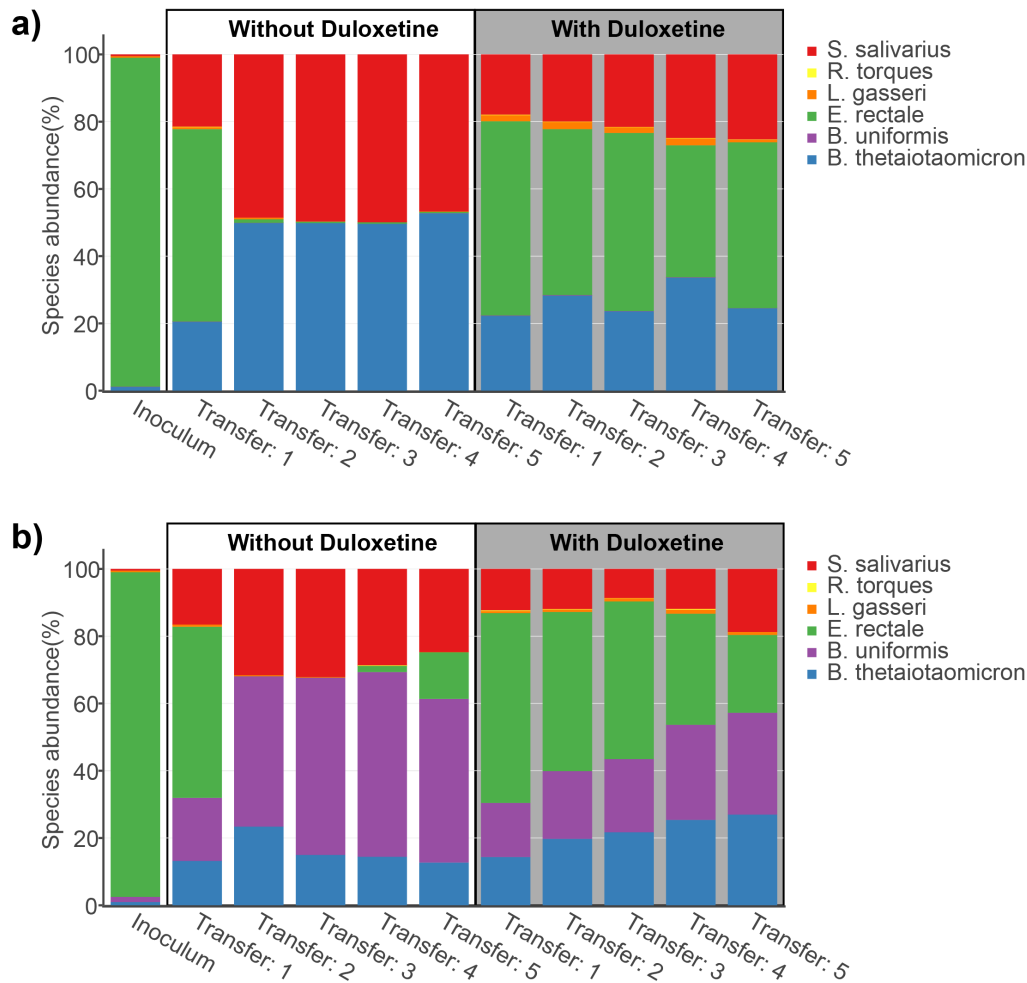


Figure 15: Community composition of duloxetine assembly assay.

Species abundance after transfer and 48h growth in bacterial community with and without duloxetine. Mean of relative abundance from triplicates after 16s DNA sequencing. a) Community of five bacteria, without strongly sequestering species *B. uniformis*. b) Community of six bacteria, with strongly sequestering species *B. uniformis*. DNA extraction and 16s library preparation by Melanie Tramontano (Patil group, EMBL). Analysis and visualization by Yongkyu Kim (Patil group, EMBL).

In general, the community without *B. uniformis* (Figure 15a) seems to be more stable over time than the one with *B. uniformis* (Figure 15b). In bacterial communities with *B. uniformis*, changes in relative composition can be observed during all transfers whereas without it a relatively stable state seems to be reached after the first transfer. Interestingly, in the community with *B. uniformis* not exposed to duloxetine, *E. rectale* seems to regain community membership after being depressed below detection limit in transfer 2 and 3 (Figure 15b). In the same community exposed to duloxetine *E. rectale* is slowly diminishing in relative abundance across all transfers. The opposite is true for *B. uniformis*. It slowly

diminishes in relative abundance without duloxetine, while gaining in the community exposed to duloxetine.

Duloxetine is depleted in all transfers except for the first transfer of the community without *B. uniformis* (Figure 16a). Duloxetine is always stronger depleted in the community with *B. uniformis* than without it. This corresponds to a higher fraction of duloxetine sequestering bacteria (*B. thetaiotaomicron*, *B. uniformis*, *S. salivarius*) in the community with *B. uniformis* than in the one without it (Figure 16b).

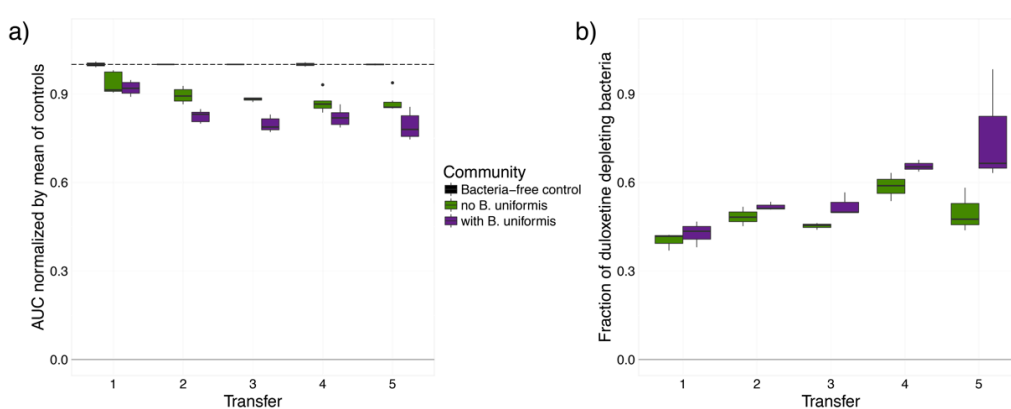


Figure 16: Duloxetine depletion in community assembly assay.

a) Duloxetine depletion (indirect extraction) at the end of each transfer of bacterial community. Dashed line indicates mean of control. b) Percentage of bacteria sequestering duloxetine in each transfer, as assessed with 16s DNA sequencing. All interactions tested in triplicates.

3.3 Summary and Discussion

The aim of these experiments was to investigate whether duloxetine and duloxetine sequestering bacteria have an effect on bacterial community composition and whether this effect could be explained by the effect duloxetine has on bacteria grown in monocultures. It was found that duloxetine induced a higher diversity within the tested bacterial synthetic communities. Unexpectedly, *E. rectale*, the community member most sensitive to duloxetine, showed a stronger survival in bacterial communities exposed to duloxetine. Additionally, communities with duloxetine-sequester *B. uniformis* seem to be less stable over

transfers, potentially caused by *E. rectale* and *B. uniformis* competing with each other.

A shift induced by xenobiotics has been observed before in host-mediated communities (Cai et al. 2015; Catry et al. 2015; Davey et al. 2013) and as such a shift in community composition upon duloxetine exposure was to be expected. A change in bacterial community might be associated with side effects of duloxetine, such as weight fluctuations (Bahra et al. 2015). Changes in gut microbiome have also been implicated in development of depression and other mental diseases (Sharon et al. 2016). As literature regarding this has been reviewed in the chapter before and in the introduction to this chapter, I would like to focus in the following on the ecological interpretation of the conducted experiments.

Ecological theory can give ideas as to the reason of the change in bacterial community composition (for an review on ecological theory in microbiology see Hibbing et al. 2010). The stress-gradient hypothesis suggests that competitive interactions between species dominate in resource-rich environments (competitive exclusion principle) whereas facilitative, complementary interactions are often seen in stressful environments. Here, they enhance the realized niches of species, which cannot persist in highly competitive environments, e.g. through cross-feeding or motility (Maestre et al. 2009; Malkinson & Tielbörger 2010) For bacteria this theory has been successfully tested in soil communities (Li et al. 2013).

All bacteria except possibly *B. uniformis* are stressed by duloxetine (Figure 14). Additionally, subinhibitory concentrations of xenobiotics have been shown to change the metabolism or behavior of bacteria (de Freitas et al. 2016; Cecil et al. 2011). Thus, some of the community members might secrete additional nutrients or change their metabolism or behavior otherwise, which reduces competition and hence induces a better survival of *E. rectale* and *L. gasseri*. Additionally, *E. rectale* recovers most from little changes in duloxetine concentration (Figure 14). In both duloxetine treated communities duloxetine sequestering species are the majority and twenty to thirty percent of duloxetine is sequestered from the medium. Thus, *E. rectale* might recover the most from a disturbance of their

bacterial physiology by the presence of duloxetine-depleting bacteria and gain a competitive advantage, but only in presence of duloxetine.

In structured environments like biofilms but also non-shaking lab cultures differences in competition can be observed in comparison to free-living or well mixed communities (Hibbing et al. 2010). Structured environments allow for different niches to be formed, as gradients of nutrient and other supplies like oxygen establish. Additionally, a common good trait like siderophore production for iron scavenging or other excreted enzymes like proteases mainly benefits closely related neighboring cells (Hibbing et al. 2010).

The experiment was set up as a non-shaken culture, furthermore duloxetine potentially induces aggregation. A noisier growth with duloxetine than without was observed for *L. gasseri* or *R. torques* in monocultures, and corresponded to a stronger aggregation of bacteria in the culture as observed by eye. Thus, aggregation and consequently escape from competition by occupying a new niche might contribute to the survival of *L. gasseri* in the duloxetine treated samples. *E. rectale* could be similarly affected, although the effect in monocultures is not as pronounced as for *L. gasseri*. *Bacteroides* cultures in turn are well dispersed in monoculture and duloxetine seems not to induce aggregation in these species. Thus, they might not gain an advantage in niche specialization.

It has also been shown that bacteria do act very differently in community than in monoculture (Chiu et al. 2014; Lawrence et al. 2012). Within a community a shift in metabolic state and hence a shift in the member species' sensitivity towards duloxetine is conceivable. Therefore, a prediction of community composition from monoculture growth data is not always possible.

To test some of the suggested hypothesis, new experiments should be designed. The community assembly assay showed to be a suitable and reproducibly robust tool to investigate bacterial communities. However, a five or six member community might still be too large to disentangle the underlying interactions. To test whether duloxetine and duloxetine sequestering bacteria have an effect, a three-member community could be designed. One duloxetine sensitive species, e.g. *E. rectale*, one sequestering species, e.g. *B. uniformis*, and one not

affected species e.g. *B. vulgatus* could be used to test duloxetine effects. Potentially, *B. uniformis* can be substituted in a community with its not-sequestering strain *B. uniformis* HM715. Besides using a smaller community, treatments in evolved communities could be reverted after five transfers. A duloxetine-exposed evolved community should revert to a state similar to non-exposed communities as soon as the stress is removed. Additionally, evolved communities as a whole could be tested for duloxetine sensitivity and thus show whether tolerance can evolve as a community trait.

Another important aspect in the causes of a shift in community composition is the shift in metabolic state of the affected bacteria. If we can show how affected bacteria itself change and potentially how they change their respective environment, we could start to understand how they impact a community. For example, if duloxetine is blocking import of certain nutrients or induces excretion of nutrients, this might explain why *E. rectale* unexpectedly gains a growth advantage in community as to monoculture alone. Thus, another potential route to be explored experimentally is investigation of the metabolic response towards duloxetine exposure.

In conclusion, duloxetine induces a consistent change in microbial communities. This change cannot be fully explained by the observed behavior of bacterial species in monoculture. Duloxetine-sequestering bacteria potentially additionally alter this change, as duloxetine bioaccumulation is stronger in communities consisting of more duloxetine sequestering bacteria. However, as all tested communities consist of duloxetine-sequestering bacteria before further conclusions are made additional experiments should be undertaken.

3.4 Clarification of contribution

I planned and conducted the duloxetine dilution growth curves assay and the community assembly assay. For the dilution curves I also did the computational analysis and visualization. For the community assembly assay, I extracted DNA from the bacteria pellets together with Melanie Tramontano (Patil group, EMBL), subsequently Melanie prepared the 16S DNA library for sequencing in the EMBL GeneCore facility. Yongkyu Kim (Patil group, EMBL) analyzed and partially visualized the resulting data. I analyzed and visualized data from duloxetine depletion.

4 Human gut bacteria change their native metabolism upon duloxetine exposure

In this chapter I investigate the change in the extracellular metabolome of two bacteria exposed to duloxetine. I explain why and how I use untargeted metabolomics approaches, before describing the experimental set up consisting of an NMR and a mass spectrometry approach. In the result section I first describe the NMR experiment, give a short summary and explanation as to why I moved to a more sensitive mass spectrometry approach, and then describe the results from this approach in detail. In the end, I discuss different explanations for the upregulation of metabolic features from the purine pathway before concluding a likely oxidative stress response.

4.1 Introduction

4.1.1 Why investigate bacterial duloxetine metabolism?

Results from bacteria-drug interaction screen and depletion-mode assay (Chapter 2) suggest that bioaccumulation of drug compounds from the medium might be a common and specific feature of many bacteria-drug interactions. The community assembly assay (Chapter 3) indicates that duloxetine does affect bacteria in community and change their behavior resulting in differences in composition. Bioaccumulation of duloxetine affects the bacterial community additionally. Detailed reasons why I focused on the antidepressant duloxetine are outlined in the introduction to the previous chapter. In short, gut bacterial interactions with duloxetine, both for depletion and growth impairment, were plenty and reproducible. In general, antidepressants are of great interest as changes in gut microbiome composition have been associated with depression (Jiang et al., 2015) and a study found changes in gut microbiome composition associated with antidepressive treatment (Zhernakova et al., 2016). On top,

bioaccumulation can change the pharmacokinetics and efficacy of drugs (Niehues & Hensel 2009; Pierantozzi et al. 2006). To study the molecular basis of bacteria-duloxetine interactions, I focused on two bacteria, *B. uniformis* and *C. saccharolyticum*. Because metabolites are the intermediates or end products of multiple enzymatic reactions and therefore are the most informative proxies of the biochemical activity of an organism, I focus first on the metabolic interaction between bacteria and duloxetine (Alonso et al. 2015; Reaves & Rabinowitz 2011). Investigating changes in the metabolic state of the bacteria upon drug exposure can aid in generating hypothesis about the way duloxetine and bacteria interact.

4.1.2 How to investigate bacterial metabolism: Untargeted metabolomics

Untargeted metabolomics can be a great approach to explore a potential uncharacterized interaction and generate hypotheses about its underlying mechanism. In contrast to targeted approaches untargeted metabolomics avoids the need for a prior specific hypothesis on a particular set of metabolites (Alonso et al. 2015). In particular, untargeted metabolomics is a useful approach to investigate microbial drug interactions and mammalian-bacterial co-metabolism (Nichols et al. 2016). Many potential features can be reviewed at once and then promising candidates can be characterized further by isolation and identification.

Untargeted metabolomics studies are characterized by the simultaneous measurement of a large number of metabolites or potential metabolic features from each sample. Therefore, there is a need to use high performance bioinformatics tools (Booth et al. 2013). One of the most critical processes in untargeted metabolomics studies is the identification of metabolites, which is a prerequisite to relating the quantitative metabolomics data to its underlying biochemical role (Alonso et al. 2015). Identification of metabolites is regularly done by comparing the recorded spectra or masses to data found in public libraries like KEGG (Kanehisa et al. 2012) or ECMDB (Guo et al. 2013).

Untargeted metabolomics is commonly implemented with NMR spectroscopy or mass spectrometry (Alonso et al. 2015). NMR allows direct structural

elucidation of potential metabolites and their relative concentration, but is limited in its sensitivity as well as by difficulties in working with complex multicomponent mixtures. Advantages of NMR spectroscopy are that it is not selective for any compound, all compounds are measured at once and amounts estimated are truly relative to each other, which means intensities of different peaks are comparable (Alonso et al. 2015). Mass spectrometry is a powerful method as it is very sensitive and allows quantification of many small compounds in the same run (Fuhrer & Zamboni 2015). However, identification of compounds is harder than in NMR spectroscopy as only masses and their elution time from LC can be measured and very little information about the chemical structure of the compound can be assessed (Alonso et al. 2015). Thus, true identification of compounds can only be achieved by comparison to standards. With an exact mass it is possible to narrow down potential compounds to a few sum formulas, which might correspond to only a handful of compounds. This is the reason mass accuracy is an important factor in mass spectrometry (Fuhrer & Zamboni 2015). Also exact relative quantification can be problematic, as different molecules have different ionization efficiencies, thus also true quantification can only be achieved in comparison to a standard (Alonso et al. 2015).

4.1.3 Experimental Outline and Aims

I first used an NMR spectroscopy approach to investigate potential drug metabolites, which I later complemented with a more sensitive mass spectrometry approach (Figure 17). The aims of all untargeted metabolomics approaches were first to confirm bacterial drug depletion and thus to confirm the interaction of the bacteria-drug pairs found in the interaction screen (see chapter 2), which had so far only been assessed by a UPLC-UV method. Secondly, untargeted metabolomics was used to aid in generating hypothesis about the way drug and bacteria interact, based on an observable shift in the bacterial metabolome or on the appearance of potential drug metabolites.

Besides a mix of bacteria for an NMR study, two bacteria were selected for further in depth characterization of interaction with duloxetine. *B. uniformis* is

gram negative bacterium of the phylum Bacteroidetes with a high abundance and prevalence across healthy human microbiomes (Li et al. 2014). In the bacteria-drug interaction screen, it showed a strong sequestration of duloxetine but was not affected in growth (Figure 11). *C. saccharolyticum* is a gram positive bacterium of the phylum Firmicutes, the other phylum prevalent in the gut. It is less abundant but as prevalent as *B. uniformis* in the microbiome of healthy human individuals (Li et al. 2014). In the screen, *C. saccharolyticum* also strongly depletes duloxetine from the medium, but different to *B. uniformis* it is affected in its growth (Figure 11). The duloxetine IC₅₀ values are 100 μ M and 40 μ M for *B. uniformis* and *C. saccharolyticum* respectively (see Figure 13 for *B. uniformis*, appendix C for *C. saccharolyticum*).

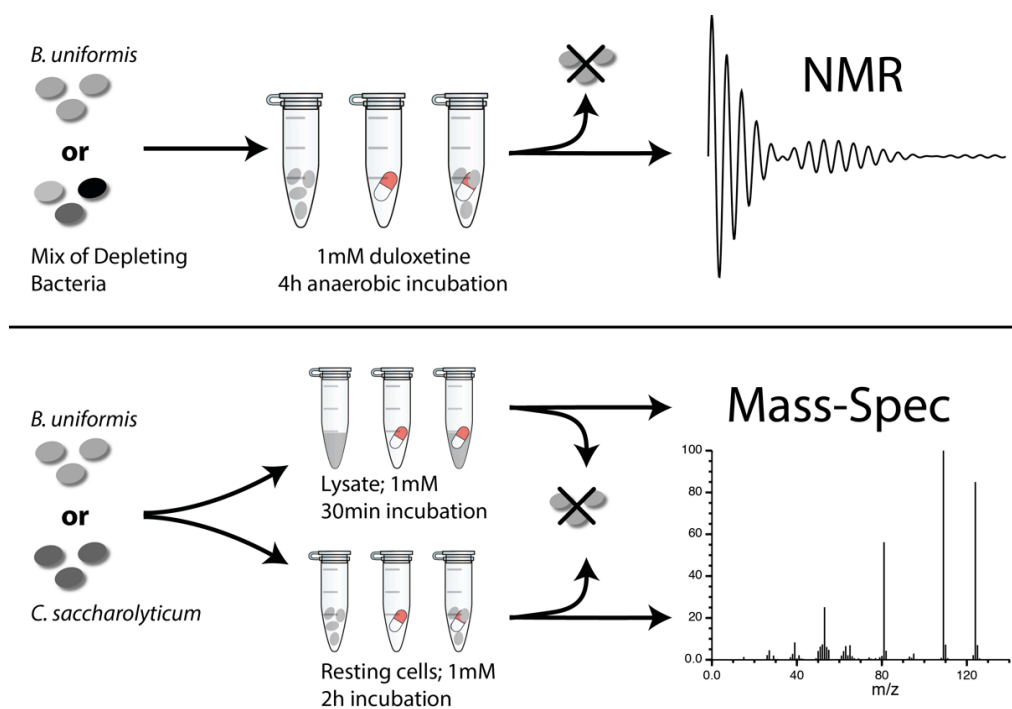


Figure 17: Outline of untargeted metabolomics experiments.

Two methods for untargeted metabolomics are used to investigate bacterial interactions with duloxetine: NMR and mass spectrometry. The mix of depleting bacteria in the NMR experiment consisted of *F. nucleatum*, *C. saccharolyticum*, *C. bolteae*, *C. ramosum*, *B. uniformis*, *B. longum subsp. longum*. All incubation was anaerobic at 37°C. In all cases bacteria are removed by centrifugation from the sample and the remaining supernatant is extracted with a mixture of ACN:MethOH. Experiments for mass spectrometry were performed in triplicates.

All experiments were conducted on resting bacterial cells or lysates, after washing the bacteria to remove extracellular metabolites and compounds from

growth medium (Figure 17). A drug-free bacteria control and a control containing only the drug but no bacteria are essential for this type of experiment, to exclude any potential confounders changing bacterial metabolism independent of the drug response. All experiments also include an extraction step to remove proteins and other debris and to concentrate low abundant metabolites. For more details please refer to method sections 7.6 and 7.7 on page 143 and 144 respectively.

4.2 Untargeted metabolomics of duloxetine interactions using ¹H NMR spectroscopy

4.2.1 Experimental setup

For NMR spectroscopy I performed two different experiments: I tested the depletion of duloxetine in a mixture of 6 bacteria (*B. longum longum*, *B. uniformis*, *C. bolteae*, *C. ramosum*, *C. saccharolyticum*, *F. nucleatum*) potentially depleting it, and I tested one specific interaction of duloxetine with *B. uniformis*. All experiments were resting cell assays (see Methods 7.5.3), comparing bacteria treated with duloxetine to bacteria not treated with duloxetine and a bacteria-free control containing only duloxetine. The bacterial mix was tested with 1mM duloxetine, the *B. uniformis* only samples with 100µM duloxetine. To record a one-dimensional proton spectrum of the molecules of interest, all samples were reconstituted in a mixture of 80% D₂O and 20% deuterated acetonitrile with half the original volume, thus doubling the concentration. 1D proton spectra for all samples were then recorded on a 500 MHz Bruker DRX NMR spectroscope.

4.2.2 Results

For exploration of the samples we first recorded few scans which resulted in less sensitive spectra. Comparing the duloxetine only spectra to spectra available in literature, we confirmed which peaks are derived from duloxetine and ensured the quality of the samples. In comparison to bacteria samples the duloxetine spectrum is less noisy, and peaks can be clearly identified. We found that peaks

belonging to duloxetine are less intense in bacteria treated samples (Table 3). A depletion of intensity of about 70% to 80% was observed on average in bacteria treated samples for both the mix of bacteria and for *B. uniformis* alone. The spectra were too noisy to look for newly appearing peaks, which might correspond to drug metabolites, in bacteria samples treated with duloxetine in comparison to non-treated bacteria.

Table 3: Duloxetine depletion in NMR spectroscopy samples. Interference indicates duloxetine peaks, which partially interfered with peaks in bacteria only treated sample.

Peak ppm	Intensity Control	Intensity Treated	% Depletion	Interference?
<i>B. uniformis</i>				
8.3926	66618879	12473273	81.28	
7.9636	71192313	24288092	65.88	yes
7.6373	214566844	48974963	77.17	yes
7.4354	117082914	47424538	59.49	yes
7.2739	66015450	13959370	78.85	
7.1646	81267273	33554120	58.71	yes
7.0418	58789654	13145173	77.64	
6.1098	83133977	9079887	89.08	
Bacteria Mix				
8.6014	231244554	69008722	70.16	
8.1448	260833964	80145756	69.27	
7.845	546049193	139189689	74.51	
7.7796	325619482	173526042	46.71	yes
7.6366	415219595	136583147	67.11	yes
7.4859	242977509	84612077	65.18	yes
7.3307	312083857	89942505	71.18	
7.2576	239460962	68593682	71.35	
6.273	376143332	92262036	75.47	

Thus, after quality control we recorded many scans of the resonance spectra to increase the signal-to-noise ratio and with this the sensitivity of the measurement. These spectra show that none of the peaks in the bacteria treated with duloxetine sample is new, as all peaks are already present either in the bacteria control or the duloxetine only control (shown for *B. uniformis* in Figure 18). These hold true for the mix of bacteria as well as for the *B. uniformis* samples. In conclusion, no potential drug metabolites were found with NMR spectrometry.

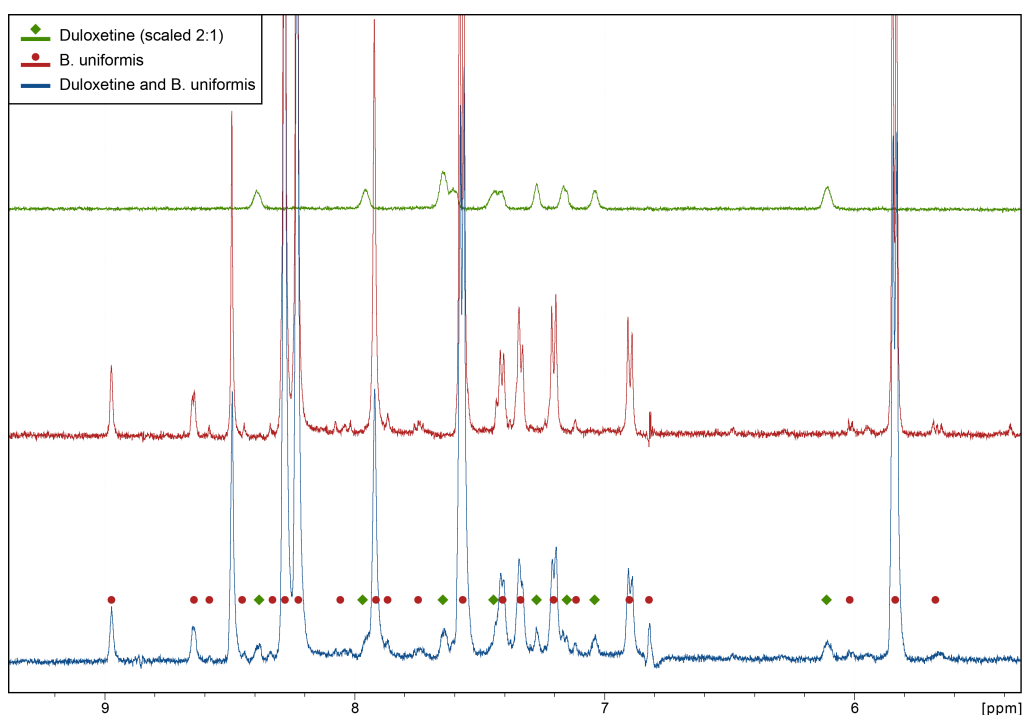


Figure 18: NMR spectra comparing *B. uniformis* treated with duloxetine to controls.

Spectra are recorded with a 500 MHz Bruker DRX NMR. Duloxetine only sample is scaled for better visibility. Concentration of duloxetine during experimental exposure for 4h was 100 μ M, but samples are reconstituted with a mixture of 80% D₂O and 20% deuterated acetonitrile in half the original volume doubling the effective concentration of metabolites for NMR study. Shapes in duloxetine treated *B. uniformis* samples indicate peaks originating from duloxetine (green diamond) or *B. uniformis* (red dot) respectively. NMR spectra recorded by Leo Nesme (Carlomagno group, EMBL).

4.2.3 Summary

There are two likely reasons a potential metabolite was not detected: either NMR spectroscopy is not a suitable method in this case or there simply is no metabolite produced in the interaction of duloxetine with bacteria. One NMR specific reason why a potentially existing drug metabolite could not be detected is sensitivity. A main challenge in these experiments was the low concentration of drug and metabolites in the samples. For small molecule NMR spectrometry the typical concentration ranges for structural elucidation start from 1mM. In this experiment the concentration of duloxetine is around 2mM, and potential metabolites can range from 1.6mM (80% of duloxetine is depleted), if there is exactly one, to much lower concentrations. As we are operating on the lower end of NMR detection, potential metabolites could be below our detection limit. While it is possible to increase NMR sensitivity (signal-to-noise ratio) through recording

many scans of a spectrum, a limit is reached fast as signal-to-noise only doubles each time the number of scans is squared. The time needed for recording each spectra in figure was 16h, and since biological samples also degrade with time we did not use a higher number of spectral scans. Another factor is that new peaks from potential drug metabolites can be hidden behind peaks from other molecules. As seen in Figure 18 the spectra from bacteria treated samples are relatively noisy containing many different peaks, even though only the aromatic range of peaks is shown. In shift ranges below 5ppm corresponding to single molecular bonds, the spectra are often consisting of many overlapping double or triple peaks, suggesting many different underlying compounds. Hence, I decided to explore the metabolic space further using a more sensitive approach with higher resolution of compounds: mass spectrometry.

4.3 Untargeted metabolomics of bacterial duloxetine depletion using LC-MS/MS

4.3.1 Experimental setup

For the mass spectrometry approach I tested the interaction of duloxetine with two bacteria, *B. uniformis* as before and *C. saccharolyticum*. Both interactions were strong, reproducible and robust in tests before and had also show depletion of duloxetine in lysate and resting cell assays (data not shown). I investigated the small molecule metabolome of a lysate and an extracellular fraction. A lysate exposes all bacterial enzymes at once to the drug and allows exploration of all possible enzymatic interactions. New features in the drug treated sample are more likely to be directly derived from duloxetine, and not to be a secondary effect of bacteria secreting metabolites in response. In contrast, the extracellular fraction of a resting cell assay explores the impact duloxetine can have on the whole bacterial metabolome. The experiment was conducted as described in short as follows, more details can be found in method section 7.7.

Bacteria were tested as lysate or resting cell assay in buffer and incubated for 30min (lysate) or 2h (intact cells) respectively. Then, debris/cells were removed by centrifugation and metabolites were extracted in ice-cold 1:1 methanol:acetonitrile containing 10 μ M Amitriptyline as an internal standard. Samples were vacuum dried, and reconstituted in 20% acetonitrile containing 250 μ M caffeine. Lysates were reconstituted in the same volume as extracted, whereas the extracellular extractions were reconstituted in half the volume, effectively doubling the concentration of metabolites. Samples were measured on a Q Exactive Plus-Orbitrap Mass Spectrometer (Thermo Fisher) in positive mode using a Kinetex C18 column for LC. Using the xcms R package from the Scripps Center for Metabolomics (Mahieu et al. 2016), I performed feature selection, peak alignment and retention time correction. Samples for lysate and extracellular fraction have been processed independently. A strict univariate analysis taking the uncertainty of the feature intensity into account followed.

4.3.2 Duloxetine is depleted in all conditions

As described before, untargeted metabolomics is sensitive to little variations in the method, because it only observes features without having a standard run side-by-side. Thus, internal standards from extraction and injection become more important to judge the quality of the mass spectrometry data. The overall variance of caffeine intensity, the internal standard for injection and run quality, is low across both fractions (extracellular: coefficient of variation (CV) = 0.054; lysate: CV=0.111) and variance was not biased to a treatment condition. The intensity of internal standard for extraction amitriptyline has also a low CV in extracellular fraction (CV=0.043) but in the lysate fraction it is slightly higher (CV=0.127). The higher variance in amitriptyline was caused by a bias in extraction towards samples containing lysed bacteria, hence I normalized the data set by the intensity of amitriptyline rather than caffeine. After normalization, the intensities of features from technical and biological replicates showed a high correlation with each other (Figure 19) in lysate and extracellular extraction respectively.

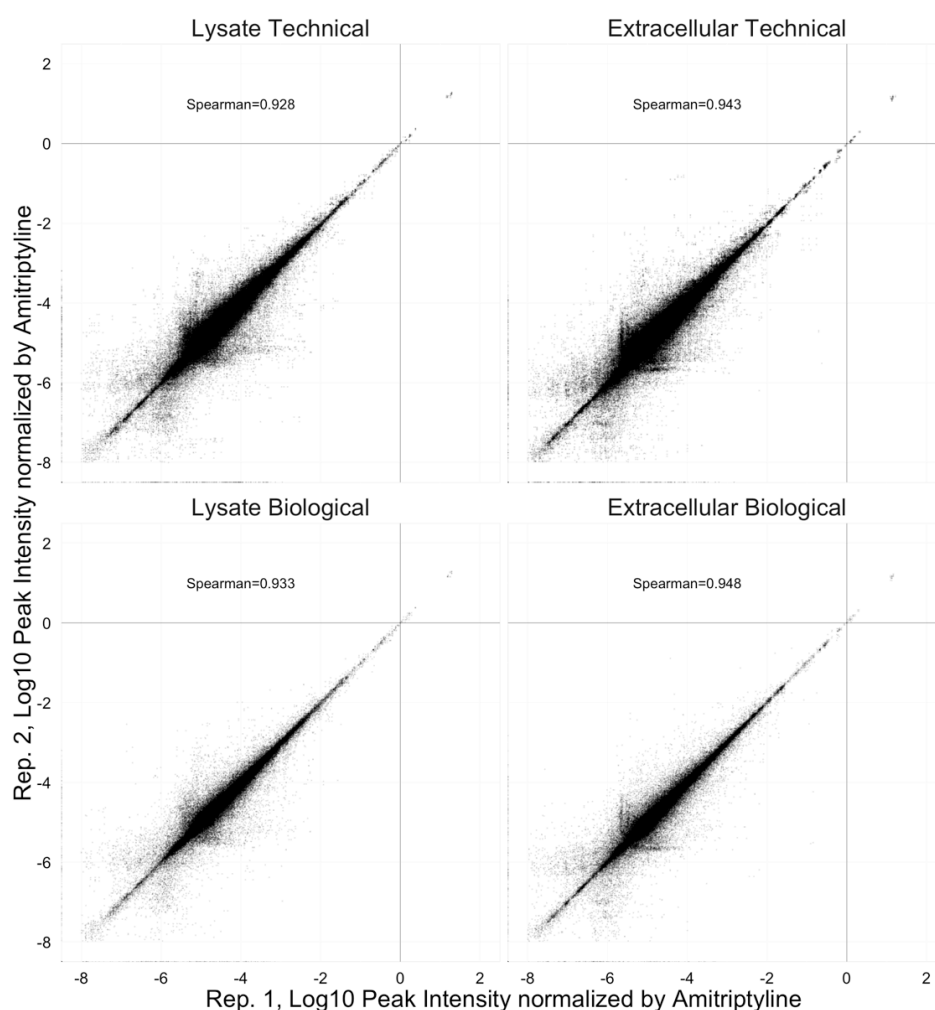


Figure 19: Technical and biological replicates of untargeted metabolomics.

Shown are log₁₀ values for LC peak intensity of detected features normalized by LC peak intensity of internal standard amitriptyline (m/z 278.18). Technical replicates represent two different mass spectrometry injections of the same biological sample, biological replicates are replicated samples of the same tested condition. Only two biological replicates are shown here for reasons of brevity, but each condition has been tested in three biological replicates.

Duloxetine is depleted in all tested conditions, but strongest in the lysate of *B. uniformis* (Figure 20). However, depletion was only roughly 20-30%, by far not as strong as the depletion in the extracellular fraction in the NMR samples. This might be explained by the shorter incubation times (2h MS samples, 4h NMR samples). All treatment groups separate spatially into different cluster after principle component analysis (Figure 21). The first two principle components explain 38.8% and 45.8% of the observed variability for extracellular and lysate fractions respectively. In the lysate, PC1 seems to separate the different bacteria from each other whereas PC2 clearly separates the bacteria from the drug. In the

extracellular fraction, no clear dominating factor is obvious for separation along PC1 axis, whereas PC2 seems to drive the separation of technical replicates. In all cases, when looking at the weights of the components, not a few features drive separation but many different features contribute (data not shown). This can indicate a global difference in the small molecule metabolome, especially in the case of extracellular extraction, as separation here is clearer than in the lysates.

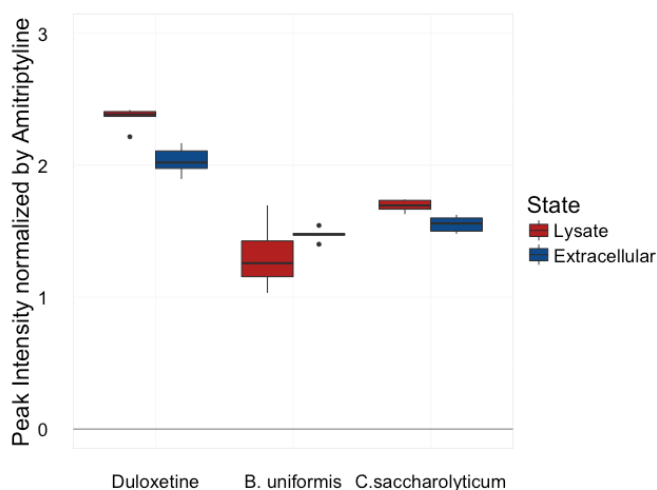


Figure 20: Depletion of duloxetine in untargeted metabolomics.

Lysates or whole cells were exposed to 1mM duloxetine, and after centrifugation to remove debris/cells soluble metabolites were extracted in MethOH/ACN. LC peak intensity of duloxetine (m/z 298.15) is normalized by LC peak intensity of internal standard amitriptyline (m/z 278.18) in respective duloxetine treated samples. Box plot represents mean and standard deviation of 3 biological replicates each injected twice.

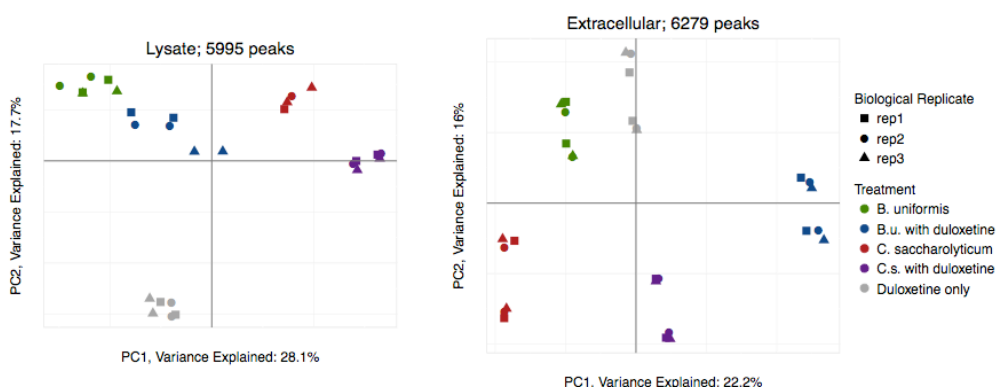


Figure 21: PCA of mass features from untargeted metabolomics.

In lysate extraction 5995 features were detected, in extracellular extractions 6270 features were detected in total. All feature intensities are normalized by amitriptyline and scaled to unit variance before analysis. Each biological replicate is injected twice, except in the case of biological replicates 1 and 2 from *C. saccharolyticum* lysates. Principle components 1 and 2 are shown, explaining 45.8% and 38.2% of total variance for lysate and extracellular extractions respectively.

4.3.3 Systemic investigation of changes in mass features

To explore this further, I compared the fold changes in the drug treated bacteria to its controls. Figure 22 shows mass features significantly changed in comparison to both controls (FDR: $\alpha < 0.05$; between treatment group $CV > 0.2$; within treatment group $CV < 0.2$) and their respective fold change. At first impression, as expected more changes occur in the extracellular fraction than in the lysate fraction. Only metabolites that are directly derived from interaction with duloxetine should significantly differ between drug-free and treated lysates. That is additionally pronounced as more features are found in extracellular samples (~6300) than in lysates (~6000), probably due to doubling of concentration in the extracellular samples when reconstituted. In general in all conditions, duloxetine has a high fold change in comparison to non-treated bacteria, and a negative fold change in comparison to the drug control as it is depleted. Other similarly behaving features might be related to the drug too, e.g. ions of adducts or fragments of duloxetine or impurities in the drug solution.

A common aspect in both extracellular extractions is that many features have a high fold change in comparison to duloxetine alone: those are likely bacteria derived molecules as they tend to have a low fold change in comparison to the bacteria control. This does not necessarily mean a difference in metabolite secretion in response to duloxetine, as despite the normalization by an extraction standard a higher amount of bacteria extracted in the treated sample could also explain the fold change. In the case of *B. uniformis* this is a possible explanation for the differences found. However, not most but only 1273 features out of 6279 total features showed a significant change in the duloxetine treated *B. uniformis* samples in comparison to the bacteria only control, which makes a methodological error unlikely (1218 out of 6279 for *C. saccharolyticum*). Additionally, in the case of *C. saccharolyticum* it is unlikely to be a methodological error, since many features are not only higher but also lower expressed than in the bacteria only control. This indicates a strong change in the metabolite profile of *C. saccharolyticum* and *B. uniformis* in response to duloxetine treatment.

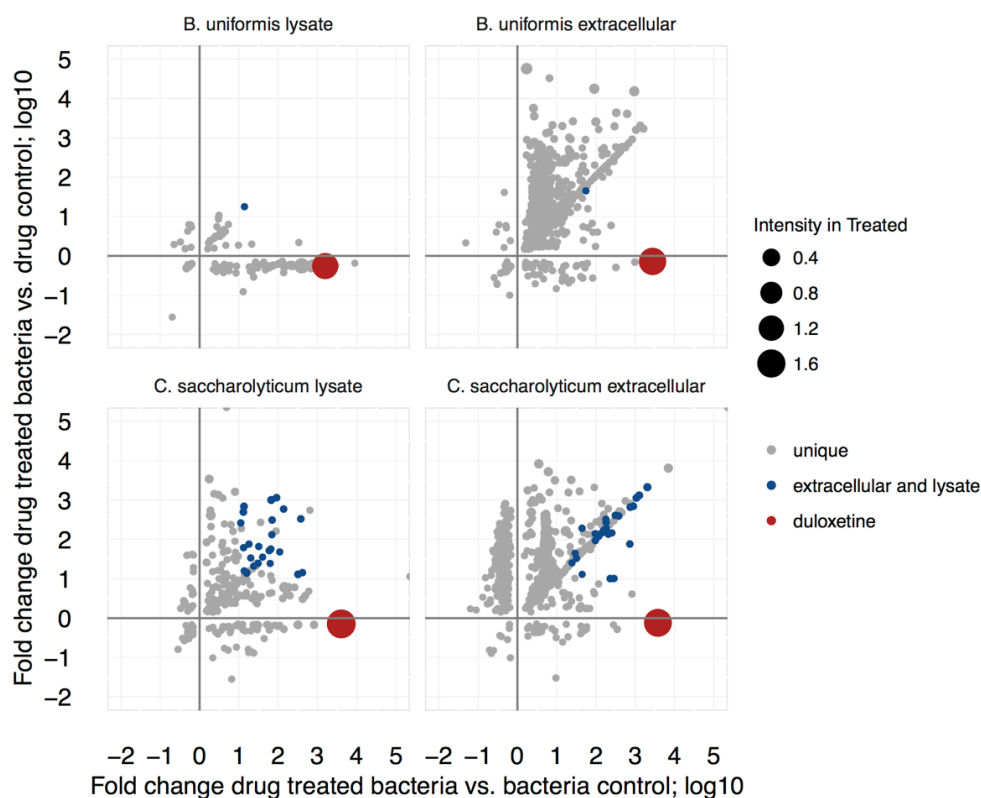


Figure 22: Comparing fold changes of duloxetine treated bacteria to controls.

Log 10 of significant (Student's t-test, FDR < 0.05) fold changes between samples treated with duloxetine and the respective drug or bacteria control. Each dot represents a m/z feature, which is significantly differentially expressed in comparison to both controls. Features have been filtered for variation before testing: CV>0.2 between conditions, CV<0.2 within one condition. Uniqueness of features has been checked for features with For mass features with a fold change above 10 in comparison to both controls and in extracellular and lysate extraction respectively, features representing the same mass in both conditions are indicated in blue.

4.3.4 Feature annotation and pathway analysis

A main aim of the metabolomics approaches was to look for potential duloxetine metabolites. Especially the experiments with lysates of bacteria were aimed to look into any enzymatic interaction with duloxetine resulting in a degradation product. Here, spectrometric features, which have the same fold change in comparison to both controls, are especially interesting as this could indicate that they are new features not observed in the controls. If the same features are also appearing in the extracellular fraction, it could be an indication for a potential duloxetine derived metabolite.

As shown in Figure 22 in *B. uniformis* lysates only one feature (674.461m/z; 1497s) is significantly and strongly upregulated (FC>10) in the duloxetine treated lysates in comparison to untreated lysate or duloxetine alone. It can be found in the extracellular extraction as well and is on the diagonal axis showing an equal fold change to both controls. This mass features is annotated in METLIN (Smith et al. 2005) as annonisin with acetonitrile adduct. However, it is likely to be an artifact and not a duloxetine derived metabolite, as no adducts similarly upregulated are found.

In *C. saccharolyticum* treated with duloxetine however, 26 features are strongly upregulated (FC>10) and found in lysate and extracellular extraction (Figure 22). In general, in *C. saccharolyticum* lysate many features are differently expressed in comparison to *B. uniformis* lysate, which can hint to improper lysis of bacteria resulting in an active metabolism with secondary effects of duloxetine treatment. The applied lysis protocol is comparatively mild (1min bead beating in PBS buffer), thus it is indeed possible that gram-positive *C. saccharolyticum* is not as effectively lysed as the gram-negative *B. uniformis*. This means that features found in *C. saccharolyticum* lysate are not directly derived from duloxetine, but could be of secondary effect. When the 26 interesting features are matched against METLIN database more than 18,000 potential metabolites are suggested, never more than two mass features having the same suggested metabolite. If compared to potential duloxetine metabolites of human detoxification metabolism described in (Lantz et al. 2003), no mass is overlapping. Thus, the search space is either too big or too small to result in a meaningful conclusion. Since an improper lysis could not be excluded as a confounding factor, no further analysis of the potential masses has been conducted.

To investigate what kind of metabolic pathways could be affected in the bacteria by duloxetine treatment, I investigated the mass features significantly changed in the extracellular fraction. I used PATHOS (Leader et al. 2011) to annotate mass features, which are differentially expressed in comparison to both controls, with metabolites from KEGG metabolic pathways. I annotated the extracellular fraction, as those show the metabolic response and include secondary

effects of duloxetine on the whole metabolism. I allowed 12 different adducts to be formed, and considered metabolites within a mass range of 5ppm. Results shown here in Table 4 show mapping against *E. coli* pathways from the KEGG database. In both cases roughly 14% of differentially expressed peaks could be annotated with metabolite masses. Mass feature to metabolite is not a one-to-one annotation, as many metabolites have the same mass e.g. sugars, and different masses can match to one metabolite due to different adducts. Thus, disturbed pathways are not ordered by their significance but rather by the number of unique ions found for that pathway. Both bacteria share many of the affected pathways, which seem to relate to amino acid and nucleotide metabolism, specifically to purine nucleotide and cysteine/methionine metabolism.

I further analyzed the data by annotating the mass features with species-specific metabolites. Data to do so was kindly provided by Daniel Sevin (Cellzome). He generated lists of species-specific metabolites by building genome-scale models for all organisms available in KEGG, and predicting their potential metabolome from the model. Unfortunately, *B. uniformis* is not available in KEGG, so instead I used the metabolome of its close relative *B. thetaiotaomicron*. For adduct-formation I used a stricter cutoff as with PATHOS, only allowing H⁺ and ACN+H⁺ adducts to be formed to annotate a mass with its potential metabolite. I used a mass accuracy of +/- 5ppm.

Table 4: KEGG Pathways enriched in significantly changed mass features.

Ordered by unique ions found as part of the pathway. Purine metabolism pathway included for *B. uniformis* because of high number of unique masses found.

KEGG Pathway Name	Mtbls found in Pathway	Total Mtbls in Pathway	Unique Masses found	Unique Ions found	p-value hypergeo. test
<i>B. uniformis</i> 123/900 masses annotated					
Purine metabolism	10	90	8	15	0.15
Cysteine and methionine metabolism	12	54	12	14	6.3 [^] 10 ⁻⁴
Methane metabolism	12	60	10	12	1.7 [^] 10 ⁻³
<i>Phenylalanine, tyrosine + tryptophan biosynt.</i>	10	31	10	11	4.3 [^] 10 ⁻⁵
<i>Glycine, serine and threonine metabolism</i>	10	45	9	11	1 [^] 10 ⁻³
Arginine and proline metabolism	14	67	10	10	0.031
<i>Histidine metabolism</i>	9	44	8	9	4 [^] 10 ⁻³
Glyoxylate and dicarboxylate metabolism	9	55	8	9	0.02
<i>Aminoacyl-tRNA biosynthesis</i>	8	24	7	9	1.4 [^] 10 ⁻⁴
Ascorbate and aldarate metabolism	13	45	7	7	1.8 [^] 10 ⁻⁵
Tyrosine metabolism	10	75	7	7	0.06
<i>Phenylalanine metabolism</i>	13	64	6	6	1 [^] 10 ⁻³
Pentose and glucuronate interconversions	12	50	6	6	2.8 [^] 10 ⁻⁴
C5-Branched dibasic acid metabolism	13	32	5	5	1.6 [^] 10 ⁻⁷
<i>C. saccharolyticum</i> 116/804 masses annotated					
Methane metabolism	15	60	13	16	1.6 [^] 10 ⁻⁵
Purine metabolism	13	90	12	14	0.013
Ascorbate and aldarate metabolism	17	45	10	13	4.2 [^] 10 ⁻⁹
Cysteine and methionine metabolism	11	54	11	12	1.3 [^] 10 ⁻³
Pentose and glucuronate interconversions	15	50	9	12	1.2 [^] 10 ⁻⁶
Arginine and proline metabolism	14	67	10	10	2.5 [^] 10 ⁻⁴
<i>Amino- and nucleotide sugar metabolism</i>	18	77	7	10	6.8 [^] 10 ⁻⁶
Tyrosine metabolism	13	75	9	9	2.6 [^] 10 ⁻³
Glyoxylate and dicarboxylate metabolism	11	55	9	9	1.5 [^] 10 ⁻³
<i>Galactose metabolism</i>	13	41	7	9	2.7 [^] 10 ⁻⁶
<i>Pentose phosphate pathway</i>	13	34	6	9	1.9 [^] 10 ⁻⁷
<i>Porphyryn and chlorophyll metabolism</i>	9	93	8	8	0.23
C5-Branched dibasic acid metabolism	15	32	7	7	6.7 [^] 10 ⁻¹⁰
<i>Naphthalene and anthracene degradation</i>	9	60	7	7	0.025
<i>Alanine, aspartate and glutamate metabolism</i>	8	25	7	7	1.3 [^] 10 ⁻³
<i>1,4-Dichlorobenzene degradation</i>	9	74	5	5	0.08

Italic letters indicate pathways not shared between *B. uniformis* and *C. saccharolyticum*

For *B. uniformis* 38 out of 900 unique mass features were annotated with 75 potential metabolites out of 686 possible metabolites. For *C. saccharolyticum* 42 out of 804 unique mass features were annotated with 93 potential metabolites out of 775 possible metabolites. A pathway enrichment analysis was not performed as many pathways were insufficiently covered by the species-specific dataset already.

The top ten significantly changed mass features with their respective potential metabolites can be found in Table 5. Sugars with the same sum formula have been summarized within one descriptive term.

Table 5: Species-specific annotations of top 10 changed mass features.

Mass feature	Name	Sum formula	FC bacteria (log10)
<i>B. uniformis</i>			
252.1090	Deoxyadenosine	C10H13N5O3	3.018
268.1035	Adenosine	C10H13N5O4	2.973
268.1035	Deoxyguanosine	C10H13N5O4	2.973
284.0989	Guanosine	C10H13N5O5	2.515
230.1858	7,8-Diaminononanoate	C9H20N2O2	2.348
182.0808	L-Tyrosine	C9H11NO3	2.327
298.0969	5'-Methylthioadenosine	C11H15N5O3S	2.204
270.1088	Deoxyuridine	C9H12N2O5	1.630
134.0446	L-Aspartate	C4H7NO4	1.627
244.0928	Cytidine	C9H13N3O5	1.620
384.1492	Disaccharides	C12H22O11	1.445
384.1492	b-D-Mannosyl-1,4-N-acetyl-D-glucosamine	C14H25NO11	1.445
<i>C. saccharolyticum</i>			
269.0881	Inosine	C10H12N4O5	3.099
284.0989	Guanosine	C10H13N5O5	2.884
261.0366	Hexose monosaccharide phosphates	C6H13O9P	2.750
244.0928	Cytidine	C9H13N3O5	2.576
112.0507	Cytosine	C4H5N3O	2.251
231.0259	Pentose monosaccharide phosphates	C5H11O8P	2.198
296.0646	Aminoimidazole ribotide	C8H14N3O7P	1.984
74.06074	Aminoacetone	C3H7NO	1.851
291.0470	Glycero-manno-Heptose 7-phosphates	C7H15O10P	1.786
291.0470	Sedoheptulose 7-phosphate	C7H15O10P	1.786
220.0811	O-Succinyl-L-homoserine	C8H13NO6	1.531
220.0811	2,4,6/3,5-Pentahydroxycyclohexanone	C6H10O6	1.531
220.0811	2-Deoxy-5-keto-D-gluconic acid	C6H10O6	1.531
220.0811	1-Keto-D-chiro-inositol	C6H10O6	1.531
220.0811	5-Deoxy-D-glucuronate	C6H10O6	1.531
220.0811	2-Dehydro-3-deoxy-D-gluconate	C6H10O6	1.531
220.0813	3-Keto-beta-D-galactose	C6H10O6	1.531

In congruency with the pathway analysis in both bacteria the purine (deoxy)ribonucleosides are strongly upregulated upon duloxetine treatment, but also the pyrimidine nucleoside cytidine is upregulated in both cases. Other nucleosides like deoxyuridine or inosine are also upregulated in one of the

bacteria respectively. While in *B. uniformis* unphosphorylated disaccharides are strongly upregulated, the sugars upregulated in *C. saccharolyticum* are phosphorylated pentose and hexose monosaccharides. *B. uniformis* has indeed a strong expression of amino acids tyrosine and aspartate upon duloxetine treatment, in *C. saccharolyticum* however no amino acid is within the top ten most changed metabolites. Amino acids and sugars are main members of the KEGG pathway “Methane metabolism” which are found enriched. It is noteworthy that in the complete list of significantly changed, annotated metabolites of *B. uniformis* and *C. saccharolyticum* a part of the Metacyc polyamine biosynthesis 1 pathway is found: agmatine → putrescine → spermidine/5'-methyl-thioadenosine (Caspi et al. 2016). In *C. saccharolyticum* aminoimidazole ribotide, a metabolite upstream of purine synthesis and unique to this pathway is also upregulated.

4.4 Summary and Discussion

One aim of the presented experiments was to confirm bacterial duloxetine depletion and thus to confirm the interaction of the bacteria-duloxetine pairs found in the interaction screen with a method complementary to UPLC-UV detection. All tested interactions showed depletion of duloxetine, both in NMR spectroscopy and mass spectrometry. However, depletion was not consistent across different samples. A strong depletion of 80% was observed in *B. uniformis* resting cell samples for NMR, and less strong in samples for mass spectrometry. As mentioned before this might be due to different incubation periods (NMR: 4h, MS: 2h) or simply due to differences in the amount of bacteria as samples were not normalized before duloxetine treatment. *B. uniformis* seems to be slightly more effective in duloxetine depletion, both in resting cell and lysate assay, but *B. uniformis* cultures often grow more dense than *C. saccharolyticum* cultures. As results from the depletion-mode assay (Figure 10) suggest that duloxetine depletion is likely not metabolic biotransformation, a difference in number of bacteria can account for a difference in depletion if a similar strength of duloxetine accumulation is assumed for both species.

Another aim of untargeted metabolomics was to aid in finding hypothesis about the way drug and bacteria interact, based on the appearance of potential drug metabolites or on an observable shift in the bacterial metabolome. In NMR spectroscopy, no new spectral peaks could be observed in *B. uniformis* samples, thus suggesting not one or two duloxetine metabolites but either no direct duloxetine metabolite or many with a concentration below the detection limit of NMR spectroscopy. In the mass spectrometry approach only one mass feature was differentially changed in *B. uniformis* lysates. In *C. saccharolyticum* samples 28 mass features are changed but are likely not directly derived from duloxetine, but of secondary effect, as improper lysis could not be excluded as confounding factor. Taking into account that also the depletion-mode assay (Figure 10) does suggest a binding without modification of duloxetine rather than a metabolic biotransformation, it is very unlikely that duloxetine is metabolically modified by *B. uniformis* or *C. saccharolyticum*.

Instead the data from mass spectrometry suggests a global difference in the extracellular small molecule metabolome of bacteria treated with duloxetine. The first two principle components separate treated bacteria well from their controls despite capturing less than 40% of the variability. Extracellular fold changes show strong differences in many features indicating a strong change in the metabolite profile of *C. saccharolyticum* and *B. uniformis* in response to duloxetine treatment. Mass feature annotation and pathway enrichment show that both bacteria share many of the affected pathways. Metabolic pathways seem to relate to amino acid and nucleotide metabolism, specifically to purine nucleotide and cysteine/methionine metabolism. A look on the species-specific annotated metabolites confirms nucleosides and sugars are strongly upregulated in both bacteria (Table 5). While in *B. uniformis* maybe part of polyamine biosynthesis is stronger affected, *C. saccharolyticum* seems to be clearly affected in its purine metabolism or synthesis.

One question, which directly arises when doing this kind of untargeted metabolomics studies, is if we just capture the most abundant metabolites in the

cell. Recently a study by Bennett et al. (2009) measured the absolute concentrations of around 100 common metabolites in whole-cell extracts of glucose-fed *E. coli*. The most abundant metabolites with a concentration of above 15mM are glutamate, glutathione and fructose-1,6-bisphosphate, followed by ATP, UDP-N-acetyl-glucosamine and hexose phosphates (Bennett et al. 2009). The latter two can be found upregulated in *C. saccharolyticum*. However, in extracellular extractions of *E. coli* hexose and pentose phosphates range around 200nM (Moses & Sharp 1972). The least abundant metabolites with a concentration below 200nM were adenosine, deoxyguanosine, adenine, guanosine and NADP⁺ (Bennett et al. 2009). All of these nucleosides except NADP⁺ are strongly upregulated in both bacteria in my experiment. Thus, I do not observe an experimental artifact but more likely a real impact of duloxetine on the purine metabolism of the two bacteria.

Duloxetine might act similar to an antibiotic as other antidepressants show antimicrobial effects, stressing or weakening the bacterial cell wall, hence the strong upregulation of extracellular compounds (Munoz-Bellido et al. 2000; Kalaycı et al. 2015). In the bacteria-drug interaction screen a slight growth defect is observed in *C. saccharolyticum*, but not *B. uniformis*. However, other bacteria like *E. rectale* are strongly affected in their growth (Figure 13, page 64). Upon administration of cell wall targeting antibiotics like ampicillin *E. coli* downregulates intracellular nucleotide levels (Belenky et al. 2015). Other antibiotics which interact with DNA or bacterial ribosome have the same effect (Belenky et al. 2015). Hoerr et al. (2016) looked into the extracellular stress response of *E. coli* respectively, and found an upregulation of thymine and alanine in response to cephalexin, and putrescine, 2-oxoglutarate, 2-phenylproprionate and 3-hydroxyisovalerate in response to ampicillin. Of those metabolites, I only found putrescine to be upregulated in my study. Duloxetine is likely not inducing a bacterial cell wall stress response and an increase in extracellular metabolite levels is not due to a leaky cell wall.

A different stress the bacteria could experience is oxidative stress upon addition of duloxetine. A study recently characterized the H₂O₂ stress response in

anaerobically grown *E. coli* using transcriptomics and found similar pathways affected, e.g. KEGG purine metabolism, alanine, aspartate and glutamate metabolism, amino sugar and nucleotide sugar metabolism pathways (Kang et al. 2013). In particular, putrescine metabolism seems to be transcriptionally upregulated and purine metabolism transcriptionally downregulated upon oxidative stress. If mainly the catabolism is affected, an accumulation and consequently secretion of purines could be the consequence. Those pathways and pattern fit best to *C. saccharolyticum*, as only one of the mentioned pathways is affected in *B. uniformis*. Interestingly, pentose phosphate pathway, which is also affected in *C. sacchaolyticum*, feeds metabolites directly into purine pathway. Disruption of the pentose phosphate pathway has been shown to increase oxidative stress as it provides NADPH for ROS decomposition (Wang et al. 2014). *B. uniformis* might be less affected by duloxetine because it is a gram-negative bacterium and its additional cell membrane prevents duloxetine from entering the cell. However, its oxidative stress response consisting of upregulation of putrescine and spermidine seems to be active as well (Tkachenko et al. 2012). However, it should also be noted that oxidative stress response is linked to starvation in bacteria and bacterial cells in this assay have been kept in nutrient-less buffer for 2h (Nguyen et al. 2011).

On an interesting side note, it can be speculated that many of the drug related mass features changed in the lysates are due to autodegradation of duloxetine. Pure duloxetine is known to have a strong autodegradation in aqueous solutions (Sinha et al. 2009). Thus, some of the effects of duloxetine on bacteria might not be direct effects of duloxetine but of its auto-metabolites as well.

In conclusion, these untargeted metabolomics data from NMR spectroscopy and mass spectrometry suggest a global change in the metabolome of the tested bacteria rather than a specific metabolic degradation of duloxetine. Duloxetine might act as an inhibitor of a protein involved in purine nucleoside synthesis or metabolism or induce a regulation of this pathway in another way. A changed metabolic state of key bacteria in the microbiome might lead to a distinct change of the microbiota composition. A change in microbiota composition is associated

with disease development: e.g. weight gain and metabolic syndrome but also psychiatric diseases like depression or autism (Heijtz et al. 2011; Foster & McVey Neufeld 2013; Jiang et al. 2015; Davey et al. 2013). The microbiome might thus contribute to some of the side effects of duloxetine treatment because it is influencing the gut-brain axis in an unfavorable way.

4.5 Clarification of contribution

I designed and conducted all experiments in this chapter. Samples for NMR were measured, analyzed and interpreted in collaboration with Leo Nesme (Carlomagno group, EMBL) and Bernd Simon (NMR core facility, EMBL). Samples for mass spectrometry were measured in the metabolomics core facility at EMBL, the MS method was setup in collaboration with Prasad Phapale (MCF, EMBL). I analyzed and interpreted the mass spectrometry data alone. Daniel Sevin (Cellzome) kindly shared data for additional feature annotation and KEGG pathway analysis.

5 Duloxetine binds to a NADH:quinone dehydrogenase and purine pathway members

In this chapter I investigate the bacterial protein targets of duloxetine in *C. saccharolyticum* using click-chemistry based methods and proteomics. I will first explain why I want to investigate the underlying mechanism of bacterial duloxetine interaction and then present the experimental outline consisting of an exploratory proteomics approach, and subsequently overexpression of candidate proteins. After presenting results from the proteomics experiments and exploratory statistical analysis, I will present duloxetine-depletion results from homo- and heterologous overexpression of duloxetine-binding protein candidates. In the end I will discuss limitations of the selected approach and suggest two molecular mechanisms for duloxetine's impact on bacterial metabolism.

5.1 Introduction

5.1.1 Why investigate protein interactions of duloxetine?

Results from the bacteria-drug interaction screen and the depletion-mode assay (Chapter 2) suggest that bioaccumulation of drug compounds from the medium might be a common and specific feature of many bacteria-drug interactions. Detailed reasons why I focused on the antidepressant duloxetine are outlined in the introduction to the previous chapters (section 3.1.1 and 4.1.1). In short, gut bacterial interactions with duloxetine, both for bioaccumulation and growth impairment, were plenty and reproducible. In general, antidepressants are of great interest as changes in gut microbiome composition have been associated with depression (Jiang et al. 2015) and a study found changes in gut microbiome composition associated with antidepressive treatment (Zhernakova et al. 2016). On top, bioaccumulation can change the pharmacokinetics and efficacy of drugs (Niehues & Hensel 2009). The metabolomics study described in the preceding

chapter suggests that duloxetine is not biotransformed by *B. uniformis* or *C. saccharolyticum*, but instead changes their native metabolism, likely affecting purine metabolism.

Untargeted metabolomics as applied in the previous chapter can only be one pillar where upon we should base a hypothesis about bacteria-duloxetine interaction. Metabolomics can give clues about the consequences of a disturbance on the whole metabolism of an organism, and potentially pinpoint the most affected metabolic pathway. However, it cannot directly point at the underlying molecular mechanism as extensive regulation and redundancies in the metabolic network often obscure the primary cause of the disturbance (Reaves & Rabinowitz 2011). Instead, the proteome is the layer of functionality a small molecule compound is usually acting on and how it is able to perturb the underlying system of regulations and functions (Szklarczyk et al. 2016). Thus, we searched for direct targets of duloxetine using a click chemistry-enabled protein pull-down and proteomics. I focused on *C. saccharolyticum* as it, in addition to sequestering duloxetine, is negatively affected in its growth upon duloxetine exposure (Figure 11 on page 52). Additionally, it is better described in KEGG and other databases, which allows for better validation of findings, and proteomics results can be complemented by the previous investigation on how duloxetine affects its metabolome.

5.1.2 Aims and Experimental Outline

The first step of exploring duloxetine interactions mechanistically on a protein level was to enrich for proteins that bind to it. This was implemented by employing click chemistry-based reactions to bind duloxetine to immobile beads and then pulling down binding proteins from a *C. saccharolyticum* lysate. The proteins were identified using mass spectrometry. After exploratory statistical analysis of the enriched proteins, I selected candidate proteins, which were overexpressed in *E. coli* and subsequently their ability to sequester duloxetine from the growth medium was assessed. I overexpressed 31 *E. coli* homologues and heterologously four *C. saccharolyticum* proteins. Homologous overexpression

was incubated anaerobically under agitation on streptavidin beads overnight at 4°C. As control, lysates with 50µM free duloxetine were also incubated on streptavidin bound duloxetine beads. After washing the beads with PBS, to release the captured proteins desthiobiotin could be substituted through biotin and the whole protein-duloxetine-desthiobiotin complex was eluted. The pull down was carried out in quadruplicates. Subsequently, Marie-Therese Mackmull (Beck group, EMBL) measured the proteins from the eluents using mass spectrometry, and analyzed the resulting data matching the measured peptides back to *C. saccharolyticum*'s *in silico* proteome. She also performed a data imputation step to increase the statistical power for proteins that were missing from the controls, and as such particular interesting. I executed the following statistical and bioinformatical analysis as described in the result section. More details of the methods can be found in section 7.8 of the method chapter.

5.1.4 Overexpression of candidate proteins

Protein enrichment from a pull down is not sufficient to demonstrate a potential mechanism for bacterial duloxetine interaction. Thus, we decided to overexpress homologues of the protein candidates in *E. coli* BW25113 $\Delta tolC$ and measure if duloxetine is sequestered from the medium in anaerobic conditions. Sequestration would indicate a potential binding of duloxetine to the respective overexpressed protein. To ensure that duloxetine molecules that enter the bacteria cell is not directly exported again, I chose the *tolC* deletion mutant as a genetic background for overexpression in *E. coli*. TolC is one of the major efflux pumps in *E. coli* (Zgurskaya et al. 2011). Additionally, for a few candidates we decided to overexpress *C. saccharolyticum* proteins heterologously to test if binding is improved with the original protein structure. Homologous overexpression mutants were readily available from a mutant library, whereas heterologous overexpression plasmids had to be newly designed.

Not all candidates could be overexpressed, as some gene overexpressions are not viable. For other candidates no potential homologue could be found in *E. coli* BW25113. In some cases, all members of a complex have been overexpressed, even

though the third member was not enriched in the pull down, e.g. since proteins homologous to XdhB and XdhC were enriched, XdhA was also overexpressed. Additionally, selection for overexpression was based on an older analysis of protein enrichment based on one unique peptide for protein identification instead of two. Thus not all potential candidates from the pull down were considered.

For heterologous overexpression I selected four proteins: HisF/HisH form a complex in *E. coli*. They are part of the histidine pathway and catalyze the last step before their product 5-Aminoimidazole-4-carboxamide ribonucleotide (AICAR) is entering the purine pathway. The other two proteins PyrD and PyrF are part of the pyrimidine pathway but do not form a complex. *In silico* predictions using the BNICE framework from a collaborator (Finley et al. 2009) suggested interaction of duloxetine with the same enzyme class as PyrF. They are one catalytic step up- and down stream respectively after Phosphoribosyl pyrophosphate (PRPP) is entering the pyrimidine pathway. PRPP is a product of the pentose phosphate pathway.

5.2 Results

5.2.1 Duloxetine binding protein enrichment

The aim of the pull-down assay was to enrich for *C. saccharolyticum* proteins, which can bind to and thus interact with duloxetine. With a threshold of at least 2 unique peptides per protein and detection in at least three out of four replicates in either control or treatment samples we detected a total of 591 proteins in the samples using mass spectrometry based proteomics. Still, many proteins were only detected in treatment samples but not controls. Thus, after log₂ transformation we performed a data imputation step to estimate missing intensities from the average intensities in samples with protein detection. Then, data was quantile normalized before calculating significant differential expression using Student's t-test controlling the false discovery rate at an alpha level below 0.1 (Figure 24).

With a threshold in \log_2 fold change between control and pulled down proteins of at least 2, 55 proteins were significantly enriched in the pull down. Of those 55 hits six proteins are so far uncharacterized. Of the five strongest hits (\log_2 fold change > 6) three proteins are uncharacterized and have homologues only to other uncharacterized proteins. The remaining two strong hits (Uniprot ID: D9R9H8, D9R9G9) contain both an iron-sulfur cluster and are part of a NADH:ubiquinone dehydrogenase complex.

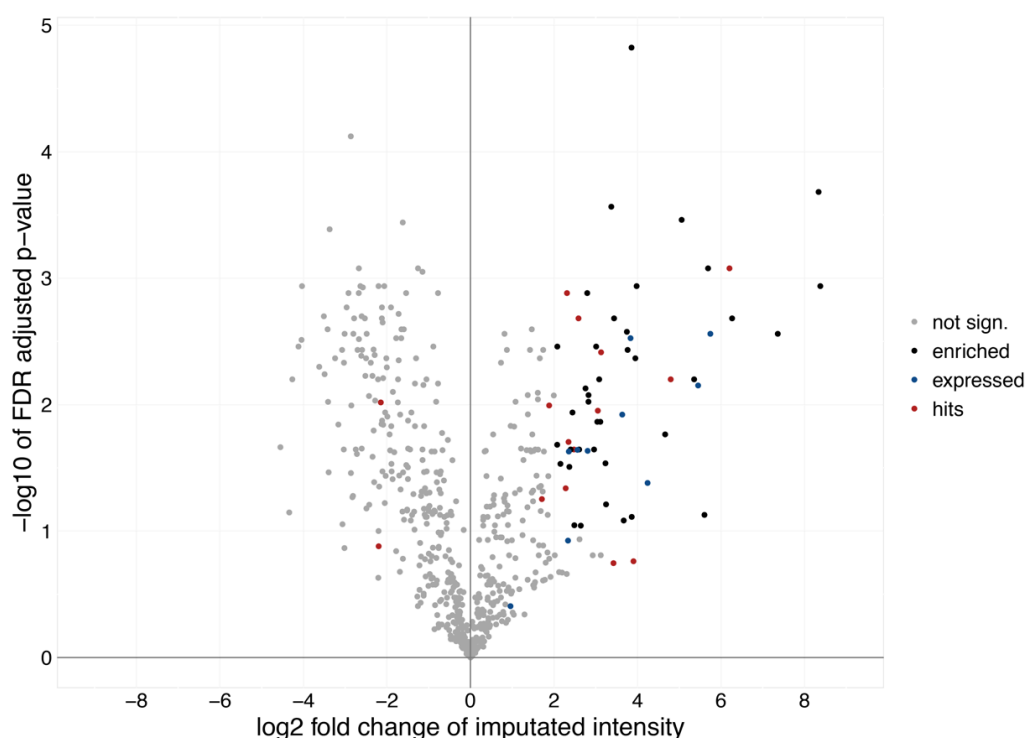


Figure 24: Volcano plot of proteins detected in pull down.

Fold change of proteins detected in duloxetine pull down of *C. saccharolyticum* lysate. Presented values are reached after imputing for not-missing-at-random from controls and correcting for an overall higher intensity in test samples in comparison to control samples. Four replicates each were tested. Color refers to: not significantly enriched proteins (grey); significantly (FDR, $\alpha < 0.1$, $\log_2(\text{Fc}) > 2$) enriched proteins (black); heterologous proteins overexpressed in *E. Coli BW25113* (blue), and a respectively significant depletion (>20%) of duloxetine (red). Mass spectrometry and data imputation by Marie-Therese Mackmull (Beck group, EMBL).

To further link the enriched proteins from *C. saccharolyticum* to their “duloxetine bioaccumulation” function, I compared their amino acid sequence similarity (Figure 25) to other species from the bacteria-drug interaction screen described in chapter 2 (Figure 11 on page 52). In there, the two *E. coli* strains IAI1 and ED1a behaved differently, with *E. coli* IAI1 sequestering duloxetine and being

slightly affected in its growth on the one hand, and *E. coli ED1a* not sequestering duloxetine nor being affected in its growth on the other hand. I included the lab *E. coli* strain BW25113 as further experiments had shown that duloxetine also affects its growth.

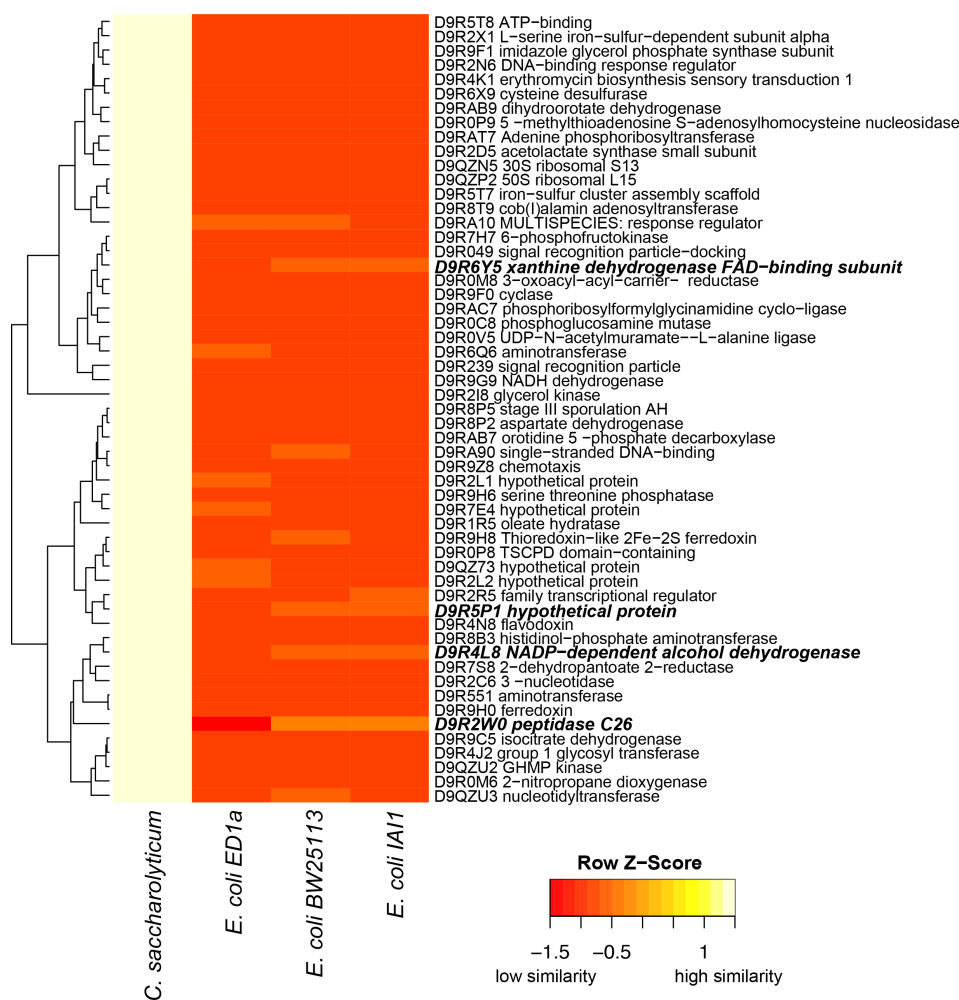


Figure 25: Heatmap of protein blast alignment.

Amino acid sequences from enriched proteins align with NCBI pblast tool to most similar sequences in target bacteria. pBlast bitscore used as distance measure, scores scaled by row. Clustering by average linking, annotation from Blast2GO analysis. Identifier is Uniprot ID. Highlighted names show divergent proteins in closely related *E. coli* strains, correlating with their diverging duloxetine response.

All *E. coli* strains have a similar phylogenetic distance to *C. saccharolyticum*, thus their protein alignments show high similarity within *E. coli* strains and very little similarity towards *C. saccharolyticum* (Figure 25). However, for four proteins the little similarity they do have is correlated with their divergent response to duloxetine (highlighted in Figure 25). This subunit of xanthine dehydrogenase

(XdhB) is strongly enriched in the pull down with a log₂ fold change over 5. This enzyme is part of the purine metabolism pathway as annotated by KEGG. Albeit peptidase C26 has the strongest divergence in its alignment similarity, and its matching gene sequence is annotated as *puuD* in *E. coli* BW25113. The respective protein is a gamma-glutamyl-gamma-aminobutyrate hydrolase, which is part of the KEGG Arginine and proline metabolism pathway and involved in putrescine degradation. The other two protein sequences map to no or to uncharacterized proteins in *E. coli*.

To enable analysis of the functionality of these enriched proteins I used Blast2GO (Conesa et al. 2005) to annotate proteins with their respective GO terms and EC numbers. I used Blast2GO to align the enriched proteins against the NCBI database restricted to Firmicutes only, and used the top five hits and their respective annotation to annotate the query proteins. Enrichment analysis of annotated GO terms can be directly done within Blast2GO (Table 6). To analyze enrichment for KEGG metabolic pathways (Table 7), I extracted the annotated EC numbers from Blast2GO (33 complete EC numbers in total) and used the EC2KEGG tool (Porollo 2014).

Table 6: GO term enrichment (most specific) for 55 enriched proteins.

GO-ID	Term	Category	FDR	#Enrich	#Ref	Uniprot ID
GO:0048037	Cofactor binding	Function	4.41E-03	10	19	D9R7S8; D9R4N8; D9R6Y5; D9R0M8; D9R8B3; D9R9G9; D9R9C5; D9R1R5; D9R8P2; D9R6Q6
GO:0008137	NADH dehydrogenase (ubiquinone) activity	Function	2.60E-02	3	0	D9R9H8; D9R9H0; D9R9G9
GO:0006120	Mitochondrial electron transport; NADH to ubiquinone	Process	2.60E-02	3	0	D9R9H8; D9R9H0; D9R9G9
GO:0006744	Ubiquinone biosynthetic process	Process	2.60E-02	3	0	D9R9H8; D9R9H0; D9R9G9

The GO term enrichment indicates that many of the enriched proteins bind to cofactors. A closer look into the annotation reveals that those cofactors are pyridoxal 5'-phosphate, flavin mononucleotide, FAD, NADP and NAD. While

pyridoxal-5'-phosphate is mainly involved in the transfer of amino and carboxyl groups, the other cofactors are all involved in electron transfer. The remaining three GO terms all refer to the same three proteins and in each case cover all potential members of the respective GO term. They indicate a strong enrichment for proteins of the NADH dehydrogenase with ubiquinone as an electron acceptor. Two out of the three members are strongly enriched in the pull down ($\log_2 \text{FC} > 6$). In the same genomic region (Biocyc access NC_014376-66) in total six enriched proteins can be found, distributed across three operons. Besides the NADH dehydrogenase and a hydrogenase, the other proteins are a ferredoxin like protein and a protein serine/threonine phosphatase, and the imidazole glycerol phosphatase subunits HisH and HisF.

The KEGG pathway enrichment analysis reveals that many enzyme classes enriched in the duloxetine pull down are part of the purine pathway or the cysteine and methionine pathway (Table 7). The enzyme classes in the purine pathway are represented by seven different proteins, in the methionine pathway by three different proteins. The same pathways were also enriched in the metabolomics data for *C. saccharolyticum* (Table 4, p. 88). Four enriched enzyme functions (2.6.1.1; 2.6.1.5; 2.6.1.57; 2.6.1.9) are shared in several amino acid metabolic pathways. However, these four enzyme annotations are based on one protein only: Histidinol-phosphate aminotransferase (Uniprot: D9R8B3). The NADH:quinone dehydrogenase proteins mentioned before are the only enriched proteins involved in oxidative phosphorylation. Albeit it is important to notice that EC2KEGG does not take incomplete EC numbers into account. Thus, for example the histidine pathway proteins D9R9F0/HisF and D9R9F1/HisH with EC:4.1.3.- and EC:2.4.2.- respectively are not considered for enrichment analysis even though a identification by sequence similarity is possible.

The pathway analysis also shows nicely why species-specific comparisons are important, especially when working with relatively little described organisms. Of 33 EC numbers annotated for the 55 enriched proteins only 20 could be mapped to KEGG pathways for *C. saccharolyticum*. As an example, only 46 proteins are so far annotated as members of the purine pathway in KEGG, while in total 107

potential proteins are known. A comparison to a general pathway map would underestimate the enrichment for any given pathway in *C. saccharolyticum*. It also indicates that some significant pathway enrichments like “Isoquinoline alkaloid biosynthesis” are not meaningful, as so far no protein has been found to be part of that pathway in *C. saccharolyticum*. However, for reasons of completeness they are listed here.

Table 7: KEGG Pathway enrichment analysis for 55 enriched proteins represented by 33 EC numbers.

KEGG Pathway Name	Total in KEGG	Total in Csh	In 55 enriched	ECs enriched	P-value	FDR
Purine metabolism	107	46	6	1.17.1.4; 2.4.2.7; 3.2.2.1; 3.6.1.15; 3.6.1.3; 6.3.3.1	0	0
Cysteine and methionine metabolism	74	22	6	2.6.1.1; 2.6.1.5; 2.6.1.57; 3.2.2.16; 3.2.2.9; 4.3.1.17	0	0
Tyrosine metabolism	61	5	4	2.6.1.1; 2.6.1.5; 2.6.1.57; 2.6.1.9	0	0
Phenylalanine metabolism	66	7	4	2.6.1.1; 2.6.1.5; 2.6.1.57; 2.6.1.9	0	0
Novobiocin biosynthesis	12	3	4	2.6.1.1; 2.6.1.5; 2.6.1.57; 2.6.1.9	0	0
Isoquinoline alkaloid biosynthesis	51	0	3	2.6.1.1; 2.6.1.5; 2.6.1.57	0	0
Tropane; piperidine and pyridine alkaloid biosynthesis	27	0	4	2.6.1.1; 2.6.1.5; 2.6.1.57; 2.6.1.9	0	0
Phenylalanine; tyrosine and tryptophan biosynthesis	39	17	4	2.6.1.1; 2.6.1.5; 2.6.1.57; 2.6.1.9	0.00001	0.00008
Oxidative phosphorylation	11	4	2	1.6.5.3; 1.6.99.3	0.0008	0.00587
Fatty acid biosynthesis	17	7	2	1.1.1.100; 2.3.1.85	0.00188	0.01273
Thiamine metabolism	23	12	2	2.8.1.7; 3.6.1.15	0.00465	0.02728
Pantothenate and CoA biosynthesis	30	12	2	1.1.1.169; 2.2.1.6	0.00465	0.02728
Biosynthesis of unsaturated fatty acids	16	1	1	1.1.1.100	0.01487	0.06887
Ubiquinone and other terpenoid-quinone biosynthesis	40	3	1	2.6.1.5	0.02953	0.11298
Pyrimidine metabolism	63	32	2	1.3.5.2; 4.1.1.23	0.02611	0.11298
D-Glutamine and D-glutamate metabolism	12	3	1	6.3.2.8	0.02953	0.11298
C5-Branched dibasic acid metabolism	21	3	1	2.2.1.6	0.02953	0.11298
Glutathione metabolism	38	5	1	1.1.1.42	0.04397	0.15477
Biotin metabolism	20	5	1	1.1.1.100	0.04397	0.15477

5.2.2 Homologous overexpression of protein candidates

The aim of overexpressing candidate proteins was to reinforce the evidence for duloxetine interaction by functional assessment of duloxetine sequestration. For homologous overexpression, I selected 31 candidate proteins, which might potentially interact with duloxetine. Selection was mainly based on a preliminary analysis of protein enrichment and limited to matching homologues in *E. coli*, thus only 17 of the 55 enriched proteins in the final bioinformatics analysis were part of the overexpressed proteins.

Homologous overexpression showed a significant depletion of duloxetine in all cases (Figure 26). If a minimal depletion of at least 20% is required, 19 out of 30 overexpressed genes sequester duloxetine from the medium (highlighted in Figure 24). The two strongest candidates with a depletion of over 30% are AroK, a shikimate kinase I that is part of the phenylalanine, tyrosine and tryptophan biosynthesis pathway, and CpdB, a 3'-nucleotidase or 2':3'-cyclic-nucleotide 2'-phosphodiesterase, which is part of purine and pyrimidine pathways. Both of these candidates were not strongly enriched in the pull-down assay in the final bioinformatics analysis, but showed rather strong enrichment in a preliminary analysis, which was based on one unique peptide per protein identification instead of two. As depletion is not corrected for strength of protein overexpression and bacterial cell density, differences in depletion strength need to be interpreted carefully. Additionally, none of the hits was stronger than 35% depletion, indicating that maybe unspecific binding might play a role. *E. coli BW25113 ΔtolC* was tested before and did not show any depletion of duloxetine. Albeit in comparison to wild type *E. coli BW25113* it had stronger growth impairments at 50 μM duloxetine. Interestingly, the two different clones of *norW* overexpression showed differently strong depletion of duloxetine. One clone was not impaired in growth by duloxetine and depletes duloxetine stronger than the clone that is impaired in growth.

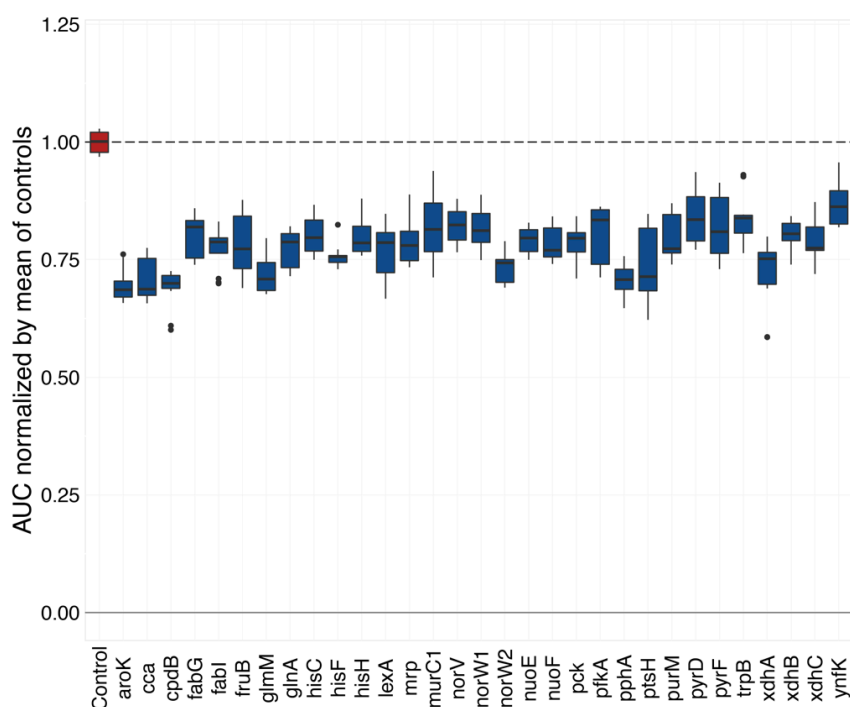


Figure 26: Duloxetine depletion in *E. coli* homologous overexpression.

Homologues of candidate proteins are overexpressed in *E. coli* BW25113 tolC deletion mutant. Results from 48h incubation, induction by 200 μ M IPTG from beginning, 50 μ M duloxetine added after 8h. Depletion of duloxetine after indirect extractions, in comparison to plate-specific control. Bacteria-free control indicated in red. Experiment performed in biological triplicates.

5.2.3 Heterologous overexpression of protein candidates

To test if binding is improved with the original protein structure, I overexpressed *C. saccharolyticum* protein heterologously in *E. coli* TOP10. I selected four genes for heterologous overexpression (Figure 27). As mentioned before in *C. saccharolyticum* the operon of HisF/HisH protein complex is located close to the NADH:quinone dehydrogenase complex operon, which are the strongest enriched proteins. They are part of the histidine pathway. The other two proteins PyrD and PyrF are part of the pyrimidine pathway but do not form a complex. They are one catalytic step up- and down stream respectively after PRPP is entering the pyrimidine pathway. PRPP is a product of the pentose phosphate pathway.

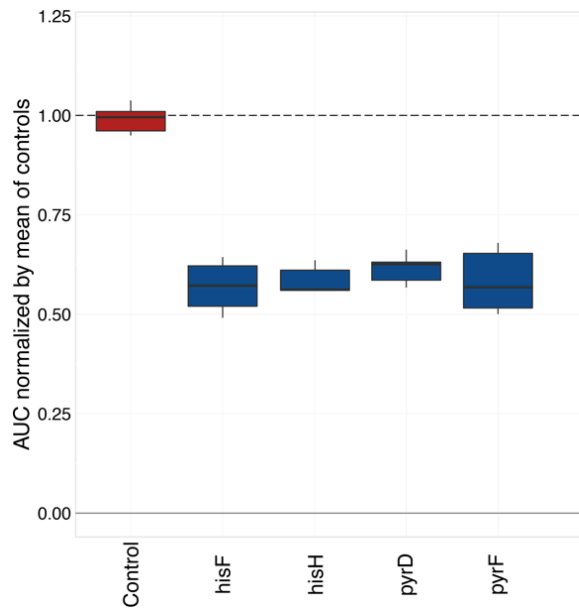


Figure 27: Duloxetine depletion in *E. coli* heterologous overexpression.

Overexpression of *C. saccharolyticum* candidate proteins in *E. coli Top10*. Depletion of duloxetine after indirect extraction in comparison to controls. Results from 48h incubation, induction by 200 μ M IPTG after 5h, 50 μ M duloxetine from beginning. Bacteria-free control indicated in red.

In all four cases heterologous overexpression of the candidates proteins lead to a depletion of duloxetine from the medium. Depletion is relatively strong in comparison to homologous overexpression and reached up to 45%. Interestingly, even though HisH and HisF form a complex separate overexpression of each gene does sequester duloxetine from the medium. However, since the wild type strain of *E. coli* was not available and thus not tested in the assay, results should be interpreted with care.

5.3 Summary and Discussion

5.3.1 Summary

The aims of these experiments were to find potential duloxetine interacting proteins and reinforce the evidence for interaction by overexpression and functional assessment of sequestration. Consequently, a potential mechanism for how duloxetine interacts with *C. saccharolyticum* and potentially other gut bacteria might come to light.

The five strongest enriched proteins from the duloxetine pull down are either part of a NADH:quinone dehydrogenase or proteins with unknown function. Many of the moderately to strongly enriched proteins are part of purine metabolism or other proteins involved in nucleotide metabolism. Additionally, the sequence alignment with pBlast showed a divergent similarity in the purine pathway member xanthine dehydrogenase (XdhB) corresponding to a divergent duloxetine response in *E. coli* strains. A different NADH dependent dehydrogenase also showed a similar behavior. The homologous overexpression of another purine pathway member showed a strong sequestration of duloxetine: CpdB, a 3'-nucleotidase or 2':3'-cyclic-nucleotide 2'-phosphodiesterase. Heterologous overexpression of pyrimidine and histidine pathway members also showed duloxetine sequestration. Metabolomics analysis had beforehand also suggested an effect in the same metabolic pathways (Table 4 on page 88).

Experimental support from the overexpression experiments should overall be considered weak as important controls are missing within the same assay. Clearly, the experiments need to be replicated with better controls like an empty vector mutant for depletion control, but also growth should be more tightly monitored to be able to correct for biomass differences. Additionally, growth might recover in mutants overexpressing duloxetine-binding proteins as the deleterious effect is titrated out. Thus, different induction strengths of protein overexpression should also be tested. Ideally, IC50 values and respective duloxetine depletion curves are determined for each overexpressed protein and induction strength to allow for assertion of the impact of the respective protein in duloxetine bioaccumulation or

functional relevant inhibition. Consequently, the following discussion is mainly based on results from the duloxetine pull-down assay, and thus rather speculative.

There are many potential mechanistic explanations possible for the observed results. Particularly as three of the five strongest enriched proteins are of unknown function there is room for speculation. I will present shortly two major thoughts in the next few paragraphs based on the two different binding site of NADH:quinone dehydrogenase (Figure 28). The underlying idea for the first is an inhibition of NADH:quinone dehydrogenase through duloxetine binding on its quinone binding site. The resulting NADH excess could lead to a change in pentose phosphate metabolism and other downstream pathways like purine metabolism. The second idea emphasizes that duloxetine itself might act as an electron acceptor, as it binds many proteins with a redox cofactor. It could bind in competition to NADH at its binding site on the NADH:quinone dehydrogenase, as the naphthalene-derived group of duloxetine could be modified into a electron donating naphtoquinone. In the end I will mention some other aspects and give a short conclusion.

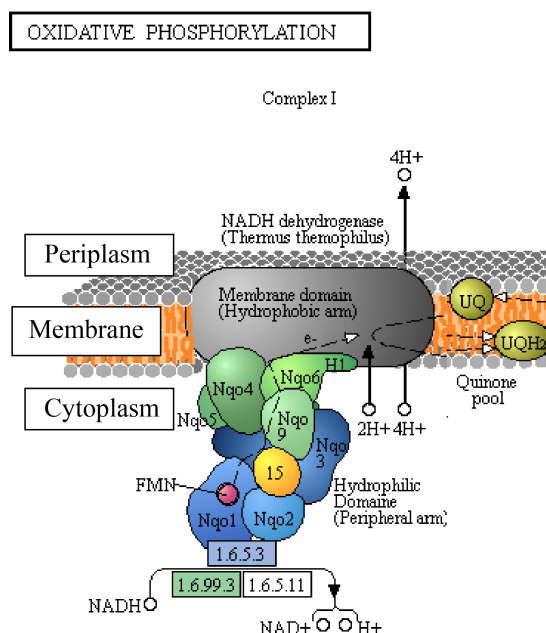


Figure 28: NADH:quinone dehydrogenase.
Figure adapted from KEGG reference pathway for Oxidative Phosphorylation (map00190).

5.3.2 Duloxetine as NADH:quinone dehydrogenase inhibitor at quinone binding site

NADH dependent quinone dehydrogenase is part of oxidative phosphorylation in the respiratory chain and thus part of the energy metabolism of most organisms (Haddock & Jones 1977). It is a complex consisting of several proteins containing iron-sulfur clusters to form an electron transport chain within the bacterial membrane build to tunnel electrons from $\text{NADH}+\text{H}^+$ to a electron acceptor, usually ubiquinone (Brandt 2006). The final electron acceptor depends on the type of fermentation or respiration employed in the bacterium. The energy freed by reducing ubiquinone is used to pump protons or Na^+ ions out of the cytosol into the periplasm to establish a proton motive force, which in turn is used to produce ATP via the ATP synthase (Brandt & Müller 2015). Ubiquinone is hydrophobic and hence embedded in the bacterial membrane, facing the cytosol. Duloxetine is also a hydrophobic potentially inserting itself into the bacterial membrane as well. As such it could potentially inhibit the electron transfer to ubiquinone and block the whole electron transport chain like the inhibitor rotenone (Singer & Ramsay 1994). NADH dehydrogenase inhibition at the ubiquinone binding side is common and other small molecule drugs like antidepressant nefazodone have been shown to act in this way (Dykens et al. 2008). Additionally, duloxetine is moderately sequestered by many bacteria with diverse phylogeny (Figure 7), which suggest a binding in the membrane rather than through a specific protein. Binding to and inhibition of the NADH:quinone dehydrogenase though might be relatively specific, as only few mainly gram-positive bacteria show growth defects upon duloxetine sequestration (Figure 11).

Usually, in aerobic respiration a high toxicity through reactive oxygen species caused by leaked electrons is observed (Fato et al. 2008). As the tested conditions are anaerobic the only effect might be an energetic loss through electron leakage, which might manifest as the decreased growth capacity of *C. saccharolyticum*. Another reason for a growth disadvantage might be that NADH cannot be oxidized by NADH dehydrogenase anymore, causing a rearrangement of

metabolic fluxes in the downstream pathways and less than optimal energy expenditure into growth. Downstream pathways like the purine, pyrimidine and histidine metabolic pathways, all depend on Phosphoribosyl pyrophosphate (PRPP) generated in the pentose phosphate pathway. They also produce NADH along the synthesis of their final metabolites. Indeed Minato and colleagues found when knocking out NADH:quinone dehydrogenase symporting sodium in *Vibrio cholera* in anaerobic conditions there was no effect on pathways related to Na⁺ use but a change in purine metabolism (Minato et al. 2014).

One drawback of this explanation is that purine pathway member proteins are enriched in the pull down, which suggest a binding to duloxetine rather than a regulation in response to it. Although the pull down was implemented overnight at 4°C, so the formation of larger protein complexes was possible, it is unlikely that pathways several metabolic steps downstream of the original binding partner are enriched in this way. Aside from this, there are different NADH:(ubi)quinone dehydrogenases potentially acting under different conditions or with different functional history in different bacterial phyla or families (Haddock & Jones 1977; Brandt 2006; Reyes-Prieto et al. 2014). For example, some are Na⁺ symporters, some do not link electron transport to proton or Na⁺ transport at all (Reyes-Prieto et al. 2014). The described mechanism is only one of several possibilities, and a detailed sequence alignment analysis and biochemical characterization has to be undertaken before making any conclusions about the function of this specific NADH:quinone dehydrogenase from *C. saccharolyticum*.

5.3.3 Duloxetine as nucleotide mimicking electron acceptor

Many purine pathway members but also other proteins from the pyrimidine pathway or cysteine and methionine pathway are enriched in the pull down. As those proteins do not directly interact with the NADH:quinone dehydrogenase another explanation seems also plausible. Several of the enriched proteins have a nucleotide-binding domain for redox cofactors. Most redox cofactors like FAD and NAD are based on adenine structures, and this might explain why enrichment occurs especially in the purine pathway. This nucleotide-binding motif is called a

Rossmann fold. It is conserved for binding dinucleotides, is widely found across kingdoms and still allows for flexibility in its structure potentially accommodating different molecules (Hanukoglu 2015) It is noteworthy that the part of the NADH:quinone dehydrogenase complex enriched is not the quinone binding protein but rather the part which binds to NADH.

Disturbing so many binding sites of redox factors should lead to a strong growth deficiency (Deris et al. 2014). This might not occur simply because duloxetine binding affinity is not high and only in a artificial environment with reduced complexity and energetic levels as in the pull down experiment binding occurs. In many cases binding in purine-binding sites might be facilitated because purines are planar double ring molecules like the naphthol ring in duloxetine, and the binding site forms a stack with planar aromatic amino acid side groups (B-Rao et al. 2012). However, unlike purines it cannot form hydrogen bonds with nearby amino acids. Thus, duloxetine affinity is low and native substrates will bind more likely than duloxetine, resulting in no to little growth defects.

Another more speculative idea why no strong growth defects occur is that duloxetine itself is used as an electron acceptor. It has a naphthol group, which might be prone to reduction. Naphthalene is degraded in anaerobic conditions by adding a carboxyl group and then reducing the ring structure by adding protons and ketone groups (Meckenstock & Mouttaki 2011; Mouttaki et al. 2012; Mihelcic & Luthy 1988; Xu et al. 2007). The in the pull-down enriched xanthine dehydrogenase is capable of catalyzing addition of ketone groups to ring structures, but usually at purine bases on a C atom situated between two N atoms. If two ketone groups are added, duloxetine might resemble the isoalloxazine group of FAD and FMN. As such it is a quinone, which can be used for electron shuttling switching between quinone and quinol states similar to ubiquinone. PyrD has a FMN binding site and preliminary experiments show a binding of duloxetine to PyrD (Vladimir Rybin (EMBL), personal communication). Docking studies suggest that duloxetine does bind in the FMN pocket (Vinita Periwal (Patil group, EMBL), personal communication). The enriched pathway co-member

PyrF is a carboxylase and could potentially activate the naphthol structure of duloxetine. In the heterologous overexpression both of them sequester duloxetine.

However, before modification duloxetine does not possess similar chemical properties to NAD or FAD. Besides the amine group close to the click chemistry linker it does not consist of any nitrogen. It is hydrophobic whereas nucleotides are highly hydrophilic. Under anaerobic conditions it is hard to modify, as it is energetically unfavorable (Meckenstock et al. 2016), although naphthene modification by gut bacteria have been described (Van de Wiele et al. 2005). Additionally, as mentioned before the discovered binding might only occur in less competitive *in vitro* environments. And finally, I found no evidence that duloxetine is biotransformed in *C. saccharolyticum*. Thus, duloxetine might bind in the suggested redox cofactor binding sites, but not be modified. A low affinity for duloxetine and strong occupation of the binding site by the native redox cofactors might explain why little growth defects occur *in vivo*.

5.3.4 Alternative explanations

Duloxetine might act in a complete different way as described here. One of the enzymes enriched was a xanthine dehydrogenase, which also showed a divergent alignment correlating with duloxetine response in *E. coli*. Clostridiales have been shown to be able to ferment purines (Durre & Andreesen 1983). The xanthine dehydrogenase is the first step in purine fermentation, and has been shown to be relatively promiscuous (Coughlan 1980). Another idea is that duloxetine blocks not the NADH or quinone binding sites of NADH:quinone dehydrogenase but a potential sodium pump function (Reyes-Prieto et al. 2014). Duloxetine could be considered a sodium pump blocker as the serotonin and noradrenaline transporters it inhibits in the mammalian brain are sodium dependent.

5.3.5 Conclusion

The protein pull down and following overexpression showed that duloxetine binds a diverse set of proteins, often associated with the purine pathway or in general with nucleotide or nucleoside binding. The strongest enrichment was seen

for a NADH:quinone dehydrogenase and duloxetine might act as an inhibitor of its electron transport function, which in turn affects oxidative phosphorylation and other downstream pathways like purine metabolism. A more detailed investigation into the structure of duloxetine binding proteins and metabolic consequences of enzyme inhibition through duloxetine should follow.

5.4 Clarification of Contribution

I designed the pull down experiment and organized the implementation. Felix Hövelmann (Schultz group, EMBL) synthesized duloxetine bound to desthiobiotin with a click chemistry enabled linker. Thomas Bock (Beck group, EMBL) conducted the pull down experiment, while I provided the bacterial lysate. Marie-Therese Mackmull (Beck group, EMBL) measured the samples with mass spectrometry and performed the peptide matching and data imputation step. I did statistical analysis and further bioinformatics.

For homologous overexpression I had help from Lucia Herrera (Typas group, EMBL) for cloning overexpression plasmids from a clone library into the $\Delta tolC$ background strain. Otherwise I designed and implemented the homologous and heterologous overexpression and accompanying duloxetine depletion analysis myself.

6 Discussion and Outlook

I will first give a short summary of all findings in this thesis, and then discuss potential implications in the context of the contemporary state of research on gut bacterial drug interactions. When discussing a specific point, I will also suggest additional paths of investigations. Finally I will give a conclusion of the findings from my PhD work. All following parts are structured by the two main thoughts behind this work: i) prevalence of drug interactions of gut bacteria and their relevance in the (host) microbiota context, and ii) mechanistic elucidation of duloxetine interactions and its effects on bacterial physiology.

6.1 Summary of Results

6.1.1 Bioaccumulation of xenobiotics is a wide-spread characteristic of the human gut bacteria and affects community dynamics

Our knowledge of the biochemical capabilities of gut bacteria to interact with or metabolize therapeutic drugs is largely incomplete (Sousa et al. 2008; Koppel & Balskus 2016). Towards filling this gap, I planned and conducted a systematic *in vitro* screen of xenobiotic-microbial interactions elucidating how wide-spread bacterial drug bioaccumulation or biotransformation is across therapeutic drugs or the gut microbiota. I tested, under anaerobic conditions, 450 drug-bacteria interactions covering 25 metabolically diverse gut bacteria and 18 structurally diverse FDA-approved drugs. This revealed almost 50 novel bioaccumulation or biotransformation links between 19 bacterial species and 10 drugs (Figure 11 on page 52). The implicated bacteria are phylogenetically diverse, including commensals, probiotics and bacteria associated with diseases. The affected drugs span diverse indication areas, from asthma (montelukast) to depression (duloxetine and aripiprazole). Among the identified interactions, around 20 could be classified as bioaccumulation and seven as potential biotransformations. Drugs

like duloxetine and montelukast showed a strong tendency to get bioaccumulated by several bacteria. Drugs like levamisole and donepezil are likely biotransformed. Interestingly, bacteria, which deplete drug compounds from the medium, are usually not affected in their growth by those compounds (at the screening concentration of 50 μ M). However, drugs like loperamide and duloxetine do affect a broader bacteria spectrum in their growth, and act both as inhibitor and promoter of bacterial growth in a strain dependent manner. Considering up to 1000 gut bacterial strains and a few thousand existing host-targeted drugs, I only tested a small part of all possible bacteria-drug interactions, and that too at only one drug concentration. Even in this limited sampling space, the number of hits found is quite high. As both the bacterial species and the affected drugs span a wide diversity, these results suggest that bioaccumulation of drugs is a common and hitherto underappreciated mode of bacteria-drug interactions.

As a case in point, the results from this bacteria-drug interaction study are followed upon in more details through investigation of interactions involving duloxetine – a widely used antidepressant. I found that duloxetine induces higher diversity in synthetic bacterial communities, and its bioaccumulation by community members affects the community dynamics (Figure 15 on page 66). The shift in community composition upon duloxetine exposure cannot be fully explained by the observed growth defects of bacterial species in monoculture as derived from duloxetine IC₅₀ estimations. Duloxetine-depleting bacteria additionally alter the dynamics of this shift, as duloxetine concentration is lower in communities consisting of more duloxetine depleting bacteria.

6.1.2 Bacterial NADH:quinone dehydrogenase and purine metabolism are likely affected by duloxetine

As I found gut bacteria-duloxetine interactions to be common *in vitro* and having an impact on bacterial community assembly, I aimed to investigate the underlying mechanisms. Using an untargeted metabolomics approach to characterize extracellular metabolites, I found that duloxetine affects the native metabolism of *B. uniformis* and *C. saccharolyticum*, in particular the purine

metabolism (Table 4 on page 88). These effects might in turn influence bacterial behavior in a community. To find the direct protein targets of duloxetine in *C. saccharolyticum*, I used click chemistry-based methods and proteomics. Two of the five strongly enriched duloxetine-binding proteins are part of a NADH:quinone dehydrogenase complex (Table 6 on page 102). Other moderately enriched proteins are part of the purine pathway (Table 7 on page 104). Figure 29 summarizes findings in the purine pathway from both metabolomics and proteomics experiments for *C. saccharolyticum*. Enriched enzymes in the purine pathway are AIR synthase, adenine phosphoribosyltransferase (ARPT), xanthine dehydrogenase (Xdh) and nucleoside-triphosphatase. Additionally, one protein of the xanthine dehydrogenase (XdhB homolog) showed a divergent sequence homology in *E. coli* strains corresponding to their divergent duloxetine response (Figure 25 on page 101). Metabolites that are products of enriched proteins like AIR or otherwise closely connected in the pathway like guanosine or pentose phosphates are enriched too. Thus, duloxetine is likely to affect bacterial metabolism in the purine pathway by directly binding to nucleotide or nucleoside binding proteins like xanthine dehydrogenase as well as by inhibiting the NADH:quinone dehydrogenase directly.

6.2 Discussion

For a more detailed discussion on effects of specific drugs see the respective discussion 2.3 on page 53. Here I will focus on more general effects and highlight implications for pharmacokinetics and gut microbiome ecology. I will mention interesting findings from other drugs but in general focus more on the case of duloxetine and depression as it has been intensively investigated in this PhD work. For each discussion point, I will also suggest further experimental approaches to test the discussed effects or mechanisms.

Albeit in general, as gut bacteria are neither functionally nor biochemically well characterized yet in comparison to model organisms like *E. coli* or *B. subtilis* and the found bacteria-drug interactions are likely sensitive to media and oxygen differences, any follow-up study will suffer from a limitation of tools. For example, genetic tools like generation of knockouts or overexpression mutants are often not easily transferable to bacteria from environmental isolates. Defined or minimal media to efficiently characterize the metabolic state of bacteria using tracer methods have not been described yet or many bacteria-drug interactions were sensitive to a change in media condition when tested. Thus, in many cases further investigations will require the adaptation of molecular biological methods to the respective investigated bacterial strain, or even strain-drug interaction.

6.2.1 Side effects of host-targeted drugs are mediated through the gut microbiota

In recent years the connection between microbiota and drug side effects has often been discussed and many links and examples have been found (Spanogiannopoulos et al. 2016; Sousa et al. 2008; Wilson & Nicholson 2016; Swanson 2015). In a few cases, drug dosages or drug side effects could be linked to bacterial drug bioaccumulation or metabolism (Hashim et al. 2014; Wallace et al. 2010). In other cases, comorbidity due to an induced shift in gut microbiota composition seems likely (Bahr et al. 2015; Bahra et al. 2015). Furthermore, the

gut microbiota can influence hepatic host drug metabolism directly (Claus et al. 2011; Selwyn et al. 2015) and indirectly through bile acid metabolism (Klaassen & Cui 2015; Sun et al. 2016).

Here, I showed that gut microbial bacteria specifically sequester drugs in many cases, and that they are affected in growth in other, often different cases. However, differences between bioaccumulation and an effect on bacterial growth might be concentration dependent as seen for duloxetine. Thus, a gut microbiota-mediated sponge-like effect altering drug dosage might occur already before a direct antimicrobial effect is observed. Furthermore, bioaccumulation did change bacterial native metabolism and community composition dynamics suggesting that drug side effects might occur through a change in microbiota composition already at comparatively low drug concentrations. It should be noted that bacteria considered probiotic like Bifidobacteria show the same tendencies for bioaccumulation as normal commensals. If we assume that gut microbiota-drug interactions are the norm rather than exception as potentially indicated by my study, then bioaccumulation is the basic bacteria-drug interaction mode and xenobiotic metabolic biotransformation of drugs are potentially more severe but also more exceptional cases.

Side effects like increased risk of heart attacks cannot always be linked to a shift in gut microbiota composition only. Often the native gut microbiota metabolism directly plays a role as is the case of bacterial trimethyl amine production from dietary choline and subsequent conversion to pro-atherosclerotic metabolite TMAO by the host (Wang et al. 2011). As bioaccumulation of drugs can lead to a change in bacterial metabolism, as shown in this study for the case of duloxetine, it can consequently cause long lasting but hard to detect side effects. Most of the tested drug compounds in this study treat chronic diseases like arteriosclerosis, asthma, or depression and patients use them for years at a time. Thus, implications of drug bioaccumulation in bacteria on development of heart diseases, obesity and other metabolic disorders in patients should be considered carefully.

As only 3 out of 12 growth affected bacteria are gram-negative, the bacteria-drug interaction screen indicates that gram-negative bacteria are better protected from growth defects than gram-positive bacteria. Of the two major phyla in the gut microbiome, Bacteroidetes is gram-negative, and Firmicutes is gram-positive. Thus, upon regular drug exposure a shift towards Bacteroidetes might occur in the gut microbiome of patients. However, as observed in the synthetic community assembly upon duloxetine exposure in this study, community dynamics can overrule expectations, and instead lead to rise in gram-positive bacteria. A high ratio of Firmicutes to Bacteroides has been associated with unfavorable developments like metabolic syndrome or obesity, and mouse models and one human case study suggests that this is causative (Musso et al. 2011; Alang & Kelly 2015). In many cases however, there is still conclusive evidence missing that a change in microbiome composition is a cause for rather than a consequence of disease development in humans. *In vitro* studies might help to point to mechanisms through which the gut microbiota interacts with the host.

For potential xenometabolic interactions like *R. gnavus* with montelukast or *B. thetaiotaomicron* and duloxetine, an untargeted metabolomics study of a time course experiment would be needed to identify bacterial drug metabolites and potential reaction mechanisms. With mutagenesis assays like the Ames test (Mortelmans & Zeiger 2000; Gatehouse 2012), cell viability assays (Hansen & Bross 2010) or Caco2 cell permeability assays (Press 2011), crude extracellular metabolite mixes of bacteria-drug interactions or specific bacterial drug metabolites once identified can be tested for host toxicity. Also effects on the protective mucus layer should be investigated *in vitro* (Liu et al. 2014; Li et al. 2015). Drug compounds with indications for strong deleterious effects in *in vitro* assays can then be further tested in *in vivo* mouse models to investigate host immune system-gut microbiota feedback interactions (Claus et al. 2011). Additionally, the same assays can be used to investigate if a shift in bacterial native metabolism or microbial community composition as caused by bioaccumulation is associated with production of toxic or otherwise unfavorable compounds.

6.2.2 Duloxetine influences depression symptoms through impact on gut microbiota

Recent research suggest that the gut microbiome is able to influence the development of depression through the immune system and the hypothalamo-pituitary-adrenocortical (HPA) axis (Kelly et al. 2015; Foster & McVey Neufeld 2013). Kelly et al. (2015) suggest a weakening of the gut barrier, respective low-grade inflammation and its influence on the HPA axis as causative in some instances of depression. Probiotics have been shown to improve barrier function and lighten mood (Kelly et al. 2015). Additionally, a diverse set of bacteria have been shown to increase production of serotonin, a major regulator in mood disorders like depression, especially by spore forming bacteria like Clostridiales species (Ridaura & Belkaid 2015).

In my study, duloxetine favored the rise of *Eubacterium rectale* in the bacterial community assembly. This bacterium is associated with short chain fatty acid production and consequently with increase in barrier function (Kelly et al. 2015; Swanson 2015). Furthermore, side effects of duloxetine like decreased appetite or constipation might be caused by a change in bacterial metabolism, which control or produce hormones controlling appetite and gut motility in the host (O'Mahony et al. 2015; Clarke et al. 2014). Side effects of antidepressants like weight gain have already been linked to a change in microbiota composition (Bahra et al. 2015). While it is possible that duloxetine directly influences serotonin production in host cells, it is also possible that duloxetine indirectly modulates serotonin levels through influencing the metabolism of Clostridiales species producing serotonin (O'Mahony et al. 2015). Thus, it is likely that duloxetine not only directly mediates relief from depression by inhibition of the serotonin reuptake in the brain, but also indirectly through the microbiota composition, which in turn can alleviate depression. In conclusion, the therapeutic targeting of the gut microbiota to alleviate depression symptoms, for example as suggested by O'Mahony et al. (2015), might already be one of the mechanisms underlying the mode of action of the antidepressants in current use. Further research in this area including

population cohort studies and placebo-controlled intervention trials as well as more mechanistic approaches in mice will likely clarify the impact of the gut microbiota on depression and respectively the impact of antidepressants on the gut microbiota in the near future.

6.2.3 Deprotonated, negatively charged drugs are less likely to be sequestered

The bacteria-drug interaction screen showed a broad potential of gut bacteria to sequester drugs from the medium. At the same time, only comparatively few bacteria were found to be affected in growth. In particular, gram-positive bacteria were more often affected (9 out of 12 affected bacteria) than gram-negative bacteria (3 out of 12 affected). It has been shown before that gram-negative bacteria are often protected from antibiotics because they possess two cell membranes instead of one like the gram-positive bacteria (Delcour 2009). Additionally, gram-negative bacteria tend to have many efflux pumps increasing their resilience (Nikaido 1996). Many of the drugs have a higher pKa than the pH of the medium in the bacteria-drug interaction screen. This means that one or several functional groups of the drug compounds are protonated in the screen and possess a positive charge. Bacterial cell walls on the other hand possess negative charge due to the deprotonation of their teichoic acids or LPS compounds. The positive charge of the drugs might facilitate binding to the negatively charged bacteria cell wall. All drugs that are not sequestered and do not affect growth in the bacteria-drug interaction screen (rosuvastatin, tolmetin, tenofovir) are likely deprotonated and thus at least partially negatively charged in screening conditions. As most drugs are also lipophilic, once they are attached to the cell wall they might easily pass into or even through the cell membrane. In gram-positive bacteria, this means that drugs reached the cytoplasm and might interfere with essential cellular functions. In gram-negative bacteria, they are more likely to get stuck in the periplasm, due to the second membrane (Delcour 2009). Additionally, gram-negative bacteria tend to have more efflux pumps increasing their resilience (Nikaido 1996). However, this balance might be overcome with a

higher concentration of the respective drug and pushed towards growth arrest in gram-negative bacteria as well. In support of this idea, IC₅₀ values would be expected, on average for a specific drug respectively, to be higher in gram-negative bacteria than in gram-positive bacteria, but bioaccumulation should be equally strong across all affected bacteria as long as they grow equally well. Tendencies of this mechanism were found for duloxetine in this study, but the idea is speculative so far. Other experiments like testing for drug sequestration through cell-free LPS or teichoic acids in different pH conditions could clarify the relevance of this idea beforehand.

6.2.4 Potential of host-targeted drugs as antibiotic adjuvants

Many compounds in the bacteria-drug interaction screen have growth inhibitory effects on specific bacterial strains. Potentially, also many drugs that are sequestered can have growth inhibitory effects in a higher concentration on the same species as demonstrated for the case of duloxetine and *B. uniformis* (Figure 13 on page 64). Others, like montelukast might not influence the growth of bacteria at physiological concentrations at all, but still have an effect on bacterial physiology as they are sequestered. These compounds could potentially aid antibiotics to overcome resistant bacteria, target antibiotics more specifically to certain strains, and have additionally the advantage of being already tried and tested for use as pharmaceuticals.

This potential has long been realized (Kristiansen & Amaral 1997) and has recently amidst the antibiotic crisis come more into focus of research again (Ejim et al. 2011; Wright 2016). Currently, other screens in our institute are aimed at finding how prevalent gut bacterial growth defects through a wide-range of host-targeted drugs are or how prevalent their antibiotic adjuvant effects are (personal communication, Typas group, EMBL). For loperamide, an antibiotic adjuvant effect has already been described, and the underlying mechanism is likely the disruption of electron potential across bacterial membranes, which facilitates uptake and effect of antibiotics (Ejim et al. 2011). A good adjuvant should induce little to no growth defect itself as to avoid adaption and evolution of resistance

mechanisms in bacteria (Wright 2016). Under aerobic conditions, loperamide induced growth defects only at concentrations in the upper mM range fulfilling the proclaimed property (Ejim et al. 2011). In anaerobic conditions however, it affects the growth of many bacteria already at a low concentration of 50 μ M (Figure 11 on page 52), giving potentially leeway to development of resistance when not used in combination with antibiotics. Nevertheless, it might also increase its efficiency as antibiotic adjuvant when used to target species in the gut.

Interestingly, duloxetine affects similar species as loperamide, but in contrast to loperamide it is also sequestered from the medium. Thus, it is possible that duloxetine has a similar destabilizing effect on the bacterial cell membrane but caused by a different mechanism than in loperamide. Indeed I could show that duloxetine potentially binds the NADH:quinone dehydrogenase, a key enzyme responsible for the establishment of proton motive force across the bacterial membrane. In this case, duloxetine might also work as an antibiotic adjuvant just like loperamide. Other antipsychotics have already been shown to have potential as antibiotic adjuvant (Jeyaseeli et al. 2012; Munoz-Bellido et al. 2000). To explore such possibilities, duloxetine and other candidates like montelukast should be tested in combination with antibiotics, and their effects on growth should be determined for individual bacterial strains. Then, it would be interesting to test the combinatorial effect of adjuvant and antibiotic in a synthetic community assembly experiment to investigate if specific bacteria can be targeted in a community.

Additionally, the bacteria-drug interaction screen indicates that bacteria, which are resistant to a certain compound, are potentially less so under anaerobic conditions. Thus, besides being a reservoir for antibiotic resistance (Penders et al. 2013), the gut microbiota is potentially also an active site for the development of bacterial resistance, which might explain its high diversity of resistance genes.

6.2.5 Duloxetine inhibits bacterial NADH:quinone dehydrogenase and affects purine metabolism

As described in the discussion of the respective chapter 5.3 on page 108 in more detail, I suggested two potential binding sites for duloxetine on the bacterial NADH:quinone dehydrogenase at the quinone binding site or the NADH binding site. Inhibiting the electron transport chain commonly occurs at the quinone-binding site (Fato et al. 2008; Singer & Ramsay 1994), and a knockout does lead to a feedback into the purine pathway and excretion of those metabolites in bacterial species (Minato et al. 2014). Indeed, duloxetine with its naphthol group shows some similarity to a known inhibitor of the quinone-binding site (Dykens et al. 2008). Thus, it would also explain the findings from the untargeted metabolomics experiment. However, not proteins of the potential quinone-binding site of the dehydrogenase complex in the membrane were enriched in the pull-down, but proteins of the respective cytosolic NADH-binding site. Furthermore, other redox factor binding proteins like AIR synthase, xanthine dehydrogenase (Xdh) and adenine ribosylphosphotransferase (ARPT), key players of the purine pathway, were also enriched in the pull-down. Additionally, homologs of Xdh but not NADH:quinone dehydrogenase show divergent sequence similarity in *E. coli* strains divergently responding to duloxetine. Xdh is comparatively promiscuous; several inhibitors at the active site have been synthesized so far (B-Rao et al. 2012; Takano et al. 2005). Deficiency in Xdh leads to accumulation of adenine (Kojima et al. 1984), deficiency of APRT to accumulation of adenine or 2,8-dihydroxyadenine (Terai et al. 1995). Adenine was not strongly enriched in *C. saccharolyticum* in the untargeted metabolomics experiments, but was enriched in *B. uniformis*.

A targeted quantitative metabolomics study of intracellular and extracellular metabolites in *C. saccharolyticum* to reveal which part of the purine metabolism is strongly affected could support these ideas, and potentially differentiate between the two explanations pointing to the primary (bacterial) target of duloxetine. Also metabolites like 2,8-dihydroxyadenine, which is produced upon inhibition of ARPT, and other indicative non-standard metabolites can be found with this

method. The metabolomics data could be used to build a metabolic model describing the expected effects of NADH:quinone dehydrogenase or purine pathway members inhibition and rearrangements in the metabolic fluxes in the downstream pathways.

Additionally, after a stringent and detailed comparison of gene homology, an improved assay of gene knockout and overexpression of *C. saccharolyticum* homologs of NADH:quinone dehydrogenase or purine pathway members in *E. coli* could give indications of binding. Overexpression mutants for proteins inhibited by duloxetine, might escape growth defects induced by duloxetine as inhibition is titrated out. If bioaccumulation is protein dependent as well, knockout mutants of proteins causative for bioaccumulation should deplete less duloxetine from the medium as non-causative protein knockout mutants. Furthermore, protein candidates from *C. saccharolyticum* can be overexpressed and purified and their duloxetine binding affinity and further biochemically properties can be characterized directly. For *in vivo* relevance, duloxetine needs to be able to bind in competition to or at least in presence of the native substrate, which can be tested in a competition assay on the purified enzyme.

6.3 Conclusion

In my PhD work, I identified almost 50 novel gut bacteria-drug interactions suggesting that similar interactions are likely to be more prevalent than expected so far. For most of the identified interactions, the drugs were bioaccumulated rather than biotransformed. Bioaccumulation is thus potentially a widespread but so far underappreciated mode of bacteria-drug interaction. My study also shows that drug bioaccumulation can impact bacterial metabolism without strong or even no effect on bacterial growth. Within a bacterial community the consequences of these effects, bioaccumulation and growth defects, are hard to predict from monoculture growth alone. For example, exposure to Duloxetine, a widely used antidepressant, led, unexpectedly, to a higher diversity in a synthetic community. As bacteria can affect the effective dose of a host-targeted drug

through bioaccumulation, and/or change its activity spectrum through biotransformation, the findings from this study have broad and far-reaching relevance for drug dosage decisions and personalized medicine. Consequently, potential bacterial off-target effects as cause for drug side effects also need to be taken into account during drug design and clinical trials.

7 Materials and Methods

7.1 Growth conditions and media

Unless otherwise indicated, all bacteria were grown as liquid cultures in Gut Microbiota Medium (GMM) (Goodman et al. 2011). Cultivations were carried out in a Vinyl Anaerobic Chamber (COY, USA) at 37°C with oxygen below 20ppm, 15% carbon dioxide and 1.8-2% hydrogen. Main gas in the anaerobic chamber is nitrogen. All experimental cultures were started from the second passage culture after inoculation from a glycerol or DMSO stock. Depending on the bacterial species, one passage might take up to 48h to grow. The recipe for GMM can be found in Table 8. All media, buffer, glass and plastic ware used had been exposed to anaerobic conditions at least 12h prior usage.

Table 8: Gut Microbiota Medium (GMM)

Component	Amount/L	Concentration	Comments
Tryptone Peptone	2 g	0.2%	
Yeast Extract	1 g	0.1%	
D-glucose	0.4 g	2.2 mM	
L-cysteine	0.5 g	3.2 mM	
Cellobiose	1 g	2.9 mM	
Maltose	1 g	2.8 mM	
Fructose	1 g	2.2 mM	
Meat Extract	5 g	0.5%	
KH ₂ PO ₄	100 mL	100 mM	1M stock solution pH 7.2
MgSO ₄ -7H ₂ O	0.002 g	0.008 mM	
NaHCO ₃	0.4 g	4.8 mM	
NaCl ₂	0.08 g	1.37 mM	
CaCl ₂	1 mL	0.80%	0.8g/100mL stock
Vitamin K (menadione)	1 mL	5.8 mM	1 mg/mL stock solution
FeSO ₄	1 mL	1.44 mM	0.4 mg FeSO ₄ /mL stock solution
Histidine Hematin Solution	1 mL	0.1%	1.2 mg hematin/mL in 0.2M histidine
Tween 80	2 mL	0.05%	25% stock solution
ATCC Vitamin Mix	10 mL	1%	
ATCC Trace Mineral Mix	10 mL	1%	
Acetic acid	1.7 mL	30 mM	
Isovaleric acid	0.1 mL	1 mM	
Propionic acid	2 mL	8 mM	
Butyric acid	2 mL	4 mM	
Resazurin	4 mL	4 mM	0.25 mg/mL stock solution
pH 7.2 corrected with 10M KCl			

For conjugation of overexpression plasmids bacteria were grown in LB liquid medium or on LB agar plates (2% w/v). LB recipe can be found in Table 9.

Table 9: Recipe for LB medium.

<u>LB medium</u>
1% (w/v) Bacto tryptone
0.5 % (w/v) Bacto yeast extract
0.5 % (w/v) NaCl

7.2 UPLC methods

7.2.1 UPLC-UV methods

Liquid chromatography is a method widely used to separate specific compounds from a mixture and identify them based on comparisons to standards. The methods used here use UV absorption and elution time for identification. To be able to measure all selected drugs within one screen with the available instrument, chromatographic conditions needed to be optimized using a maximum of 4 different mobile phases, while two of them needed to be water and an organic phase respectively. Another parameter for optimization was time. For optimal separation of compounds a longer chromatography with a less steep gradient is usually preferable. However, this would increase the measurement time for the whole screen strongly since approximately 6000 injections were to be expected. Once established, the same methods were used throughout the whole study.

All liquid chromatography methods are run on a Waters Acquity UPLC H-Class instrument with a PDA detector and a quaternary solvent system. All established methods are 5 minutes long, have a flow rate of 0.5ml/min and run on a CSH C18 column (Waters, Part number 186005297) in reverse mode. The column is heated to 40°C and samples are kept at 6°C. All methods use 50% acetonitrile (Biosolve, ULC grade) for washing buffer, and 50% methanol (Biosolve, ULC grade) for purging buffer. As organic mobile phase acetonitrile was used. The assay was optimized using only two buffers besides water as hydrophilic mobile phase: 5mM formic acid (Biosolve, ULC grade) of pH 3.2 and

5mM ammonium formate (Ammonium hydroxide, ACS grade, Sigma) with pH adjusted to 8.3 using the formic acid buffer. Table 10 lists the five different chromatographic methods established for the different drugs. The specific chromatographic method used for identification of each drug compound can be found in Table 11.

Table 10: UPLC methods.

	From min	To min	Acetonitrile	Formic Acid Buffer	Ammonium Formate Buffer	Water
Method A	0	1.5	5%	0%	65%	30%
	2.5	3	60%	0%	40%	0%
	3.5	5	5%	0%	65%	30%
Method B	0	1.5	5%	65%	0%	30%
	2.5	3	60%	40%	0%	0%
	3.5	5	5%	65%	0%	30%
Method C	0	1.5	20%	60%	0%	20%
	2.5	3	80%	20%	0%	0%
	3.5	5	20%	60%	0%	20%
Method D	0	1.5	5%	0%	95%	0%
	2.5	3	50%	0%	50%	0%
	3.5	5	5%	0%	95%	0%
Method E	0	1.5	40%	60%	0%	0%
	2.5	3	95%	5%	0%	0%
	3.5	5	40%	60%	0%	0%

Table 11: UPLC method description by drug

Drug compound	UV absorption (nm)	Second channel (nm)	UPLC Method	Peak elution time (min)	Caffeine elution time (min)
Acetaminophen	244	-	A	1.5	3
Aripiprazole	255	-	B	3.3	3
Donepezil	268	-	B	3.2	3
Duloxetine	230	-	B	3.3	3
Digoxin	220	-	B	3.5	3
Ezetimibe	234	-	C	3.5	0.7
Loperamide	220	-	B	3.5	3
Metformin	234	-	D	0.7	3.1
Montelukast	344	274	E	3.8	0.5
Metronidazole	330	274	A	1.9	3
Levamisole	225	-	A	3.5	3
Ranitidine	313	274	A	3.3	3
Roflumilast	245	-	C	3.6	0.7
Rosiglitazone	247	-	B	3.1	3
Rosuvastatin	241	-	C	3.3	0.7
Simvastatin	247	-	E	3.7	0.5
Sulfasalazine	254	-	C	3.7	0.7
Tenofovir	260	-	B	3.4	3
Tolmetin	320	274	C	3.4	0.7

7.2.2 Data analysis

A general approach to analysis data from UPLC methods is described here. If not indicated otherwise, all chromatographic data is handled this way. For data analysis of the bacteria-drug interaction screen, see respective method 7.3.3.

All chromatograms are annotated with the vendor specific program Empower 3, and manually curated for peak identification. Readout for all chromatograms is baseline corrected area under the curve of the drug peak and the internal standard peak respectively. This raw data is further analyzed using statistics software environment R and respective packages.

Each drug peak is normalized by the respective caffeine peak (used as internal standard) from the same chromatogram. If a new peak appeared in the drug-free bacteria control, which is coeluting with the drug peak, the mean of the normalized values from the control was subtracted from the mean of the normalized values from the experimental samples. Corrected normalized means of the experiment samples were then compared to the mean of the respective bacteria-free drug control and a Student's t-test was used to assess if they are significantly different. If more than 10 interactions were tested in one assay, the false discovery rate was controlled at alpha level 0.05 using Benjamini-Hochbergs method (Benjamini & Hochberg 1995).

If samples from different experimental batches or different UPLC runs were compared with each other, all samples were normalized by the mean of the bacteria-free control from the respective batch. This allows statistical testing comparisons by keeping the relative mean and variation of the respective batch, but adjusting for differences in absolute means caused by methodological differences.

7.3 Bacteria-Drug Interaction Screen

7.3.1 Drug Selection

As a starting point I used the SIDER database (Kuhn et al. 2010), listing 4492 unique side effects for 996 medical drugs as accessed on 7.2.2014. The SIDER database extracts these side effects from publicly available websites and patient information leaflets. I defined two sets of side effects: one loosely associated with symptoms related to the gut or gut microbiome including symptoms like “Vitamin B deficiency” or “Atherosclerosis” (190 terms in Appendix A), the other one more strict only focusing on terms directly related to the gut like “Flatulence” or “Weight fluctuations” (36 terms in Appendix A). For 121 of the 996 drugs, more than 10% of their respective side effects were loosely associated with the gut, and for 93 drugs more than 5% of their respective side effects were strictly associated with the gut. 63 drugs fulfilled both conditions, and were further scrutinized.

I enriched the list with drugs that have a high sales volume (indicative of clinical relevance), drugs that had been withdrawn from the market for side effects that might involve the microbiome as a cause, and drugs that are on the WHO list of essential medicine (World Health Organization 2015). Additionally, drugs that had already been shown to impact the gut microbiome as collected by the Pharmacomicromicrobiomics database (Saad et al. 2012) were considered for the screen. I manually curated this list of approximately 120 drugs, and annotated it with data from ChEMBL (Bento et al. 2014) and DrugBank (Law et al. 2014).

From these compounds I selected only drugs that are administered orally to the patient. This could increase the chance of exposure of the gut microbiome to the drug before first pass metabolism, especially if the drug is poorly absorbed in the stomach. Thus, I prioritized drugs with a long biological half-life and low bioavailability. I excluded antibodies or other peptide-like drugs as I assumed a high likelihood of them being metabolized as nutritional source. Also drugs with a molecular weight higher than 500 Dalton were generally excluded to focus on small molecule drugs. The resulting roughly 60 drugs were manually curated and

selected for availability from vendors and implementation of UPLC methods within a screening context. For the 18 drugs listed in Table 2 on page 40 I established reliable chromatographic methods as described in the previous method section 7.2.

7.3.2 Experimental setup

For all drugs, I used a fixed concentration of 50 μM , which in most cases approximates the concentration of one pill (0.02-3 mmol) diluted in the volume of the gut (approx. 2.5 L). As shown in the plate outline in Figure 30, I used one bacteria-free control per plate and drug, but triplicates for each bacteria-drug interaction. The screen was carried out under anaerobic conditions in 96-well plates (Nunclon Delta Surface 163320, NUNC) with 150 μl GMM as the growth medium sealed with a Breathe-Easy[®] sealing membrane (Z380059, Sigma-Aldrich). Plates containing 100 μl of the medium and 75 μM of the drug were prepared beforehand, stored at -20°C and used as needed.

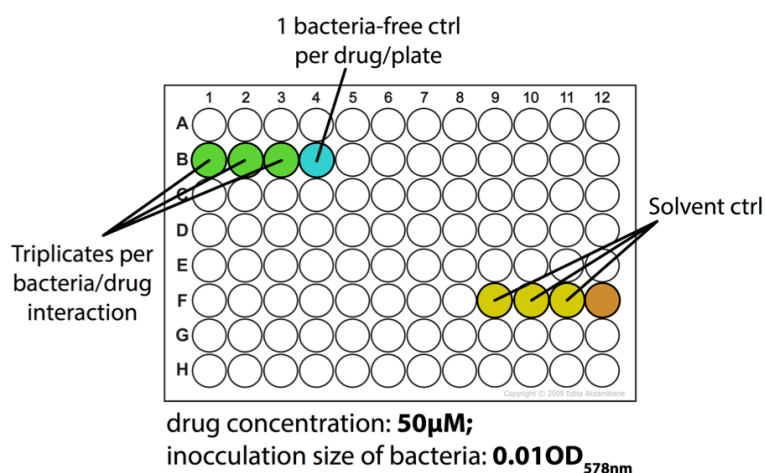


Figure 30: Outline of bacteria-drug interaction screening plates.

Each sample involving the growth of bacteria is tested in triplicates per plate. Drug controls, which are bacteria-free, are tested in singlets per plate. Per plate one bacterium is tested with all drugs in the screen.

Frozen plates were introduced into the anaerobic chamber the evening before inoculation. Wells were inoculated with 50 μl of a second overnight culture with an end OD_{578} of 0.01. Growth was monitored with measurements of the optical density at 578 nm using an Eon Microplate Spectrophotometer (BioTek) approximately every 2h for the first 10h, then approximately every 6h. After 48h,

plates were removed from the anaerobic chamber and the bacteria spun down (4000 rpm, 10 min). Then, 100 μ l of the supernatant was extracted in 300 μ l ice cold acetonitrile:methanol (Biosolve, ULC grade) in 500 μ l polypropylene plates (Corning Costar 3957) to remove compounds interfering with liquid chromatography. Plates were closed with a lid (Corning, storage mat 3080) and after shaking and 15 minutes incubation at 4°C, samples were centrifuged at 4000 rpm for 10 min at 4°C and 300 μ l of the supernatant were transferred to a new plate (Corning Costar 3362). All liquid handling outside of anaerobic chamber was done using a liquid handling robot (FXp, Biomek). Sample plates were then left overnight in a chemical hood to evaporate the organic phase, before being stored at -20°C. For estimating the drug concentration in the samples with the UPLC, samples were reconstituted in 50 μ l 20% acetonitrile solution containing 250 μ M caffeine (Sigma) as an internal standard. The bacteria-drug interaction screen was conducted with two biological replicates. Table 1 contains a list of bacteria in the screen.

Under the same conditions I tested also two different mixes of five bacteria each. One mix consisting of bacteria depleting many drugs: *C. saccharolyticum*, *C. ramosum*, *B. uniformis*, *B. animalis lactis*, and *F. nucleatum*; the other mix consisting of bacteria not depleting drugs: *L. plantarum*, *L. paracasei*, *B. fragilis*, *L. lactis*, and *B. vulgatus*. Second overnight cultures from those bacterial strains were mixed before inoculation, and wells were inoculated with 50 μ l of the premix resulting in an end OD₅₇₈ of 0.01 for each bacterium. Otherwise, mixes were treated as described above for monocultures.

7.3.3 Data analysis

For drug depletion analysis, area under the curve (AUC) from drug peak was normalized by AUC from the internal standard caffeine (corresponding peak of the same chromatogram). Then for the triplicates for each bacteria-drug interaction the mean was compared to the bacteria-free control from the same plate. If the bacteria-free control was contaminated for that interaction, the triplicates were compared to the median of controls from the same column batch

(all plates measured on the same LC column). If for both biological replicates the difference was 30% or more, the interaction was considered a hit. For each hit the mean depletion from both biological replicates was then calculated.

For growth effect analysis, growth curves were manually annotated with maximum OD reached, to correct for irreproducible “overgrowing” for certain species of bacteria. Triplicates of bacteria-drug samples were then compared to triplicates of solvent control with Student’s t-test, and if differences were significant in both biological replicates, the interaction was considered a hit. For each hit, the mean of the differences of maximum OD from both biological replicates was then calculated as the effect size.

7.4 Community Assembly Assay

7.4.1 Experimental Setup

Two different species mixes were prepared, one with *B. uniformis* and one without. Other species in the mix were *B. thetaiotaomicron*, *E. rectale*, *L. gasseri*, *R. torques* and *S. salivarius*. Overnight cultures of the bacteria were diluted to OD₅₇₈ 0.5 and 500 µl of each species culture was mixed in a 5ml eppendorf tube (5+GMM or 6 species respectively). A 10 mM working solution of duloxetine and DMSO in PBS was prepared to be used throughout the assay. 5 mL polystyrene tubes (round bottom, Falcon, Corning Mexico) were prepared with 1950 µl GMM plus 10 µl drug/DMSO solution plus 40 µl species mixture for each transfer respectively. Tubes were incubated for 48h non-shaken anaerobically at 37°C. After the first inoculation, the transferred species mix was from the end point of the earlier cultivation. For DNA extraction, 1mL of the remaining culture was centrifuged for 10 min 14.000 rpm in 1.5 mL eppendorf tube. 200 µl supernatant was transferred to a new 1.5 ml eppendorf tube, rest of supernatant was removed and then the bacteria pellet was frozen at -80°C until DNA extraction. For drug extraction 600 µl of cold ACN:MethOH was added to supernatant and incubated for 15 min in fridge. Then samples were centrifuged for 10 min 14.000 rpm 4°C,

700 µl of sample was transferred to new tube and then samples were dried in a speedvac (Eppendorf Vacuum Concentrator Plus) for 5h at 30°C at V-AL mode. For UPLC measurement samples were reconstituted in 116 µl 20% ACN containing 250 µM caffeine.

7.4.2 DNA extraction and 16S barcode sequencing library preparation

Bacteria pellets were dissolved in lysis buffer and transferred into a 96 Polypropylene Deep Well plate (3959, Corning). An in-house protocol was used for DNA extraction. The GNOME DNA isolation Kit (MP Biomedicals) was adapted to be used with the Biomek® FXp Liquid Handling Automation Workstation (Beckman). Subsequently, purified DNA was obtained using ZR-96 DNA Clean & Concentrator™-5 (D4024, Zymo Research).

After the integrity of the DNA was verified by agarose gel electrophoresis, DNA concentration of the samples was determined using the Qubit dsDNA BR assay kit (Q32850, life technologies) in combination with the Infinite® M1000 PRO plate reader (Tecan). The 16S V4 amplicons were generated using an Illumina-compatible 2-step PCR protocol: In a first PCR the 16S V4 region was amplified with the primers F515/R806 (Caporaso et al. 2011) and then in a second PCR barcode sequences were introduced using the NEXTflex 16S V4 Amplicon-Seq Kit (4201-05, Bioo Scientific).

After multiplexing equal volumes of PCR products from each sample, SPRIselect reagent kit (B23318, Beckman Coulter) was used for left-side size selection. Prior to Illumina sequencing the quality of the library was controlled using the 2100 BioAnalyzer (Agilent Technologies) and the DNA concentration was determined using the Qubit dsDNA HS assay kit.

Sequencing was performed using a 250 bp paired-end sequencing protocol on the Illumina MiSeq platform (Illumina, San Diego, USA) at the Genomics Core Facility (EMBL Heidelberg).

7.4.3 16S barcode sequencing analysis

The raw Illumina paired-end reads were quality trimmed and length filtered using CUTADAPT with quality threshold of 30 and length cutoff of 150 bp (Martin 2011). The forward and reverse pairs were subsequently merged using Paired End 138ead MergerR with minimum overlap of 20 bp (Zhang et al. 2014). The merged amplicon sequences were compared to the 16S rRNA gene of the species mixed for coculture using UCLUST (Edgar 2010). Only those that have minimum 98% identity were clustered into the operational taxonomic units (OTUs). The species abundance was normalized by the 16S rRNA gene copy numbers. Data was visualized using the plotly library (Dimitrov 2014).

7.5 Other *in vitro* assays

7.5.1 Depletion-mode assay

The bacteria-drug interaction screen is designed to find potential drug interactions by screening for depletion of the drug from the medium. However, since in the screen the bacteria are removed before the extraction this leaves the question whether the drug is bound to or accumulated by the bacteria or if it is also biotransformed or metabolized. To distinguish between these two possibilities, bioaccumulation and xenometabolism, and also to further confirm the screening hits, I designed a depletion-mode assay.

Bacteria from an overnight culture are inoculated with an OD₅₇₈ of 0.01 in 1 mL GMM containing 50 µM drug of interest in 2 mL eppendorf tubes and incubated for 48h while shaking. After finishing growth, the cultures were removed from the anaerobic chamber. 800 µl of each sample was transferred to a new eppendorf tube, while the remaining 200 µl were **directly extracted** by adding 600 µl ice-cold acetonitrile:methanol solution and incubated for 15 min at 4°C. For the **indirect extraction**, the transferred culture was centrifuged for 5 min at 14.000 rpm to pellet the bacteria, and 200 µl of the bacteria-free supernatant was extracted in a new eppendorf tube respectively. After the 15 min 4°C incubation

period, all samples were centrifuged for 10min, 14.000rpm at 4°C and 700µl of the supernatant was transferred to a new eppendorf tube. Samples were dried for 5-7h at 30°C in a speedvac (Eppendorf Vacuum Concentrator Plus, V-AL mode) and stored at -20°C until used for UPLC measurement. Samples were reconstituted in 116µl 20% acetonitrile containing 250µM caffeine. All interactions and controls were tested in triplicates.

7.5.2 Growth curves for IC50 determination

A dilution curve of duloxetine ranging from 1mM to 5mM was prepared in DMSO and then added to GMM. End concentration of DMSO was 1%. Bacteria from second overnight culture were diluted to an OD₅₇₈ of 0.5. 100 µL of medium was distributed in 96 well plates (Nunclon Delta Surface 163320, NUNC), inoculated with 1 µl to a final OD₅₇₈ of 0.005 and sealed with a Breathe-Easy® sealing membrane (Z380059, Sigma-Aldrich). Growth was monitored every hour for 24h using an Eon Microplate Spectrophotometer (BioTek) equipped with BioStack Microplate Stacker (BioTek) and a surrounding self-designed incubator.

For IC50 calculation a local regression curve was fitted to data from triplicates using R's loess function with a span parameter of 0.5. From this half the maximum OD was inferred. Then the closest time point was selected where bacteria growth first passed half the maximum OD, being a close estimate to the turning point of the exponential growth phase. For this time point the fitted ODs from the duloxetine dilution curve were used for estimation of 50% of total the concentration inhibiting 50% of the growth (IC50).

7.5.3 Resting Cell and Lysate assay

For further characterization of hits from the bacteria-drug interaction screen with metabolomics and proteomics methods, interactions were tested in media-free conditions. The use of media-free conditions allowed reducing the complexity due to media components and highly active endogenous bacterial metabolism.

Bacteria were grown in a volume of 30 mL or more in standard conditions to maximum OD₅₇₈, approaching or reaching stationary phase. Cultures were pooled

in 50 mL falcons and pelleted by centrifugation (2000-4000 rpm, 10 min). Media was discarded; cells were resuspended in 2 mL buffer and transferred to an eppendorf tube. Cells were washed 2 more times in 2 mL buffer (centrifugation 9.000 rpm, 5 min, 4°C) before used further.

For a resting cell assay, cells were resuspended in buffer, and exposed to experimental conditions as indicted. At the end of the experiment, all samples were extracted **indirectly** in a ratio of 1:3 sample:organic phase, as described in the depletion-mode assay method 7.5.1.

For a lysate assay, up to 1mL cell suspension was added to 500µl 300µm glassbeads in a screw cap tube and cells were lysed for 1min at 4°C using a bead beater. Then, cell debris and beads were spinned down (14.000 rpm, 5min). The cell lysate was then exposed to experimental conditions as indicated.

While all transfers were anaerobic, centrifugation, bead beating and ultrasound steps had to be implemented outside the anaerobic chamber. Eppendorf and screw cap tubes close tight enough for minimal oxygen exposure during these steps.

7.5.4 Duloxetine pull down assay

To enable a pull down of proteins interacting with duloxetine we decided in collaboration with Schultz group at EMBL to introduce an alkyne group at the methyl group of duloxetine. Felix Hövelmann (Schultz group, EMBL) synthesized the molecule. After synthesis and clean up, he linked the functionalized duloxetine to desthiobiotin using a click-chemistry enabled reaction. In collaboration with Thomas Bock (Beck group, EMBL) we could consequently captured the functionalized desthiobiotin-duloxetine on streptavidin magnetic beads.

Bacterial suspensions of *Clostridium saccharolyticum* (1 ml, anaerobic conditions) were lysed by bead disruption (lysate preparation see method 7.5.3) and additional sonication at 4 C (two times at 75% amplitude/0.5 s cycle for one minute, Hielscher sonicator). Supernatant after centrifugation at 20000 x g at 4 C for 10 minutes containing protein lysate was recovered and protease inhibitors (aprotinin 10 µg/mL, leupeptin 5 µg/mL) were added.

For all duloxetine-protein pull-downs, Strep-Tactin® Sepharose® 50% suspension (#2-1201-025, IBA) was used. For each sample, 400 µl Strep-Tactin Sepharose (50% suspension) was pre-washed three times using 400 µl PBS (pH=7) at room temperature. Beads were bound to duloxetine before addition of the protein lysate by resuspension in 400 µl PBS containing 50 µM duloxetine (control) or 50 µM duloxetine linked to desthiobiotin (for pull-down) on a rotating wheel at room temperature for 30 minutes. Unbound drug was removed by three PBS wash cycles (400 µl each).

Protein lysates were incubated with drug-bound beads on a rotating wheel at 4°C over night. Unbound proteins were removed by washing the beads with cold PBS. Bound proteins were recovered by competitive elution using PBS containing 5 mM Biotin. After an SDS gel using stain-free SDS-PAGE imaging technology (BioRad) showed protein integrity, samples were further processed for mass spectrometry-based protein identification. The pull down was conducted in quadruplicates for each treated and control sample.

7.5.5 Homologous overexpression of protein candidates

First, selected strains from an overexpression plasmid library were conjugated into *E. coli* BW25113 Δ tolC::aphT background. The low copy expression plasmid clone library (Transbac library (Otsuka et al. 2015)) in the diaminopimelic acid (DAP) auxotrophic BW38029 (Hfr by CIP8) background was grown on LB agar plates supplemented with 10 µg ml⁻¹ tetracycline and 0.3 mM DAP. The selected donor strains were manually picked from the library and arrayed in 96-format onto one LB agar plate.

The receiver strain (BW25113 Δ tolC::aphT) was grown to stationary phase, diluted to an OD₅₇₈ of 1 and streaked out on a mating plate (LB supplemented with DAP). Plates were dried for 1 hour at 37°C and the donor strains were pinned on top of the donor strain layer using a Singer robot. Conjugation was carried out at 37°C for 5 – 6 hours. After conjugation mixtures were pinned on LB plates supplemented with tetracycline. Three selection rounds ensured successful mating events. For glycerol stocks conjugated bacteria were inoculated in 100 µl

LB supplemented with 10 µg ml⁻¹ tetracycline in a 96 well plate and after overnight incubation at 37°C 20µl of a sterile 80% glycerol solution was added. Glycerol stocks were kept at -80°C.

Overexpression was conducted in 96-well plates (Nunclon Delta Surface 163320, NUNC) in 100µl GMM supplemented with 10µg/ml tetracycline. Bacteria from second pre-culture in GMM supplemented with 10µg/ml tetracycline and 200µM IPTG were inoculated with a final OD₅₇₈ of approximately 0.01 and plates were sealed with a Breathe-Easy® sealing membrane (Z380059, Sigma-Aldrich). After 8h incubation at 37°C membranes were removed, 50µl of the same media additionally containing 50µM duloxetine or respective amount of DMSO as control was added and plates were sealed again for a further 43h incubation. Plates were then extracted and further treated as described for the bacteria-drug interaction screen, method section 7.3.2.

For data analysis after normalization by caffeine internal standard, samples were normalized by mean of bacteria-free drug control from the respective plates and then compared using student's t-test with an alpha level below 0.05.

7.5.6 Heterologous overexpression of protein candidates

E. coli TOP10 strains with a pET151/D-TOPO plasmid containing the codon-optimized gene for the respective *C. saccharolyticum* protein candidate were designed at and ordered from Genart (Thermo Scientific). Plasmids encoded for ampicillin resistance. Overexpression was conducted in 96-well plates (Nunclon Delta Surface 163320, NUNC) in 150 µl GMM supplemented with 100 µg/ml ampicillin. Bacteria from second pre-culture in GMM supplemented with 100 µg/ml ampicillin and 50 µM duloxetine were inoculated with a final OD₅₇₈ of 0.01 and plates were sealed with a Breathe-Easy® sealing membrane (Z380059, Sigma-Aldrich). After 5h incubation at 37°C membranes were removed, 1.5 µl 20 mM IPTG solution added to induce overexpression and plates were sealed again for a further 43h incubation. Plates were then extracted and further treated as described for the bacteria-drug interaction screen, method section 7.3.2.

For data analysis after normalization by caffeine internal standard, samples were normalized by mean of bacteria-free drug control from the respective plates and then compared using Student's t-test with an alpha level below 0.05.

7.6 Untargeted Metabolomics with NMR

For NMR spectroscopy I performed two different experiments. First, I tested one specific interaction, that of duloxetine with *B. uniformis*. Samples were collected from resting cell assays (method 7.5.3), and duloxetine concentration was 100 μ M. Samples were exposed for 4h before further processed. Secondly, I tested the depletion of duloxetine in a mixture of 6 bacteria (*B. longum longum*, *B. uniformis*, *C. bolteae*, *C. ramosum*, *C. saccharolyticum*, *F. nucleatum*). For this resting cell assay PBS buffer was supplemented with 1 mM $MgCl_2$ and pH was adjusted to 6.5 using 1 M HCl. For the bacteria mix, bacteria were grown to end of exponential phase/beginning of stationary phase before preparing the resting cell assay. For this cells were diluted and mixed in the same ratio at a final OD_{578} of 3.75 before exposed to experimental conditions of 1 mM duloxetine for 4h and further processed.

All experiments were resting cell assays (see Methods 7.5.3) with duloxetine or respective amount of DMSO in control, comparing bacteria treated with duloxetine to bacteria not treated with duloxetine and a bacteria-free control containing only duloxetine. To record a one-dimensional proton spectrum of duloxetine, proton containing water molecules, which make up almost 100% of the sample, need to be replaced by deuterated, heavy water with no protons. After drying in a speedvac (Eppendorf Vacuum Concentrator Plus), all samples were reconstituted in a mixture of 80% D_2O and 20% deuterated acetonitrile with half the original volume, thus doubling the concentration. 1D proton NMR spectra for all samples were then recorded on a 500 MHz Bruker DRX at 27 degrees or equivalent.

7.7 Untargeted Metabolomics with LC-MS/MS

7.7.1 Experimental setup

I tested the depletion of duloxetine and change in the metabolome of *Clostridium saccharolyticum* and *Bacteroides uniformis* upon addition of the drug. Bacteria from a 20 mL overnight culture were washed and prepared for a resting cell and lysate assay as described in the method section 7.5.3. For the resting cell assay bacteria were reconstituted in 3.6 mL PBS, pH 6.5 containing 1 mM MgCl₂, sample volume was 600 µl. For the lysate assay, bacteria were reconstituted in 1 mL PBS, lysed, and then 360 µl of the recovered lysate was diluted with 1080 µl PBS. Thus, finale sample volume for each lysate replicate was 240 µl. Resting cells were incubated for 2h, lysates were incubated for 30 min with duloxetine or with DMSO as control respectively. As another control, buffer with duloxetine was incubated for the respective time in the respective sample volume. Duloxetine concentration was 1 mM for both assay, and all interactions were tested in triplicates. Extraction buffer contained 10 µM amitriptyline as internal standard, and all extractions were **indirect**, meaning cells/lysate was centrifuged (14.000 rpm, 10 min, 4°C) and only the supernatant was extracted. Resting cell samples were reconstituted in 225 µl reconstitution buffer, doubling the respective concentration of small molecules in comparison to the original sample. Lysate samples were reconstituted in 187.5 µl, concentration in comparison to the original culture remained constant.

7.7.2 Mass spectrometry method

Samples were measured on a Q Exactive Plus-Orbitrap Mass Spectrometer (Thermo Fisher) in positive mode using a Kinetex C18 column for LC. The LC method used was 35 min long, and used acetonitrile and 5 mM formic acid as liquid phase. Gradient were. Injection volume was 5 µl, samples were injected in three rounds representing three technical replicates including washing injection every ten injections.

Scan mode was FTMS + p ESI Full ms and scan range was from 60-800 m/z. Resolution was set to 70.000, AGC target to 1.000.000 ions, maximum IT to 150 ms. For secondary MS resolution was set to 17.500, AGC target to 100.000 ions, and maximum IT to 60 ms, allowing 5 secondary scans ranging from 200-2000 m/z per full scan at a collision energy of 35. In any case unknown charges or charges higher than 2 were excluded from analysis.

7.7.3 Data analysis

Data analysis was aimed at comparing the two bacteria *C. saccharolyticum* and *B. uniformis* in two different experimental condition and trying to investigate if a potential drug metabolite is generated in the presence of bacteria and drug. After no potential drug metabolite could be isolated, data analysis switched to identifying mass features.

Raw data was converted from ThermoFisher .raw format into the open mzXML format using RawConverter program (He et al. 2015). For feature selection, peak alignment, grouping and retention time shift correction from the raw data the XCMS R package was used. Parameters for first round of density grouping of peaks were bw=30, minfrac=0.5, minsamp=3, mzwid=0.025, max=50. For retention time correction parameters were family="symmetric", plottype="mdevden"; Lysates were corrected with span = .4 instead of default value. For second round of grouping parameters were bw=10, minfrac=0.5, minsamp=3, mzwid=0.025, max=50. Then missing peaks were filled using "chrom" method. Samples for lysate and extracellular fraction have been processed independently. One technical injection replicate was excluded as strong difference to other two injections was observed, potentially based on less washing injections between sample injection. Thus, following statistical analysis was based on three biological replicates with two technical replicates each.

Statistical analysis was loosely based on Vinaixa et al. 2012 and Ortmayr et al. 2017. Vinaixa et al. describe a general approach how to analyze untargeted metabolomics data focusing on statistical pitfalls and general workflow. Ortmayr et al. describe an alternative approach to the common Student's t-test or variance

analysis approach, taking the uncertainty in fold change calculation into account. All data analysis and scripting was done in R.

Using PATHOS (Leader et al. 2011) or other tools like MBROLE (Lopez-Ibanez et al. 2016) for data exploration comparisons to databases like METLIN (Smith et al. 2005), Biocyc (Caspi et al. 2016) or KEGG (Tanabe & Kanehisa 2012) were based on 5ppm accuracy. As reference/background, *C. saccharolyticum* or *B. uniformis* was used if possible. Otherwise *C. saccharobutilyticum* or *B. thetaiotaomicron* was used respectively. If none of the options were given for data comparison, *E. coli* was used. For KEGG pathway enrichment using PATHOS I allowed all 12 ACN or H adducts to be formed, and compared to *E. coli* as a background for statistical tests (Fisher's exact test). I further analyzed the data by annotating the mass features with species-specific metabolites. Data was kindly provided by Daniel Sevin (Cellzome). He generated lists of species-specific metabolites by building genome-scale models for all organisms available in KEGG, and predicting their potential metabolome from the model. For adduct-formation I used a stricter cutoff as with PATHOS, only allowing H⁺ and ACN+H⁺ adducts to be formed to annotate a mass with its potential KEGG metabolite.

7.8 Proteomics

7.8.1 Sample preparation

For the identification of recovered proteins by mass spectrometry, protein eluates were rebuffered into 4 M urea/0.2% rapigest (final concentration) and sonicated in a vial tweeter (Hielscher) for two times 30 seconds (100%/0.5 seconds cycle). Disulfide bridges between cysteins were disrupted by reduction with 10 mM DTT at 37 C for 30 minutes. Following that, free cysteins were alkylated using 15 mM iodoacetamide at room temperature in the dark for 30 minutes. Protein digestion was performed using 1:100 (w/w) Lys-C endoproteinase (Wako Chemicals GmbH, Germany) at 37 °C for 4 hours and then finalized (after the urea concentration was diluted to 1.6 M) with 1:50 (w/w) trypsin (Promega

GmbH, Germany) at 37 °C over night. Rapigest was cleaved by acidification below pH=3 using 10% (v/v) TFA at room temperature for 30 minutes and removed by desalting of the peptide mixture using C18 spin columns (Harvard Apparatus, USA) according to the manufacturers procedures. Desalted peptides were vacuum dried and stored at -20 C until further use.

7.8.2 Mass spectrometry method and protein identification

For shot-gun experiments, samples were analyzed using a nanoAcquity UPLC system (Waters GmbH) connected online to a LTQ-Orbitrap Velos Pro instrument (Thermo Fisher Scientific GmbH). Peptides were separated on a BEH300 C18 (75 µm x 250 mm, 1.7 µm) nanoAcquity UPLC column (Waters GmbH) using a stepwise 90 min gradient between 3 and 85% (v/v) ACN in 0.1% (v/v) FA. Data acquisition was performed by collision-induced dissociation using a TOP-20 strategy with standard parameters. Charge states 1 and unknown were rejected.

For the quantitative label-free analysis, raw files from the Orbitrap were analyzed using MaxQuant (version 1.5.3.28) (Cox & Mann 2008). MS/MS spectra were searched against the *Clostridium saccharolyticum* (strain ATCC 35040 / DSM 2544 / NRCC 2533 / WM1) entries of the Uniprot KB (database release 2016_04, 7212 entries) using the Andromeda search engine (Cox et al. 2011).

The search criteria were set as follows: full tryptic specificity was required (cleavage after lysine or arginine residues, unless followed by proline); 2 missed cleavages were allowed; carbamidomethylation (C) was set as fixed modification; oxidation (M) and acetylation (protein N-term) were applied as variable modifications, if applicable; mass tolerance of 20 ppm (precursor) and 0.5 Da (fragments). The reversed sequences of the target database were used as decoy database. Peptide and protein hits were filtered at a false discovery rate of 1% using a target-decoy strategy (Elias & Gygi 2007). Additionally, only proteins identified by at least 2 unique peptides were retained. Only proteins identified in

at least 2 replicates were considered when comparing protein abundances between control and drug treatment.

7.8.3 Data analysis

To reduce technical variation, data was quantile-normalized using the preprocessCore library (Gentleman et al. 2004). Protein differential expression was evaluated using the limma package. Differences in protein abundances were statistically determined using the Student's t-test moderated by Benjamini-Hochberg's method (Benjamini & Hochberg 1995) at alpha level of 0.05. Significant regulated proteins were defined by a cut-off of log₂ fold change ≥ 2 and p-value ≤ 0.1 .

For gene ontology term and pathway enrichment analysis, significantly changed proteins were annotated using Blast2GO (Conesa et al. 2005) with default parameters using the NCBI blast search. GO term enrichment can be done within Blast2GO and significantly enriched (FDR corrected p-value < 0.05) most specific GO terms were listed. For KEGG pathway enrichment analysis EC numbers from Blast2Go annotation were extracted and the EC2KEGG tool (Porollo 2014) was used to annotate respective species specific KEGG pathways and perform enrichment analysis (uncorrected p-value < 0.05).

References

- Abubucker, S. et al., 2012. Metabolic reconstruction for metagenomic data and its application to the human microbiome. *PLoS Comput. Biol.*, 8(6), p.e1002358.
- Alang, N. & Kelly, C.R., 2015. Weight Gain After Fecal Microbiota Transplantation. *Open Forum Infectious Diseases*, 2(1), p.ofv004-ofv004.
- Allison, K., Brynildsen, M. & Collins, J., 2011. Metabolite-enabled eradication of bacterial persisters by aminoglycosides. *Nature*, 473(7346), pp.216–220.
- Alonso, A., Marsal, S. & Julià, A., 2015. Analytical methods in untargeted metabolomics: state of the art in 2015. *Frontiers in bioengineering and biotechnology*, 3(March), p.23.
- Aura, A.-M. et al., 2011. Drug metabolome of the simvastatin formed by human intestinal microbiota in vitro. *Molecular bioSystems*, 7(2), pp.437–446.
- Ayaz, M. et al., 2015. Sertraline enhances the activity of antimicrobial agents against pathogens of clinical relevance. *Journal of biological research (Thessalonikē, Greece)*, 22(1), p.4.
- Azad Khan, A.K. et al., 1983. Tissue and bacterial splitting of sulphasalazine. *Clin. Sci.*, 64(3), pp.349–54.
- B-Rao, C. et al., 2012. Identification of novel isocytosine derivatives as xanthine oxidase inhibitors from a set of virtual screening hits. *Bioorganic and Medicinal Chemistry*, 20(9), pp.2930–2939.
- Bahr, S.M. et al., 2015. Use of the second-generation antipsychotic, risperidone, and secondary weight gain are associated with an altered gut microbiota in children. *Translational Psychiatry*, 5(9), p.e652.
- Bahra, S.M. et al., 2015. Risperidone-induced weight gain is mediated through shifts in the gut microbiome and suppression of energy expenditure. *EBioMedicine*, 2(11), pp.1725–34.
- Balani, S.K. et al., 1997. Metabolic profiles of montelukast sodium (singulair), a potent cysteinyl leukotriene1 receptor antagonist, in human plasma and bile. *Drug Metabolism and Disposition*, 25(11), pp.1282–1287.
- Basit, A.W. & Lacey, L.F., 2001. Colonic metabolism of ranitidine: implications for its delivery and absorption. *International journal of pharmaceuticals*, 227(1–2), pp.157–65.
- Belenky, P. et al., 2015. Bactericidal Antibiotics Induce Toxic Metabolic Perturbations that Lead to Cellular Damage. *Cell Reports*, 13(5), pp.968–980.
- Benjamini, Y. & Hochberg, Y., 1995. Controlling the False Discovery Rate: A Practical and Powerful Approach to Multiple Testing. *Journal of the Royal Statistical Society. Series B (Methodological)*, 57(1), pp.289–300.
- Bennett, B.D. et al., 2009. Absolute metabolite concentrations and implied enzyme active site occupancy in *Escherichia coli*. *Nature chemical biology*, 5(8), pp.593–599.
- Bento, A.P. et al., 2014. The ChEMBL bioactivity database: An update. *Nucleic Acids Research*, 42(D1).

- Berger, M., Gray, J.A. & Roth, B.L., 2009. The expanded biology of serotonin. *Annual Review of Medicine*, 60(August 2016), pp.355–366.
- Björkholm, B. et al., 2009. Intestinal microbiota regulate xenobiotic metabolism in the liver. *PloS One*, 4(9), p.e6958.
- Blaser, M. et al., 2013. The microbiome explored: recent insights and future challenges. *Nat. Rev. Microbiol.*, 11(3), pp.213–7.
- Bohnert, J.A. et al., 2011. Efflux inhibition by selective serotonin reuptake inhibitors in *Escherichia coli*. *The Journal of antimicrobial chemotherapy*, 66(9), pp.2057–60.
- Booijink, C.C.G.M. et al., 2010. Metatranscriptome analysis of the human fecal microbiota reveals subject-specific expression profiles, with genes encoding proteins involved in carbohydrate metabolism being dominantly expressed. *Appl. Environ. Microbiol.*, 76(16), pp.5533–40.
- Booth, S.C., Weljie, A.M. & Turner, R.J., 2013. Computational Tools for the Secondary Analysis of Metabolomics Experiments. *Computational and Structural Biotechnology Journal*, 4(5), pp.1–13.
- Brandt, K. & Müller, V., 2015. Hybrid rotors in F1Fo ATP synthases: subunit composition, distribution, and physiological significance. *Biological Chemistry*, 396(9–10), pp.1031–42.
- Brandt, U., 2006. Energy converting NADH:quinone oxidoreductase (complex I). *Annual Review of Biochemistry*, 75(Complex I), pp.69–92.
- Burris, K.D. et al., 2002. Aripiprazole, a novel antipsychotic, is a high-affinity partial agonist at human dopamine D2 receptors. *The Journal of pharmacology and experimental therapeutics*, 302(1), pp.381–389.
- Cai, J. et al., 2015. The Anti-Oxidant Drug Tempol Promotes Functional Metabolic Changes in the Gut Microbiota. *Journal of proteome research*, 15(2), pp.563–71.
- Caporaso, J.G. et al., 2011. An Introduction to Illumina Next-Generation Sequencing Technology for Microbiologists Welcome to Next-Generation Sequencing. *Proc Natl Acad Sci U S A.*, (108), pp.4516–4522.
- Carmody, R.N. & Turnbaugh, P.J., 2014. Host-microbial interactions in the metabolism of therapeutic and diet-derived xenobiotics. *The Journal of clinical investigation*, 124(10), pp.4173–81.
- Caspi, R. et al., 2016. The MetaCyc database of metabolic pathways and enzymes and the BioCyc collection of pathway/genome databases. *Nucleic Acids Research*, 44(D1), pp.D471–D480.
- Catry, E. et al., 2015. Ezetimibe and simvastatin modulate gut microbiota and expression of genes related to cholesterol metabolism. *Life Sciences*, 132, pp.77–84.
- Cecil, A. et al., 2011. Modeling antibiotic and cytotoxic effects of the dimeric isoquinoline IQ-143 on metabolism and its regulation in *Staphylococcus aureus*, *Staphylococcus epidermidis* and human cells. *Genome biology*, 12(3), p.R24.
- Chhabra, R.S., 1979. Intestinal absorption and metabolism of xenobiotics. *Environ Health Perspect.*, 33, pp.61–9.
- Chiu, H.-C., Levy, R. & Borenstein, E., 2014. Emergent Biosynthetic Capacity in

- Simple Microbial Communities C. A. Ouzounis, ed. *PLoS Computational Biology*, 10(7), p.e1003695.
- Cimperman, L. et al., 2011. A randomized, double-blind, placebo-controlled pilot study of *Lactobacillus reuteri* ATCC 55730 for the prevention of antibiotic-associated diarrhea in hospitalized adults. *J. Clin. Gastroenterol.*, 45(9), pp.785–9.
- Clarke, G. et al., 2014. Minireview: Gut Microbiota: The Neglected Endocrine Organ. *Molecular Endocrinology*, 28(8), pp.1221–1238.
- Claus, S.P.S. et al., 2011. Colonization-induced host-gut microbial metabolic interaction. *MBio*, 2(2), p.8.
- Clayton, T.A. et al., 2006. Pharmaco-metabonomic phenotyping and personalized drug treatment. *Nature*, 440(7087), pp.1073–7.
- Clayton, T.A. et al., 2009. Pharmacometabonomic identification of a significant host-microbiome metabolic interaction affecting human drug metabolism. *Proc. Natl. Acad. Sci. U.S.A.*, 106(34), pp.14728–33.
- Collins, S.M. & Bercik, P., 2009. The Relationship Between Intestinal Microbiota and the Central Nervous System in Normal Gastrointestinal Function and Disease. *Gastroenterology*, 136(6), pp.2003–2014.
- Conesa, A. et al., 2005. Blast2GO: A universal tool for annotation, visualization and analysis in functional genomics research. *Bioinformatics*, 21(18), pp.3674–3676.
- Costello, E. & Stagaman, K., 2012. The application of ecological theory toward an understanding of the human microbiome. *Science*, 336(6086), pp.1255–1262.
- Coughlan, M.P., 1980. Aldehyde Oxidase, Xanthine Oxidase and Xanthine Dehydrogenase. In M. P. Coughlan, ed. *Molybdenum and Molybdenum-Containing Enzymes*. Pergamon Press, pp. 139–140.
- Cox, J. et al., 2011. Andromeda: A peptide search engine integrated into the MaxQuant environment. *Journal of Proteome Research*, 10(4), pp.1794–1805.
- Cox, J. & Mann, M., 2008. MaxQuant enables high peptide identification rates, individualized p.p.b.-range mass accuracies and proteome-wide protein quantification. *Nature biotechnology*, 26(12), pp.1367–72.
- Czyż, D.M. et al., 2014. Host-directed antimicrobial drugs with broad-spectrum efficacy against intracellular bacterial pathogens. *mBio*, 5(4), pp.e01534–e01514.
- Das, A. et al., 2016. Xenobiotic metabolism and gut microbiomes. *PLoS ONE*, 11(10), p.e0163099.
- Davey, K.J. et al., 2013. Antipsychotics and the gut microbiome: olanzapine-induced metabolic dysfunction is attenuated by antibiotic administration in the rat. *Translational psychiatry*, 3, p.e309.
- Delcour, A.H., 2009. Outer membrane permeability and antibiotic resistance. *Biochimica et biophysica acta*, 1794(5), pp.808–16.
- Dent, R. et al., 2012. Changes in body weight and psychotropic drugs: A systematic synthesis of the literature S. Alessi-Severini, ed. *PLoS ONE*, 7(6), p.e36889.
- Deris, Z.Z. et al., 2014. A secondary mode of action of polymyxins against Gram-negative bacteria involves the inhibition of NADH-quinone oxidoreductase

- activity. *The Journal of Antibiotics*, 67(2), pp.147–151.
- Dimitrov, A., 2014. Plotly graphs in IPython Notebook. *Undocumented Matlab*. Available at: <http://undocumentedmatlab.com/blog/plotly-graphs-in-ipython-notebook>.
- Donaldson, G.P., Lee, S.M. & Mazmanian, S.K., 2015. Gut biogeography of the bacterial microbiota. *Nature Reviews Microbiology*, 14(1).
- Dragosits, M. & Mattanovich, D., 2013. Adaptive laboratory evolution--principles and applications for biotechnology. *Microbial cell factories*, 12(1), p.64.
- Dunne, C., 2001. Adaptation of bacteria to the intestinal niche: probiotics and gut disorder. *Inflamm. Bowel Dis.*, 7(2), pp.136–45.
- Durre, P. & Andreesen, J.R., 1983. Purine and glycine metabolism by purinolytic clostridia. *Journal of Bacteriology*, 154(1), pp.192–199.
- van Duynhoven, J. et al., 2011. Metabolic fate of polyphenols in the human superorganism. *Proc. Natl. Acad. Sci. U.S.A.*, 108 Suppl, pp.4531–8.
- Dykens, J.A. et al., 2008. In vitro assessment of mitochondrial dysfunction and cytotoxicity of nefazodone, trazodone, and buspirone. *Toxicological Sciences*, 103(2), pp.335–345.
- Edgar, R.C., 2010. Search and clustering orders of magnitude faster than BLAST. *Bioinformatics*, 26(19), pp.2460–2461.
- Ejim, L. et al., 2011. Combinations of antibiotics and nonantibiotic drugs enhance antimicrobial efficacy. *Nature chemical biology*, 7(6), pp.348–50.
- Ekins, S., 2004. Predicting undesirable drug interactions with promiscuous proteins in silico. *Drug Discov. Today*, 9(6), pp.276–85.
- Elias, J.E. & Gygi, S.P., 2007. Target-decoy search strategy for increased confidence in large-scale protein identifications by mass spectrometry. *Nature Methods*, 4(3), pp.207–214.
- Falcony, G. et al., 2016. Population-level analysis of gut microbiome variation. *Science*, 352(6285), pp.560–564.
- Fato, R. et al., 2008. Mitochondrial production of reactive oxygen species: role of complex I and quinone analogues. *BioFactors (Oxford, England)*, 32(1–4), pp.31–39.
- FDA, 1997. *FDA Pharmacology Review for Montelukast (Singulair)*.
- Finley, S., Broadbelt, L. & Hatzimanikatis, V., 2009. Computational framework for predictive biodegradation. *Biotechnology & genetic engineering reviews*, 104(6), pp.1086–1097.
- Forslund, K. et al., 2015. Disentangling type 2 diabetes and metformin treatment signatures in the human gut microbiota. *Nature*, 528(7581), pp.262–266.
- Foster, J.A. & McVey Neufeld, K.-A., 2013. Gut-brain axis: how the microbiome influences anxiety and depression. *Trends in neurosciences*, 36(5), pp.305–12.
- de Freitas, M.C.R. et al., 2016. Exploratory Investigation of *Bacteroides fragilis* Transcriptional Response during In vitro Exposure to Subinhibitory Concentration of Metronidazole. *Frontiers in microbiology*, 7, p.1465.
- Fuhrer, T. & Zamboni, N., 2015. High-throughput discovery metabolomics. *Current Opinion in Biotechnology*, 31, pp.73–78.
- Gad, S.C. ed., 2007. *Toxicology of the Gastrointestinal Tract*, CRC Press.
- Gao, J., Ellis, L.B.M. & Wackett, L.P., 2011. The University of Minnesota Pathway

- Prediction System: multi-level prediction and visualization. *Nucleic Acids Res.*, 39(Web Server issue), pp.W406-11.
- Gatehouse, D., 2012. Bacterial mutagenicity assays: Test methods. *Methods in Molecular Biology*, 817, pp.21–34.
- Gauffin Cano, P. et al., 2012. *Bacteroides uniformis* CECT 7771 ameliorates metabolic and immunological dysfunction in mice with high-fat-diet induced obesity. *PLoS ONE*, 7(7).
- Gentleman, R.C. et al., 2004. Bioconductor: open software development for computational biology and bioinformatics. *Genome Biology*, 5(10), p.R80.
- Goldman, P., Peppercorn, M.A. & Goldin, B.R., 1974. Metabolism of drugs by microorganisms in the intestine. *Am. J. Clin. Nutr.*, 27(11), pp.1348–55.
- Goodman, A.L. et al., 2011. Extensive personal human gut microbiota culture collections characterized and manipulated in gnotobiotic mice. *Proceedings of the National Academy of Sciences of the United States of America*, 108(15), pp.6252–7.
- Gu, Q. et al., 2014. Prescription Cholesterol-lowering Medication Use in Adults Aged 40 and Over: United States, 2003–2012 Key findings Data from the National Health and Nutrition Examination Survey. *NCHS Data Brief*, 177.
- Guo, A.C. et al., 2013. ECMDB: The *E. coli* Metabolome Database. *Nucleic Acids Research*, 41(D1).
- Haddock, B.A. & Jones, C.W., 1977. Bacterial respiration. *Bacteriological reviews*, 41(1), pp.47–99.
- Haiser, H.J. et al., 2014. Mechanistic insight into digoxin inactivation by *Eggerthella lenta* augments our understanding of its pharmacokinetics. *Gut microbes*, 5(2), pp.233–8.
- Haiser, H.J. et al., 2013. Predicting and manipulating cardiac drug inactivation by the human gut bacterium *Eggerthella lenta*. *Science*, 341(6143), pp.295–8.
- Haiser, H.J. & Turnbaugh, P.J., 2013. Developing a metagenomic view of xenobiotic metabolism. *Pharmacol. Res.*, 69(1), pp.21–31.
- Hansen, J. & Bross, P., 2010. A Cellular Viability Assay to Monitor Drug Toxicity. In *Methods in molecular biology (Clifton, N.J.)*. pp. 303–311.
- Hanukoglu, I., 2015. Proteopedia: Rossmann fold: A beta-alpha-beta fold at dinucleotide binding sites. *Biochemistry and Molecular Biology Education*, 43(3), pp.206–209.
- Hao, W.-L. & Lee, Y.-K., 2004. Microflora of the gastrointestinal tract: a review. *Methods Mol. Biol.*, 268, pp.491–502.
- Hashim, H. et al., 2014. Eradication of *Helicobacter pylori* Infection Improves Levodopa Action, Clinical Symptoms and Quality of Life in Patients with Parkinson's Disease T. M. Doherty, ed. *PLoS ONE*, 9(11), p.e112330.
- He, L. et al., 2015. Extracting Accurate Precursor Information for Tandem Mass Spectra by RawConverter. *Analytical Chemistry*, 87(22), pp.11361–11367.
- Heijtz, R., Wang, S. & Anuar, F., 2011. Normal gut microbiota modulates brain development and behavior. *Proceedings of the ...*, 108(7), pp.3047–3052.
- Hibbing, M.E. et al., 2010. Bacterial competition: surviving and thriving in the microbial jungle. *Nature reviews. Microbiology*, 8(1), pp.15–25.
- Hickson, M., 2011. Probiotics in the prevention of antibiotic-associated diarrhoea

- and *Clostridium difficile* infection. *Therap Adv Gastroenterol*, 4(3), pp.185–97.
- Hoerr, V. et al., 2016. Characterization and prediction of the mechanism of action of antibiotics through NMR metabolomics. *BMC Microbiology*, 16(1), p.82.
- Holzhütter, H.-G. et al., 2012. The virtual liver: a multidisciplinary, multilevel challenge for systems biology. *Wiley Interdiscip Rev Syst Biol Med*, 4(3), pp.221–35.
- Hooper, L., Littman, D. & Macpherson, A., 2012. Interactions between the microbiota and the immune system. *Science*, 336(6086), pp.1268–1273.
- Human Microbiome Project Consortium., 2012. Structure, function and diversity of the healthy human microbiome. *Nature*, 486(7402), pp.207–14.
- Jackson, M.A. et al., 2016. Proton pump inhibitors alter the composition of the gut microbiota. *Gut*, 65(5), pp.749–56.
- Jacobs, D.M. et al., 2008. (1)H NMR metabolite profiling of feces as a tool to assess the impact of nutrition on the human microbiome. *NMR Biomed*, 21(6), pp.615–26.
- Jakoby, W.B. & Ziegler, D.M., 1990. The enzymes of detoxication. *J. Biol. Chem.*, 265(34), pp.20715–8.
- Jeyaseeli, L. et al., 2006. Antimicrobial potentiality of the thioxanthene flupenthixol through extensive in vitro and in vivo experiments. *International Journal of Antimicrobial Agents*, 27(1), pp.58–62.
- Jeyaseeli, L. et al., 2012. Evidence of significant synergism between antibiotics and the antipsychotic, antimicrobial drug flupenthixol. *European Journal of Clinical Microbiology & Infectious Diseases*, 31(6), pp.1243–1250.
- Jiang, H. et al., 2015. Altered fecal microbiota composition in patients with major depressive disorder. *Brain, behavior, and immunity*.
- Johnson, C.H. et al., 2012. Xenobiotic metabolomics: major impact on the metabolome. *Annu. Rev. Pharmacol. Toxicol.*, 52, pp.37–56.
- Kalaycı, S., Demirci, S. & Sahin, F., 2015. Antimicrobial Properties of Various Psychotropic Drugs Against Broad Range Microorganisms. *Current Psychopharmacology*, 3(3), pp.195–202.
- Kaminsky, L.S. & Zhang, Q.-Y., 2003. The small intestine as a xenobiotic-metabolizing organ. *Drug Metab Dispos.*, 31(12), pp.1520–5.
- Kanehisa, M. et al., 2014. Data, information, knowledge and principle: back to metabolism in KEGG. *Nucleic acids research*, 42(Database issue), pp.D199–205.
- Kanehisa, M. et al., 2012. KEGG for integration and interpretation of large-scale molecular data sets. *Nucleic Acids Res.*, 40(Database issue), pp.D109–14.
- Kang, A. et al., 2013. Systems-level characterization and engineering of oxidative stress tolerance in *Escherichia coli* under anaerobic conditions. *Molecular bioSystems*, 9(2), pp.285–95.
- Kaufman, J. & Griffiths, T., 2009. Effects of mesalamine (5-aminosalicylic acid) on bacterial gene expression. *Inflammatory bowel ...*, 15(7), pp.985–996.
- Kelly, J.R. et al., 2015. Breaking down the barriers: the gut microbiome, intestinal permeability and stress-related psychiatric disorders. *Frontiers in cellular neuroscience*, 9, p.392.

- Khersonsky, O. & Tawfik, D.S., 2010. Enzyme promiscuity: a mechanistic and evolutionary perspective. *Annu. Rev. Biochem.*, 79, pp.471–505.
- Khoury, P. et al., 2006. Effect of montelukast on bacterial sinusitis in allergic mice. *Annals of allergy, asthma & immunology : official publication of the American College of Allergy, Asthma, & Immunology*, 97(3), pp.329–35.
- Klaassen, C.D. & Cui, J.Y., 2015. Review: Mechanisms of How the Intestinal Microbiota Alters the Effects of Drugs and Bile Acids. *Drug metabolism and disposition: the biological fate of chemicals*, 43(10), pp.1505–21.
- Klünemann, M., Schmid, M. & Patil, K.R., 2014. Computational tools for modeling xenometabolism of the human gut microbiota. *Trends in biotechnology*, 32(3), pp.157–65.
- Kojima, T. et al., 1984. Biochemical studies on the purine metabolism of four cases with hereditary xanthinuria. *Clinica chimica acta; international journal of clinical chemistry*, 137(2), pp.189–98.
- Kolmeder, C.A. et al., 2012. Comparative metaproteomics and diversity analysis of human intestinal microbiota testifies for its temporal stability and expression of core functions. *PLoS ONE*, 7(1), p.e29913.
- Koppel, N. & Balskus, E.P., 2016. Exploring and Understanding the Biochemical Diversity of the Human Microbiota. *Cell Chemical Biology*, 23(1), pp.18–30.
- Kristiansen, J.E. & Amaral, L., 1997. The potential management of resistant infections with non-antibiotics. *Journal of Antimicrobial Chemotherapy*, 40(3), pp.319–327.
- Kuhn, M. et al., 2010. A side effect resource to capture phenotypic effects of drugs. *Molecular systems biology*, 6, p.343.
- Kuhn, M. et al., 2016. The SIDER database of drugs and side effects. *Nucleic Acids Research*, 44(D1), pp.D1075–D1079.
- Kuo, F. et al., 2004. Synthesis and biological activity of some known and putative duloxetine metabolites. *Bioorganic and Medicinal Chemistry Letters*, 14(13), pp.3481–3486.
- Lantz, R.J. et al., 2003. Metabolism, excretion, and pharmacokinetics of duloxetine in healthy human subjects. *Drug Metabolism and Disposition*, 31(9), pp.1142–1150.
- Law, V. et al., 2014. DrugBank 4.0: Shedding new light on drug metabolism. *Nucleic Acids Research*, 42(D1).
- Lawrence, D. et al., 2012. Species interactions alter evolutionary responses to a novel environment. *PLoS biology*, 10(5), p.e1001330.
- Leader, D.P. et al., 2011. Pathos: A web facility that uses metabolic maps to display experimental changes in metabolites identified by mass spectrometry. *Rapid Communications in Mass Spectrometry*, 25(22), pp.3422–3426.
- Lee, H. et al., 2010. Bacterial charity work leads to population-wide resistance. *Nature*, 467(7311), pp.82–85.
- Lenski, R.E. et al., 1991. Long-Term Experimental Evolution in *Escherichia coli*. I. Adaptation and Divergence During. *The American Naturalist*, 138, pp.1315–1341.
- Li, H. et al., 2013. Shifting Species Interaction in Soil Microbial Community and Its Influence on Ecosystem Functions Modulating. *Microbial Ecology*, 65(3),

- pp.700–708.
- Li, H. et al., 2015. The outer mucus layer hosts a distinct intestinal microbial niche. *Nature communications*, 6(May), p.8292.
- Li, J. et al., 2014. An integrated catalog of reference genes in the human gut microbiome. *Nat Biotech*, advance on(8), pp.834–41.
- Liu, M. et al., 2014. Developments of mucus penetrating nanoparticles. *Asian Journal of Pharmaceutical Sciences*, 10(4), pp.275–282.
- Lopez-Ibanez, J., Pazos, F. & Chagoyen, M., 2016. MBROLE 2.0-functional enrichment of chemical compounds. *Nucleic Acids Research*, 44(W1), pp.W201–W204.
- Maestre, F.T. et al., 2009. Refining the stress-gradient hypothesis for competition and facilitation in plant communities. *Journal of Ecology*, 97(2), pp.199–205.
- Mahieu, N.G., Genenbacher, J.L. & Patti, G.J., 2016. A roadmap for the XCMS family of software solutions in metabolomics. *Current Opinion in Chemical Biology*, 30, pp.87–93.
- Mahmood, S. et al., 2015. Detoxification of azo dyes by bacterial oxidoreductase enzymes. *Critical Reviews in Biotechnology*, 36(4), pp.1–13.
- Malkinson, D. & Tielbörger, K., 2010. What does the stress-gradient hypothesis predict? Resolving the discrepancies. *Oikos*, 119(10), pp.1546–1552.
- Martin, M., 2011. Cutadapt removes adapter sequences from high-throughput sequencing reads. *EMBnet.journal*, 17(1), pp.10–12.
- Martin, M. et al., 2016. Laboratory evolution of microbial interactions in bacterial biofilms. *Journal of Bacteriology*, 198(19), pp.2564–2571.
- Maurice, C.F., Haiser, H.J. & Turnbaugh, P.J., 2013. Xenobiotics shape the physiology and gene expression of the active human gut microbiome. *Cell*, 152(1–2), pp.39–50.
- Meckenstock, R.U. et al., 2016. Anaerobic degradation of benzene and polycyclic aromatic hydrocarbons. *Journal of Molecular Microbiology and Biotechnology*, 26(1–3), pp.92–118.
- Meckenstock, R.U. & Mouttaki, H., 2011. Anaerobic degradation of non-substituted aromatic hydrocarbons. *Current Opinion in Biotechnology*, 22(3), pp.406–414.
- Mihelcic, J.R. & Luthy, R.G., 1988. Degradation of polycyclic aromatic hydrocarbon compounds under various redox conditions in soil-water systems. *Applied and Environmental Microbiology*, 54(5), pp.1182–1187.
- Minato, Y. et al., 2014. Roles of the sodium-translocating NADH:Quinone oxidoreductase (Na⁺-NQR) on *Vibrio cholerae* metabolism, motility and osmotic stress resistance J. H. Weiner, ed. *PLoS ONE*, 9(5), p.e97083.
- Morgan, A.P. et al., 2014. The Antipsychotic Olanzapine Interacts with the Gut Microbiome to Cause Weight Gain in Mouse M. M. Heimesaat, ed. *PLoS ONE*, 9(12), p.e115225.
- Mortelmans, K. & Zeiger, E., 2000. The Ames Salmonella/microsome mutagenicity assay. *Mutation Research - Fundamental and Molecular Mechanisms of Mutagenesis*, 455(1–2), pp.29–60.
- Moses, V. & Sharp, P.B., 1972. Intermediary Metabolite Levels in *Escherichia coli*. *Microbiology*, 71(1), pp.181–190.

- Mouttaki, H., Johannes, J.J. & Meckenstock, R.U., 2012. Identification of naphthalene carboxylase as a prototype for the anaerobic activation of non-substituted aromatic hydrocarbons. *Environmental Microbiology*, 14(10), pp.2770–2774.
- Munoz-Bellido, J., Munoz-Criado, S. & Garcia-Rodríguez, J., 2000. Antimicrobial activity of psychotropic drugs: Selective serotonin reuptake inhibitors. *International Journal of Antimicrobial Agents*, 14(3), pp.177–180.
- Musso, G., Gambino, R. & Cassader, M., 2011. Interactions between gut microbiota and host metabolism predisposing to obesity and diabetes. *Annual review of medicine*, 62(1), pp.361–80.
- Nguyen, D. et al., 2011. Active starvation responses mediate antibiotic tolerance in biofilms and nutrient-limited bacteria. *Science (New York, N.Y.)*, 334(6058), pp.982–6.
- Nichols, R.G. et al., 2016. Omics Approaches To Probe Microbiota and Drug Metabolism Interactions. *Chemical Research in Toxicology*, p.acs.chemrestox.6b00236.
- Nicholson, J., 2002. Understanding 'global' systems biology: metabonomics and the continuum of metabolism. *Nat Rev Drug Discov*, 2(8), pp.668–676.
- Niehues, M. & Hensel, A., 2009. In-vitro interaction of L-dopa with bacterial adhesins of *Helicobacter pylori*; an explanation for clinical differences in bioavailability? *Journal of Pharmacy and Pharmacology*, 61(10), pp.1303–1307.
- Nikaido, H., 1996. Multidrug efflux pumps of gram-negative bacteria. *Journal of bacteriology*, 178(20), pp.5853–9.
- O'Mahony, S.M. et al., 2015. Serotonin, tryptophan metabolism and the brain-gut-microbiome axis. *Behavioural Brain Research*, 277, pp.32–48.
- Oguri, K., 1994. Regiochemistry of Cytochrome P450 Isozymes. *Annu. Rev. Pharmacol. Toxicol.*, 34(1), pp.251–279.
- Ortmayr, K. et al., 2016. Uncertainty budgeting in fold change determination and implications for non-targeted metabolomics studies in model systems. *The Analyst*.
- Otsuka, Y. et al., 2015. GenoBase: comprehensive resource database of Escherichia coli K-12. *Nucleic acids research*, 43(Database issue), pp.D606–17.
- Patterson, A.D. & Turnbaugh, P.J., 2014. Microbial Determinants of Biochemical Individuality and Their Impact on Toxicology and Pharmacology. *Cell metabolism*, 20(5), pp.761–768.
- Penders, J. et al., 2013. The human microbiome as a reservoir of antimicrobial resistance. *Frontiers in Microbiology*, 4(APR).
- Pérez-Cobas, A.E. et al., 2013. Gut microbiota disturbance during antibiotic therapy: a multi-omic approach. *Gut*, 62(11), pp.1591–601.
- Pierantozzi, M. et al., 2006. Helicobacter pylori eradication and L-dopa absorption in patients with PD and motor fluctuations. *Neurology*, 66(12), pp.1824–1829.
- PMLive, 2015. Top 50 pharmaceutical products by global sales. Available at: http://www.pmlive.com/top_pharma_list/Top_50_pharmaceutical_products_by_global_sales [Accessed December 7, 2016].

- Ponomarova, O. & Patil, K.R., 2015. Metabolic interactions in microbial communities: Untangling the Gordian knot. *Current Opinion in Microbiology*, 27, pp.37–44.
- Porollo, A., 2014. EC2KEGG: a command line tool for comparison of metabolic pathways. *Source code for biology and medicine*, 9(1), p.19.
- Press, B., 2011. Optimization of the Caco-2 permeability assay to screen drug compounds for intestinal absorption and efflux. *Methods in Molecular Biology*, 763, pp.139–154.
- Qin, J. et al., 2010. A human gut microbial gene catalogue established by metagenomic sequencing. *Nature*, 464(7285), pp.59–65.
- Ravcheev, D.A. & Thiele, I., 2016. Genomic analysis of the human gut microbiome suggests novel enzymes involved in quinone biosynthesis. *Frontiers in Microbiology*, 7(FEB), p.128.
- Reaves, M.L. & Rabinowitz, J.D., 2011. Metabolomics in systems microbiology. *Current opinion in biotechnology*, 22(1), pp.17–25.
- Rey, F.E. et al., 2013. Metabolic niche of a prominent sulfate-reducing human gut bacterium. *Proc. Natl. Acad. Sci. U.S.A.*, 110(33), pp.13582–7.
- Reyes-Prieto, A., Barquera, B. & Juárez, O., 2014. Origin and evolution of the sodium -pumping NADH: Ubiquinone oxidoreductase G. Greub, ed. *PLoS ONE*, 9(5), p.e96696.
- Ridaura, V. & Belkaid, Y., 2015. Gut Microbiota: The Link to Your Second Brain. *Cell*, 161(2), pp.193–194.
- Riley, M. & Wertz, J., 2002. Bacteriocins: evolution, ecology, and application. *Annu. Rev. Microbiol.*, 56(1), pp.117–37.
- Saad, R., Rizkallah, M.R. & Aziz, R.K., 2012. Gut Pharmacomicrobiomics: the tip of an iceberg of complex interactions between drugs and gut-associated microbes. *Gut Pathog*, 4(1), p.16.
- Schmidt, K. et al., 2014. Prebiotic intake reduces the waking cortisol response and alters emotional bias in healthy volunteers. *Psychopharmacology*.
- Schomburg, I. et al., 2013. BRENDA in 2013: integrated reactions, kinetic data, enzyme function data, improved disease classification: new options and contents in BRENDA. *Nucleic Acids Res.*, 41(Database issue), pp.D764-72.
- Segata, N. et al., 2013. Computational meta'omics for microbial community studies. *Mol. Syst. Biol.*, 9(666), p.666.
- Selwyn, F.P., Cui, J.Y. & Klaassen, C.D., 2015. RNA-seq quantification of hepatic drug processing genes in germ-free mice. *Drug Metabolism and Disposition*, 43(10), pp.1572–1580.
- Sharon, G. et al., 2016. The Central Nervous System and the Gut Microbiome. *Cell*, 167(4), pp.915–932.
- Shu, Y.Z. et al., 1991. Metabolism of levamisole, an anti-colon cancer drug, by human intestinal bacteria. *Xenobiotica*, 21(6), pp.737–50.
- Singer, T.P. & Ramsay, R.R., 1994. The reaction sites of rotenone and ubiquinone with mitochondrial NADH dehydrogenase. *BBA - Bioenergetics*, 1187(2), pp.198–202.
- Sinha, V.R., Kumria, R. & Bhinge, J.R., 2009. Stress degradation studies on duloxetine hydrochloride and development of an RP-HPLC method for its

- determination in capsule formulation. *Journal of chromatographic science*, 47(7), pp.589–593.
- Smith, C.A. et al., 2005. METLIN A Metabolite Mass Spectral Database. *Proceedings of the 9Th International Congress of Therapeutic Drug Monitoring & Clinical Toxicology*, 27(6), pp.747–751.
- Soni C Banerjee, P.U., 2005. Biotransformations for the production of the chiral drug (S)-Duloxetine catalyzed by a novel isolate of *Candida tropicalis*. *Appl Microbiol Biotechnol*, 67, pp.771–777.
- Sorg, R.A. et al., 2014. Collective Resistance in Microbial Communities by Intracellular Antibiotic Deactivation. *PLOS Biology*, 14(12), p.e2000631.
- Sousa, T. et al., 2008. The gastrointestinal microbiota as a site for the biotransformation of drugs. *Int J Pharm*, 363(1–2), pp.1–25.
- Sowada, J. et al., 2014. Degradation of benzo[a]pyrene by bacterial isolates from human skin. *FEMS microbiology ecology*, 88(1), pp.129–39.
- Spanogiannopoulos, P. et al., 2016. The microbial pharmacists within us: a metagenomic view of xenobiotic metabolism. *Nature Reviews Microbiology*, 14(5).
- Stadie, J. et al., 2013. Metabolic activity and symbiotic interactions of lactic acid bacteria and yeasts isolated from water kefir. *Food Microbiology*, 35(2), pp.92–98.
- Sun, R. et al., 2016. Orally administered berberine modulates hepatic lipid metabolism by altering microbial bile acid metabolism and the intestinal FXR signaling pathway. *Molecular Pharmacology*.
- Swanson, H.I., 2015. Drug Metabolism by the Host and Gut Microbiota: A Partnership or Rivalry? *Drug metabolism and disposition: the biological fate of chemicals*, 43(10), pp.1499–504.
- Szklarczyk, D. et al., 2016. STITCH 5: Augmenting protein-chemical interaction networks with tissue and affinity data. *Nucleic Acids Research*, 44(D1), pp.D380–D384.
- Takano, Y. et al., 2005. Selectivity of febuxostat, a novel non-purine inhibitor of xanthine oxidase/xanthine dehydrogenase. *Life Sciences*, 76(16), pp.1835–1847.
- Tamura, M., Hoshi, C. & Hori, S., 2013. Xylitol affects the intestinal microbiota and metabolism of daidzein in adult male mice. *International journal of molecular sciences*, 14(12), pp.23993–4007.
- Tanabe, M. & Kanehisa, M., 2012. Using the KEGG database resource. *Current protocols in bioinformatics / editorial board, Andreas D. Baxevanis ... [et al.]*, Chapter 1, p.Unit1.12.
- Terai, C. et al., 1995. Adenine phosphoribosyltransferase deficiency identified by urinary sediment analysis: cellular and molecular confirmation. *Clinical genetics*, 48(5), pp.246–250.
- Tillisch, K. et al., 2013. Consumption of fermented milk product with probiotic modulates brain activity. *Gastroenterology*, 144(7).
- Tkachenko, A.G. et al., 2012. Polyamines reduce oxidative stress in *Escherichia coli* cells exposed to bactericidal antibiotics. *Research in Microbiology*, 163(2), pp.83–91.

- Turnbaugh, P.J. et al., 2009. The effect of diet on the human gut microbiome: a metagenomic analysis in humanized gnotobiotic mice. *Science translational medicine*, 1(6), p.6ra14.
- Valerio, L.G. & Long, A., 2010. The in silico prediction of human-specific metabolites from hepatotoxic drugs. *Curr Drug Discov Technol*, 7(3), pp.170–87.
- Vernocchi, P., Del Chierico, F. & Putignani, L., 2016. Gut Microbiota Profiling: Metabolomics Based Approach to Unravel Compounds Affecting Human Health. *Frontiers in Microbiology*, 7.
- Vinaixa, M. et al., 2012. A Guideline to Univariate Statistical Analysis for LC/MS-Based Untargeted Metabolomics-Derived Data. *Metabolites*, 2(4), pp.775–795.
- Wallace, B. et al., 2010. Alleviating cancer drug toxicity by inhibiting a bacterial enzyme. *Science*, 330(6005), pp.831–835.
- Wang, J.H. et al., 2014. Sigma S-dependent antioxidant defense protects stationary-phase *Escherichia coli* against the bactericidal antibiotic gentamicin. *Antimicrobial Agents and Chemotherapy*, 58(10), pp.5964–5975.
- Wang, Z. et al., 2011. Gut flora metabolism of phosphatidylcholine promotes cardiovascular disease. *Nature*, 472(7341), pp.57–63.
- Wernicke, J.F. et al., 2005. Safety and adverse event profile of duloxetine. *Expert opinion on drug safety*, 4(6), pp.987–93.
- Wexler, P., 2001. TOXNET: an evolving web resource for toxicology and environmental health information. *Toxicology*, 157(1–2), pp.3–10.
- Van de Wiele, T. et al., 2005. Human colon microbiota transform polycyclic aromatic hydrocarbons to estrogenic metabolites. *Environmental health perspectives*, 113(1), pp.6–10.
- Wikoff, W. & Anfora, A., 2009. Metabolomics analysis reveals large effects of gut microflora on mammalian blood metabolites. *Proc. Natl. Acad. Sci. U.S.A.*, 106(10), pp.3698–3703.
- Wilson, I.D. & Nicholson, J.K., 2016. Gut microbiome interactions with drug metabolism, efficacy, and toxicity. *Translational Research*.
- World Health Organization, 2015. 19th WHO Model List of Essential Medicines. [Http://www.who.int/medicines/publications/essentialmedicines/En](http://www.who.int/medicines/publications/essentialmedicines/En), (April), pp.1–43.
- Wright, G.D., 2016. Antibiotic Adjuvants: Rescuing Antibiotics from Resistance. *Trends in Microbiology*, 24(11), pp.862–871.
- Wu, S., Zhang, L. & Chen, J., 2012. Paracetamol in the environment and its degradation by microorganisms. *Appl. Microbiol. Biotechnol.*, 96(4), pp.875–84.
- Xu, H. et al., 2007. Anaerobic metabolism of 1-amino-2-naphthol-based azo dyes (Sudan dyes) by human intestinal microflora. *Applied and Environmental Microbiology*, 73(23), pp.7759–7762.
- Yang, H. et al., 2005. Niche heterogeneity determines bacterial community structure in the termite gut (*Reticulitermes santonensis*). *Environ. Microbiol.*, 7(7), pp.916–32.
- Zgurskaya, H.I. et al., 2011. *Mechanism and function of the outer membrane*

- channel TolC in multidrug resistance and physiology of enterobacteria,*
- Zhang, J. et al., 2014. PEAR: A fast and accurate Illumina Paired-End reAd mergeR. *Bioinformatics*, 30(5), pp.614–620.
- Zheng, P. et al., 2016. Gut microbiome remodeling induces depressive-like behaviors through a pathway mediated by the host's metabolism. *Molecular psychiatry*, (February), pp.1–11.
- Zheng, X. et al., 2013. Melamine-induced renal toxicity is mediated by the gut microbiota. *Sci Transl Med*, 5(172), p.172ra22.
- Zhernakova, A. et al., 2016. Population-based metagenomics analysis reveals markers for gut microbiome composition and diversity. *Science*, 352(6285), pp.565–569.

Appendix

A. Side effect keywords

Table 12: Indirect gut related side effects from SIDER database.

"Abdominal bloating", "Abdominal colic", "Abdominal cramps", "Abdominal discomfort", "Abdominal distension", "Abdominal distension gaseous", "Abdominal distress", "Abdominal infection", "Abdominal pain", "Abdominal pain generalised", "Abdominal pain lower", "Abdominal pain upper", "Abdominal rigidity", "Abdominal symptom", "Abdominal tenderness", "Abnormal bowel sounds", "Abnormal faeces", "Abnormal weight gain", "Acne", "Acne fulminans", "Acne infantile", "Acneiform eruption", "Acquired megacolon", "Acute abdomen", "Acute gastroenteritis", "Acute interstitial nephritis", "Aminoaciduria", "Anaemia vitamin B12 deficiency", "Anal atresia", "Anal discomfort", "Anal inflammation", "Anal pruritus", "Anorectal discomfort", "Anorectal disorder", "Anorexia", "Anus disorder", "Arterial stenosis", "Arterial thrombosis", "Arterial thrombosis limb", "Arteriosclerosis", "Arteriosclerosis coronary artery", "Arthritis bacterial", "Arthritis infective", "Atherosclerosis", "Atypical mycobacterial infection", "Avitaminosis", "Bacterial infection", "Bacterial prostatitis", "Bacteriuria", "Bloating feeling", "Blood gastrin increased", "Blood glucose abnormal", "Blood glucose decreased", "Blood glucose increased", "Body odor", "Borborygmi", "Bowel sounds decreased", "Bowel spasm", "Caecitis", "Carbohydrate craving", "Carbohydrate tolerance decreased", "Carotid bruit", "Central obesity", "Cerebral arteriosclerosis", "Change of bowel habit", "Cholangitis", "Cholangitis sclerosing", "Clostridial infection", "Clostridium colitis", "Clostridium difficile colitis", "Colicky", "Colitis", "Colitis ischaemic", "Colitis microscopic", "Colitis ulcerative", "Colon atonic", "Colonic obstruction", "Colonic pseudo-obstruction", "Constipation", "Constipation chronic", "Coronary artery occlusion", "Crohn's disease", "Defaecation urgency", "Delayed gastric emptying", "Diarrhoea", "Diarrhoea haemorrhagic", "Diarrhoea, Clostridium difficile", "Digestion impaired", "Discomfort rectal", "Distress gastrointestinal", "Diverticulitis", "Diverticulum", "Diverticulum intestinal", "Dysentery", "Encopresis", "Enlargement abdomen", "Enteritis", "Enterocolitis", "Epigastric discomfort", "Epigastric distress", "Epigastric fullness", "Epigastric pain", "Excessive flatulence", "Faecal incontinence", "Faecalith", "Faecaloma", "Faeces discoloured", "Faeces hard", "Flatulence", "Gas", "Gas in stomach", "Gas pain", "Gastric dilatation", "Gastric disorder", "Gastric erosions", "Gastric flu", "Gastric irritation", "Gastric pH decreased", "Gastric ulcer", "Gastric ulcer haemorrhage", "Gastric ulcer perforation", "Gastrin increased", "Gastrinoma", "Gastritis", "Gastritis erosive", "Gastritis haemorrhagic", "Gastroduodenitis", "Gastroenteritis", "Gastroenteritis bacterial", "Gastrointestinal candidiasis", "Gastrointestinal discomfort", "Gastrointestinal disorder", "Gastrointestinal infection", "Gastrointestinal obstruction", "Gastrointestinal pain", "Gastrointestinal sounds abnormal", "Gastrointestinal stoma complication", "Gastrointestinal symptom NOS", "Gastrointestinal toxicity", "Gastrointestinal tract irritation", "Gastrointestinal ulcer", "Helicobacter gastritis", "Helicobacter infection", "Hypovitaminosis", "Impaired gastric emptying", "Infection susceptibility increased", "Infrequent bowel movements", "Intestinal obstruction", "Intestinal stoma complication", "Intestinal ulcer", "Irritable bowel syndrome", "Large intestinal obstruction", "Lymphocytic colitis", "Malabsorption", "Malnutrition", "Markedly reduced dietary intake", "Megacolon", "Megacolon toxic", "Melaena", "Metabolic acidosis", "Metabolic alkalosis", "Metabolic disorder", "Mucous stools", "Neutropenic colitis", "Neutropenic enterocolitis", "Obesity", "Obstipation", "Pneumatosis", "Pneumatosis cystoides intestinalis", "Pneumatosis intestinalis", "Post procedural diarrhoea", "Proctocolitis", "Protein-losing gastroenteropathy", "Pseudomembranous colitis", "Pseudomembranous enterocolitis", "Serum gastrin increased", "Steatorrhoea", "Stools watery", "Tarry stools", "Ulcerative enterocolitis", "Unspecified disorder of intestine", "Vitamin B complex deficiency", "Vitamin B12 deficiency", "Vitamin B6 deficiency", "Vitamin D deficiency", "Vitamin K deficiency", "Watery diarrhoea", "Weight decreased", "Weight fluctuation", "Weight increased"

Table 13: Direct gut related side effects from SIDER database.

"Abdominal bloating", "Abdominal distension gaseous", "Abnormal bowel sounds", "Abnormal faeces", "Bloating feeling", "Borborygmi", "Bowel sounds decreased", "Change of bowel habit", "Constipation", "Defaecation urgency", "Diarrhoea", "Diarrhoea, Clostridium difficile", "Digestion impaired", "Distress gastrointestinal", "Excessive flatulence", "Faecal incontinence", "Faeces discoloured", "Faeces hard", "Flatulence", "Gas", "Gas in stomach", "Gastrointestinal sounds abnormal", "Impaired gastric emptying", "Infection susceptibility increased", "Infrequent bowel movements", "Intestinal obstruction", "Malabsorption", "Malnutrition", "Obstipation", "Steatorrhoea", "Stools watery", "Tarry stools", "Watery diarrhoea", "Weight decreased", "Weight fluctuation", "Weight increased"

B. Bacteria-Drug Interactions

Table 14: Drug depletion in bacteria-drug interaction screen.

Depleting bacteria	Depleted drug	Mean depletion in percent
Escherichia coli ED1a	Acetaminophen	100
Fusobacterium nucleatum nucleatum	Acetaminophen	100
Bacteroides uniformis	Aripiprazole	44.27540983
Clostridium saccharolyticum	Aripiprazole	41.06687518
Escherichia coli iAi1	Aripiprazole	41.15933652
Eggerthella lenta	Digoxin	100
Fusobacterium nucleatum nucleatum	Donepezil	39.22195301
Bacteroides uniformis	Duloxetine	51.53810786
Clostridium bolteae	Duloxetine	48.68194393
Clostridium saccharolyticum	Duloxetine	53.84738298
Coprococcus comes	Duloxetine	37.43557749
Escherichia coli iAi1	Duloxetine	40.60557131
Lactobacillus paracasei	Duloxetine	52.11007663
Lactobacillus plantarum	Duloxetine	44.54516384
Ruminococcus gnavus	Duloxetine	57.22155512
Bifidobacterium animalis lactis	Ezetimibe	57.34494054
Clostridium ramosum	Ezetimibe	62.76817906
Mix Degrad	Ezetimibe	66.779273
Mix No	Ezetimibe	50.61135839
Bacteroides uniformis	Levamisole	68.47070953
Bacteroides uniformis HM716	Levamisole	74.79411704
Bifidobacterium animalis lactis	Levamisole	43.84127641
Bifidobacterium longum infantis	Levamisole	55.62754501
Clostridium bolteae	Levamisole	48.05907875
Clostridium saccharolyticum	Levamisole	58.2917914
Coprococcus comes	Levamisole	62.47539067
Fusobacterium nucleatum nucleatum	Levamisole	87.38600047
Bacteroides vulgatus	Metronidazole	100
Bifidobacterium animalis lactis	Metronidazole	98.69099719
Clostridium bolteae	Metronidazole	100
Escherichia coli ED1a	Metronidazole	100
Escherichia coli iAi1	Metronidazole	100
Lactobacillus plantarum	Metronidazole	100
Lactococcus lactis	Metronidazole	100
Mix Degrad	Metronidazole	100
Mix No	Metronidazole	100
Streptococcus salivarius	Metronidazole	100
Bacteroides uniformis HM715	Montelukast	39.14008877
Bifidobacterium animalis lactis	Montelukast	47.83326001
Bifidobacterium longum infantis	Montelukast	45.68743593
Clostridium bolteae	Montelukast	49.09396904
Coprococcus comes	Montelukast	43.2711665
Fusobacterium nucleatum nucleatum	Montelukast	42.07705466
Lactobacillus plantarum	Montelukast	43.4526419
Mix Degrad	Montelukast	46.00337988

Ruminococcus gnavus	Montelukast	66.10601682
Clostridium bolteae	Ranitidine	39.85594525
Eggerthella lenta	Ranitidine	100
Escherichia coli iAi1	Ranitidine	39.82398937
Fusobacterium nucleatum nucleatum	Ranitidine	32.7098203
Lactobacillus gasseri	Ranitidine	42.91659306
Ruminococcus gnavus	Ranitidine	45.6331274
Fusobacterium nucleatum nucleatum	Roflumilast	39.05930242
Lactococcus lactis	Roflumilast	79.83320576
Mix No	Roflumilast	53.1968065
Ruminococcus gnavus	Roflumilast	44.25472109
Bacteroides thetaiotaomicron	Rosiglitazone	35.28432013
Bifidobacterium animalis lactis	Rosiglitazone	44.48883462
Fusobacterium nucleatum nucleatum	Rosiglitazone	35.23351925
Lactobacillus paracasei	Rosiglitazone	41.88601157
Bacteroides thetaiotaomicron	Simvastatin	74.84471371
Bacteroides uniformis	Simvastatin	76.86857365
Bacteroides vulgatus	Simvastatin	69.9565144
Bifidobacterium animalis lactis	Simvastatin	69.83734966
Clostridium bolteae	Simvastatin	52.52299585
Clostridium ramosum	Simvastatin	66.26821933
Clostridium saccharolyticum	Simvastatin	56.35281086
Eggerthella lenta	Simvastatin	44.58606123
Fusobacterium nucleatum nucleatum	Simvastatin	54.77585933
Lactobacillus plantarum	Simvastatin	74.33695501
Mix Degrad	Simvastatin	54.37546604
Bacteroides uniformis	Sulfasalazine	100
Bacteroides uniformis HM715	Sulfasalazine	100
Bifidobacterium animalis lactis	Sulfasalazine	100
Bifidobacterium longum infantis	Sulfasalazine	100
Clostridium bolteae	Sulfasalazine	100
Clostridium ramosum	Sulfasalazine	100
Eggerthella lenta	Sulfasalazine	100
Escherichia coli iAi1	Sulfasalazine	100
Fusobacterium nucleatum nucleatum	Sulfasalazine	100
Lactobacillus gasseri	Sulfasalazine	100
Lactococcus lactis	Sulfasalazine	100
Mix Degrad	Sulfasalazine	99.64278195
Mix No	Sulfasalazine	100
Streptococcus salivarius	Sulfasalazine	100

Table 15: Growth effects from bacteria-drug interaction screen.

Drug	Affected bacteria	log2 fold change
Aripiprazole	E. coli IAI1	0.376486125
Aripiprazole	L. gasseri	0.229201218
Digoxin	E. coli IAI1	0.300498375
Digoxin	E. lenta	0.27439148
Digoxin	R. torques	0.764346284
Duloxetine	C. saccharolyticum	0.129106874
Duloxetine	E. coli IAI1	0.451924994
Duloxetine	E. rectale	lethal
Levamisole	L. lactis	0.114455594
Loperamide	B. longum subsp. infantis	lethal
Loperamide	E. coli IAI1	0.304640652
Loperamide	E. lenta	lethal
Loperamide	E. rectale	lethal
Loperamide	L. lactis	0.746548355
Metronidazole	B. fragilis	lethal
Metronidazole	B. longum subsp. infantis	lethal
Metronidazole	B. thetaiotaomicron	lethal

Metronidazole	B. uniformis	lethal
Metronidazole	B. uniformis HM715	lethal
Metronidazole	B. uniformis HM716	lethal
Metronidazole	C. ramosum	lethal
Metronidazole	C. saccharolyticum	lethal
Metronidazole	E. lenta	lethal
Metronidazole	E. rectale	lethal
Metronidazole	F. nucleatum subsp. nucleatum	lethal
Montelukast	B. uniformis HM715	0.167807495
Ranitidine	E. coli IAI1	0.4156723
Rosiglitazone	E. coli IAI1	0.365450851
Rosuvastatin	B. vulgatus	0.136144383
Simvastatin	B. uniformis HM716	0.286360254
Sulfasalazine	C. ramosum	0.297975223
Sulfasalazine	R. torques	1.239805299
Tolmetin	L. plantarum	0.11056823
Tolmetin	R. torques	0.25022290

Table 16: Drug depletion in depletion-mode assay.

Batch	Extraction	Drugs	Bacteria	Difference to Ctrl	p-value
2	dir	aripiprazole	B. uniformis	-31.30972752	0.006731675
3	dir	aripiprazole	C. bolteae	-54.84344883	0.006634478
3	ind	aripiprazole	C. bolteae	-21.70746985	0.070838531
3	dir	digoxin	E. lenta	-19.75243723	0.013396957
5	ind	digoxin	E. lenta	-10.96501077	0.003940423
1	dir	donepezil	F. nucleatum	-22.97478742	0.000865049
3	ind	donepezil	F. nucleatum	-5.304484226	0.001339369
2	dir	duloxetine	B. thetaiotaomicron	-62.43641652	1.13E-05
4	dir	duloxetine	B. thetaiotaomicron	-46.26443258	0.000322
5	dir	duloxetine	C. comes	-6.048205727	0.002312058
2	ind	duloxetine	B. thetaiotaomicron	-38.54924883	1.08E-06
3	ind	duloxetine	B. thetaiotaomicron	-42.16501325	4.04E-05
4	ind	duloxetine	B. thetaiotaomicron	-62.78030703	5.27E-08
2	ind	duloxetine	C. bolteae	-10.65210459	0.056749628
3	ind	duloxetine	C. bolteae	-39.05784799	0.043926718
5	ind	duloxetine	C. comes	-31.77858065	3.53E-09
2	ind	duloxetine	C. saccharolyticum	-26.28156478	4.77E-05
2	ind	duloxetine	R. gnavus	-16.76114904	5.17E-05
2	ind	duloxetine	S. salivarius	-14.99328111	0.000827831
3	dir	ezetimibe	B. animalis lactis	-18.33791	0.000143792
3	ind	ezetimibe	B. animalis lactis	-14.63941392	0.002263293
3	dir	levamisole	B. animalis lactis	-70.63291266	0.001432845
3	dir	levamisole	B. longum infantis	-75.93690931	0.00109915
4	dir	levamisole	B. longum infantis	-74.15933736	1.85E-05
3	dir	levamisole	B. uniformis	-52.03567202	0.005418941
1	dir	levamisole	C. comes	-60.28240374	4.40E-08
2	dir	levamisole	C. ramosum	-52.09290375	0.001769814
1	dir	levamisole	L. gasseri	-42.75016138	4.81E-07
3	ind	levamisole	B. animalis lactis	-69.33489689	1.37E-06
3	ind	levamisole	B. longum infantis	-100	1.98E-06
4	ind	levamisole	B. longum infantis	-72.6262388	2.84E-07
3	ind	levamisole	B. uniformis	-46.70492127	5.34E-05
1	ind	levamisole	C. comes	-64.86468501	0.042616736
2	dir	montelukast	B. longum infantis	-46.99429855	3.18E-05
3	dir	montelukast	C. bolteae	-6.944421862	0.052709981
1	dir	montelukast	C. comes	-12.47607532	0.017622857
1	dir	montelukast	E. rectale	-28.2121751	0.002900849
3	dir	montelukast	R. gnavus	-32.73632476	1.50E-05
5	dir	montelukast	R. gnavus	-33.6912125	0.000223934
3	dir	montelukast	S. salivarius	-50.93947424	1.82E-07

3	ind	montelukast	B. animalis lactis	-12.01544874	0.0018339
2	ind	montelukast	B. longum infantis	-37.33852858	4.15E-08
3	ind	montelukast	B. longum infantis	-20.95413808	0.014405127
2	ind	montelukast	C. bolteae	-35.22644616	5.89E-10
3	ind	montelukast	C. bolteae	-29.39436175	8.68E-07
2	ind	montelukast	C. saccharolyticum	-7.725129365	0.00295472
2	ind	montelukast	R. gnavus	-33.66419854	2.57E-06
3	ind	montelukast	R. gnavus	-33.72466057	2.90E-06
5	ind	montelukast	R. gnavus	-20.88527317	0.000556889
2	ind	montelukast	S. salivarius	-20.63055213	0.000367701
3	ind	montelukast	S. salivarius	-44.09876523	1.13E-07
1	dir	ranitidine	F. nucleatum	-33.18924222	0.000182851
2	dir	roflumilast	S. salivarius	-34.57741768	0.043745799
3	dir	roflumilast	S. salivarius	-49.94386202	0.002985216
3	ind	roflumilast	F. nucleatum	-32.32253541	4.37E-05
2	ind	roflumilast	S. salivarius	-60.05588551	0.010742064
3	ind	roflumilast	S. salivarius	-39.46763637	1.18E-06
5	ind	roflumilast	S. salivarius	-32.14895808	0.000185274
2	ind	rosiglitazone	B. thetaiotaomicron	-28.36986	1.80E-06
2	ind	rosiglitazone	C. ramosum	-15.67899709	3.30E-05
2	dir	sulfasalazine	B. thetaiotaomicron	-100	3.01E-09
2	dir	sulfasalazine	B. uniformis	-100	3.01E-09
2	dir	sulfasalazine	C. bolteae	-100	3.01E-09
2	dir	sulfasalazine	C. ramosum	-100	3.01E-09
2	dir	sulfasalazine	C. saccharolyticum	-100	3.01E-09
2	dir	sulfasalazine	E. coli IAI1	-100	3.01E-09
1	dir	sulfasalazine	F. nucleatum	-100	5.31E-09
1	dir	sulfasalazine	L. gasseri	-100	5.31E-09
2	dir	sulfasalazine	S. salivarius	-100	3.01E-09
2	ind	sulfasalazine	B. thetaiotaomicron	-100	5.46E-06
2	ind	sulfasalazine	B. uniformis	-100	5.46E-06
2	ind	sulfasalazine	C. bolteae	-100	5.46E-06
2	ind	sulfasalazine	C. ramosum	-100	5.46E-06
2	ind	sulfasalazine	C. saccharolyticum	-100	5.46E-06
2	ind	sulfasalazine	E. coli IAI1	-100	5.46E-06
2	ind	sulfasalazine	F. nucleatum	-100	5.46E-06
1	ind	sulfasalazine	F. nucleatum	-100	8.03E-10
1	ind	sulfasalazine	L. gasseri	-85.63467369	0.000211314
2	ind	sulfasalazine	S. salivarius	-100	5.46E-06

C. *saccharolyticum* growth curves and IC50

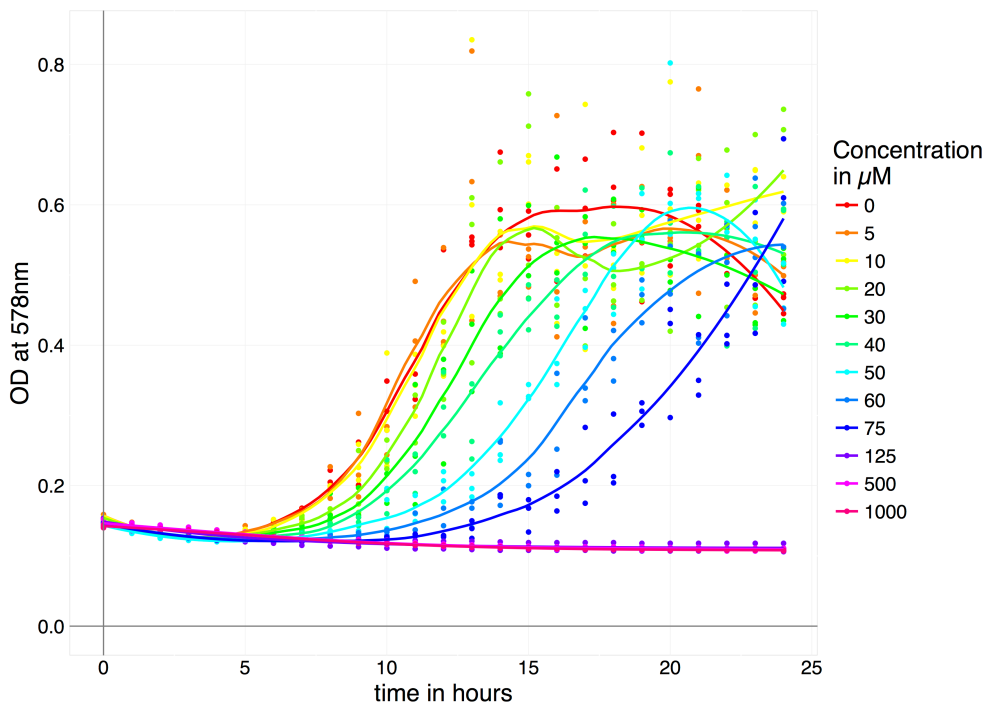


Figure 31: Growth curves of *C. saccharolyticum* exposed to a dilution series of duloxetine. 24h growth curves in GMM with respective concentration of duloxetine with 1% DMSO as solvent. Curves fitted for triplicates with local regression using R's loess function.

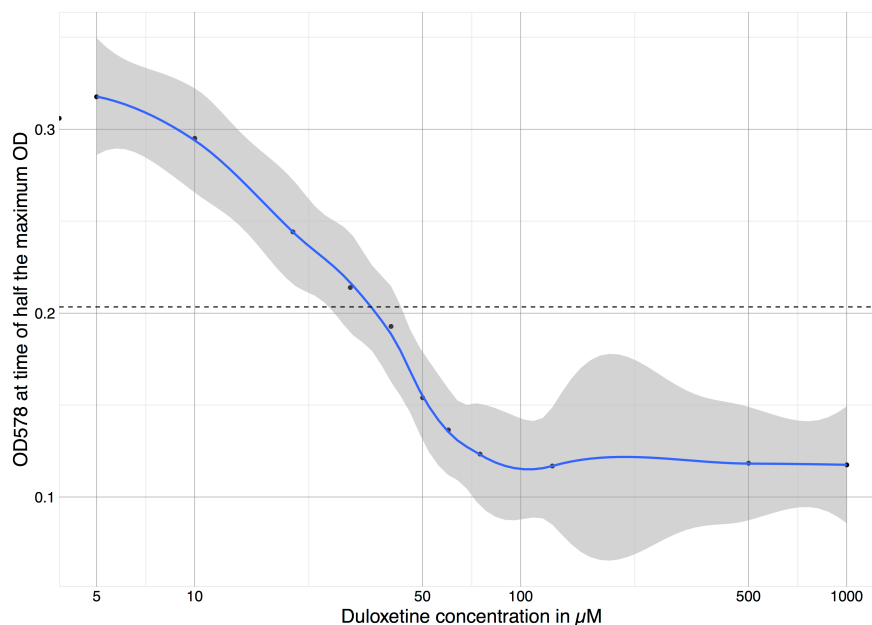


Figure 32: Duloxetine IC50 determination for *C. saccharolyticum*. Dilution series of duloxetine in 1% DMSO. Underlying growth curves taken for 24h in GMM in triplicates. OD at half maximum OD time point of control used as effect response. Dashed line indicates 50% of half-maximum OD, to estimate corresponding inhibitory concentration (IC50). Curves are fitted with R function "loess", span parameter equals 0.5.